

# ***Supplement of*** **LPJmL4 - a dynamic global vegetation model with managed land: Part II – Model evaluation**

S. Schaphoff et al.

*Correspondence to:* Sibyll.Schaphoff@pik-potsdam.de

## **1 Supplementary informations to the evaluation of the LPJmL4 model**

The here provided supplementary informations give more details to the evaluations given in [Schaphoff et al. \(submitted\)](#). All sources and data used are described in detail there. Here we present additional figures for evaluating the LPJmL4 model on a plot scale for water and carbon fluxes Fig. 1 - 16. We  
5 use gauging station to evaluate the river discharge as an integrated measure (Fig. 17 - 64). Fig. 65 and  
Fig. 66a give a comparison with the global estimation of [Carvalhais et al. \(2014\)](#) for soil organic carbon resp. biomass. Additionally we have compared aboveground biomass in Fig. 66b with estimates  
by [Liu et al. \(2015\)](#). A spatial comparison of ecosystem respiration is shown in Fig. 67.

Sowing dates have been proved to be important to simulate crop variability (Fig. 72 - 80), a comparison with MIRCA sowing dates we show in Fig. 81 - 90.  
10

Table 1 gives an overview of estimates for regional field application efficiencies, showing that LPJmL4 are in a similar range as other estimates.

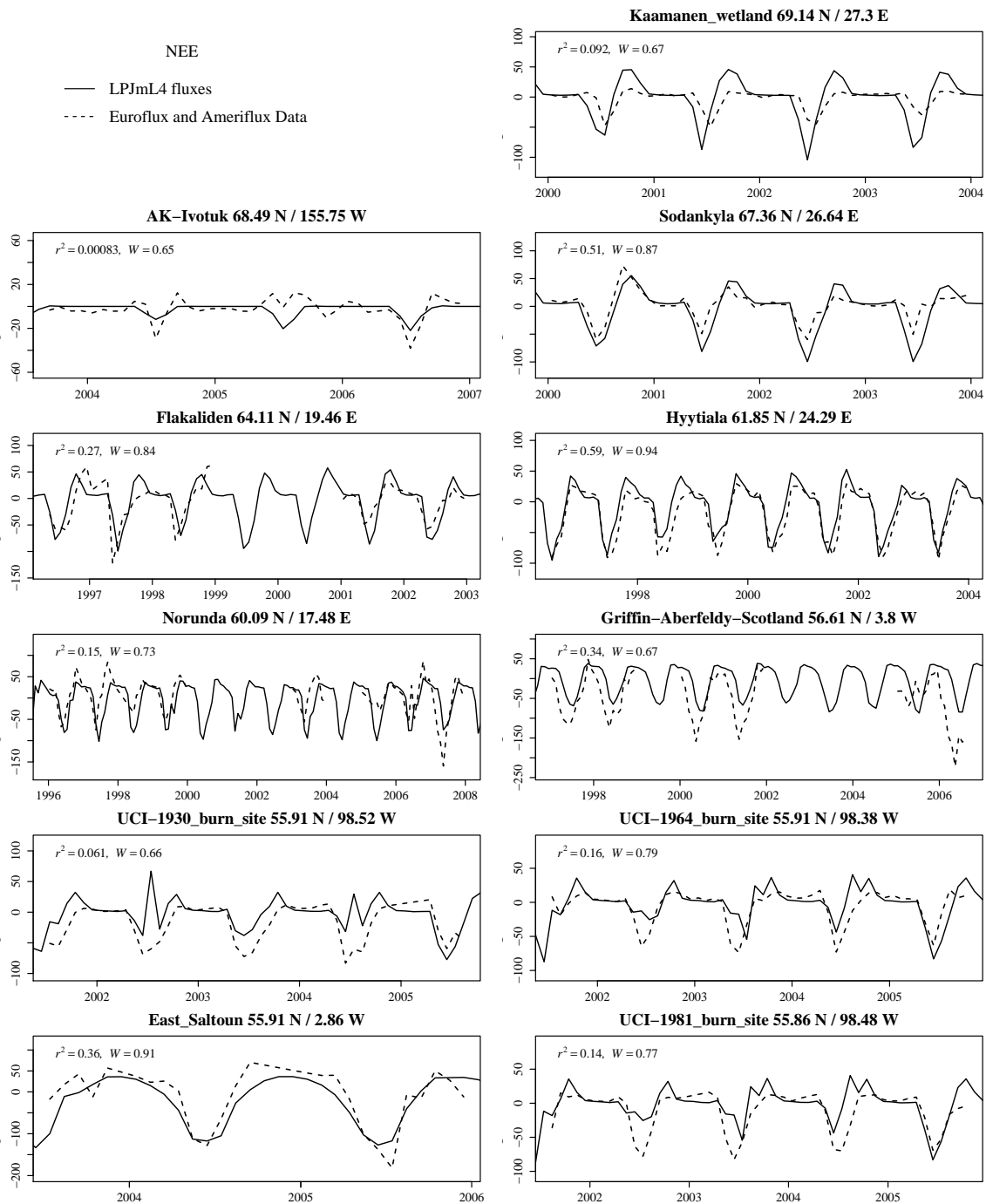


**Figure 1.** Comparison of NEE fluxes with EDDY-flux measurements.

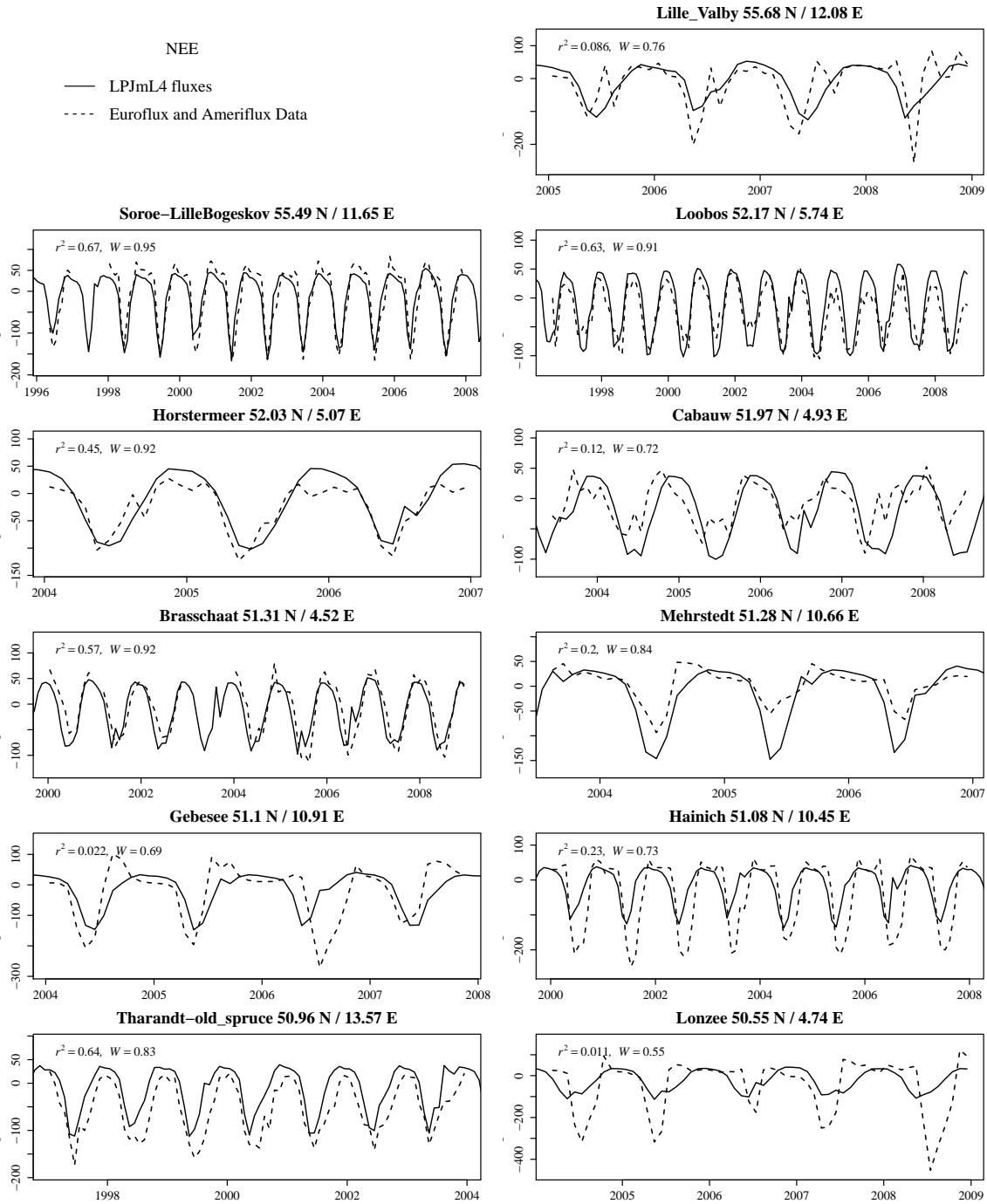


**Figure 2.** Comparison of NEE fluxes with EDDY-flux measurements.

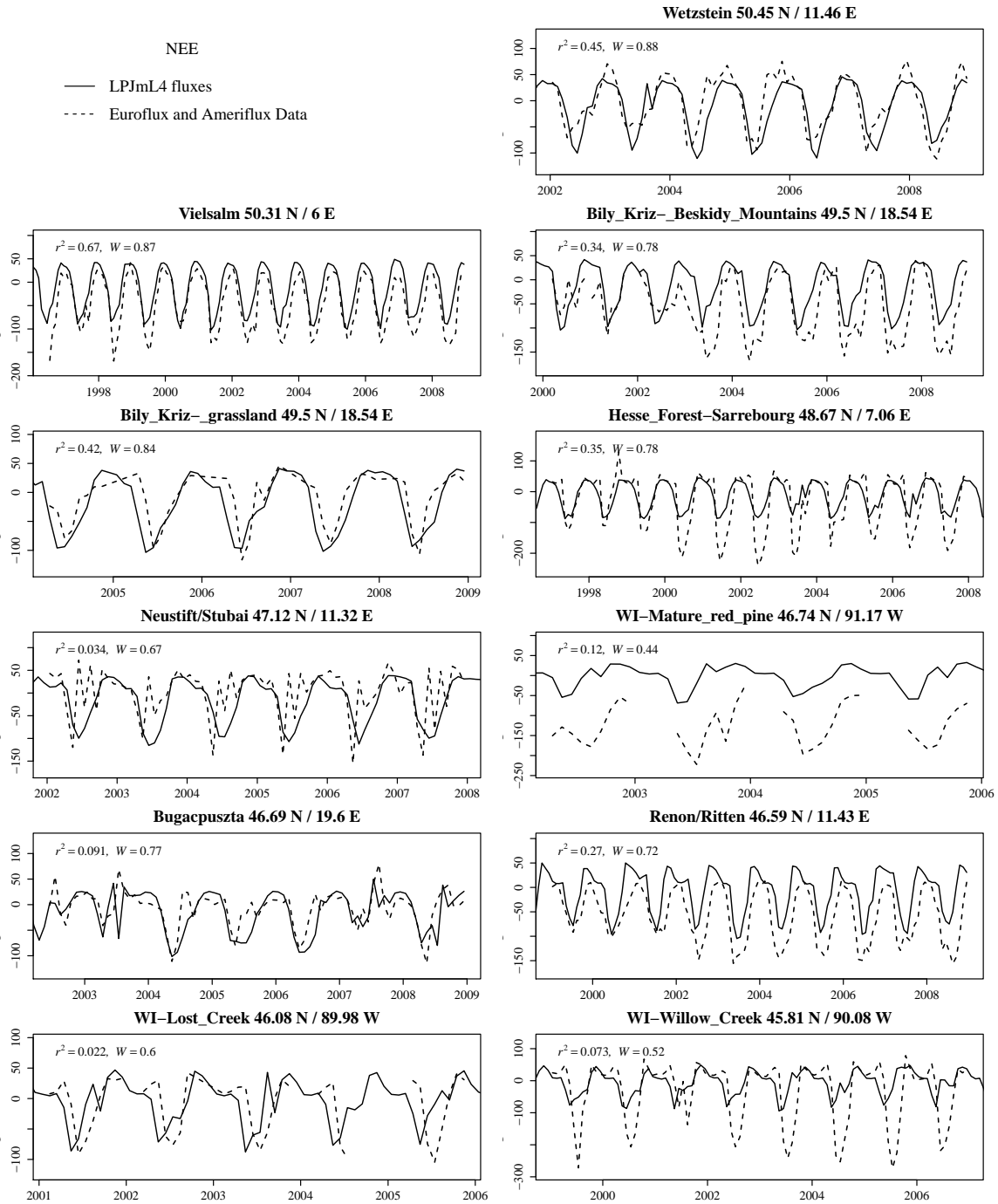


**Figure 3.** Comparison of NEE fluxes with EDDY-flux measurements.

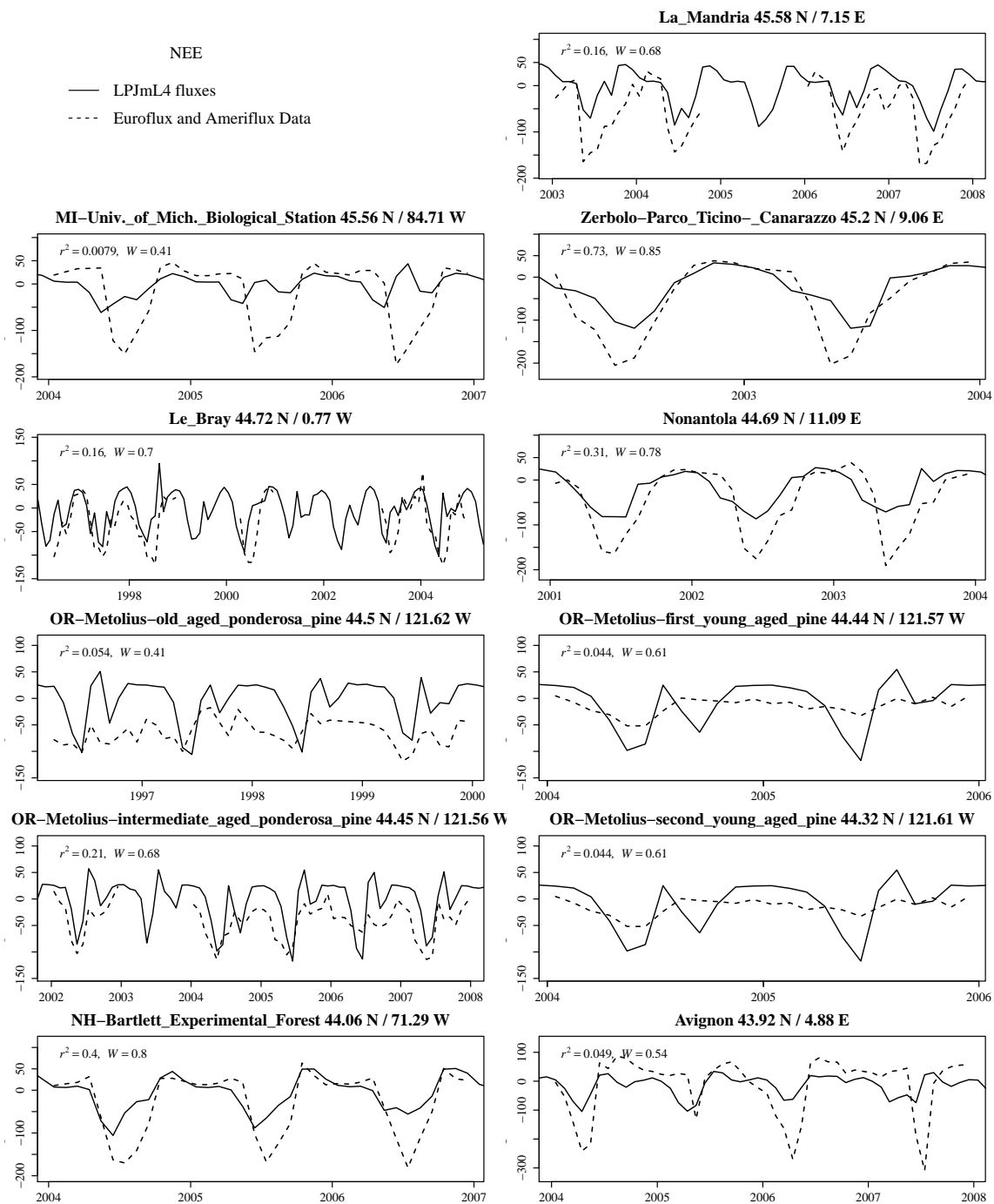


**Figure 4.** Comparison of NEE fluxes with EDDY-flux measurements.

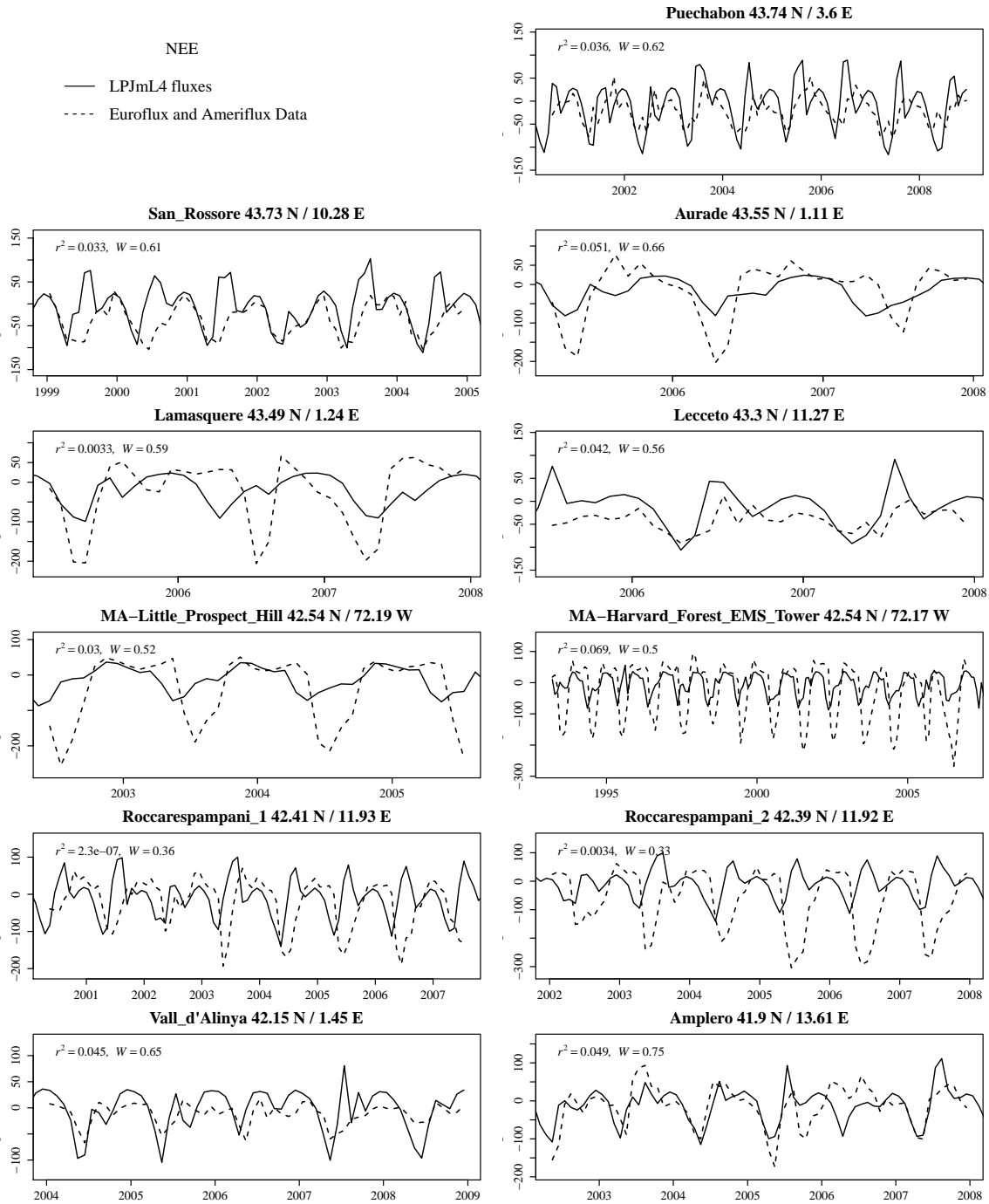
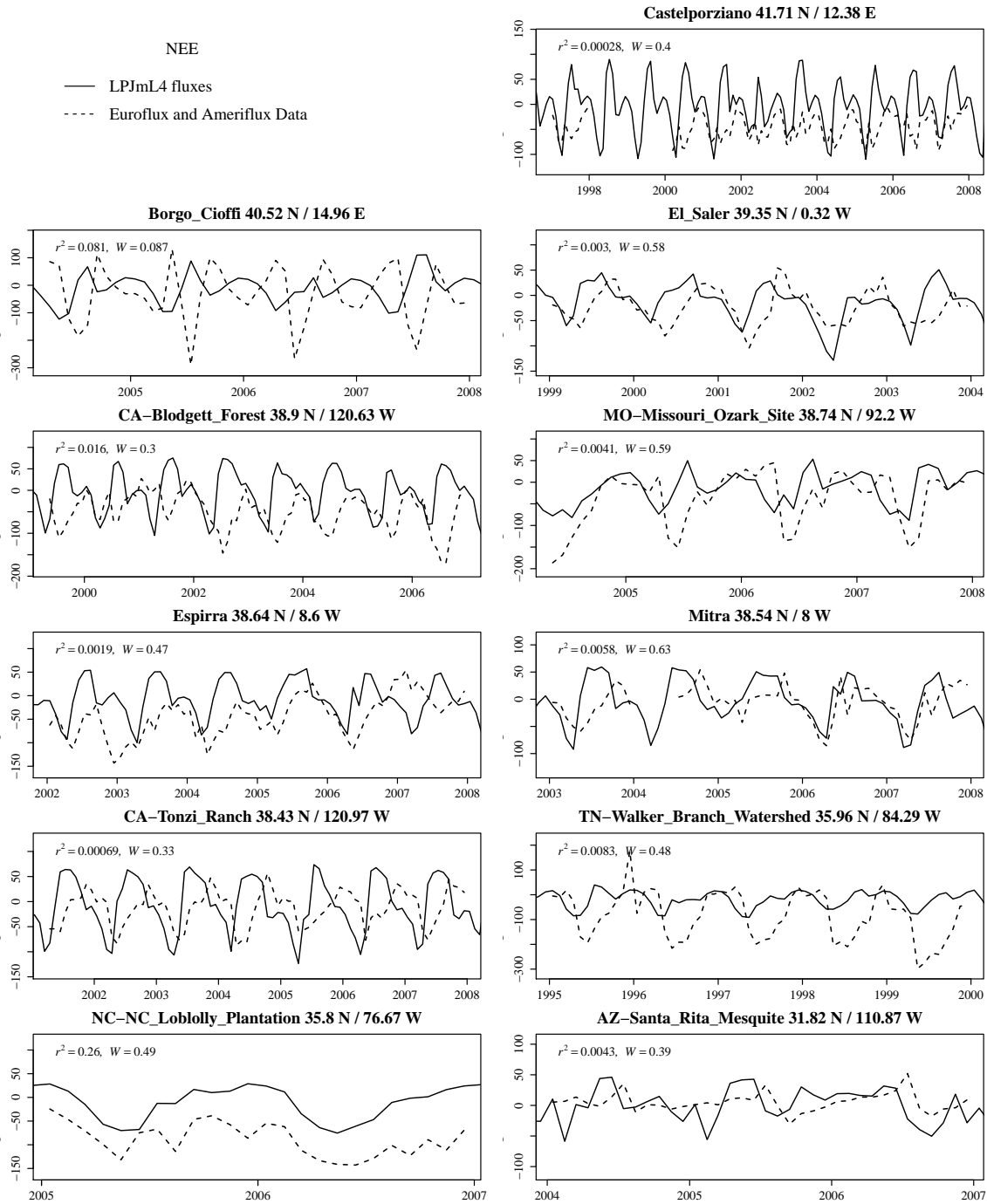
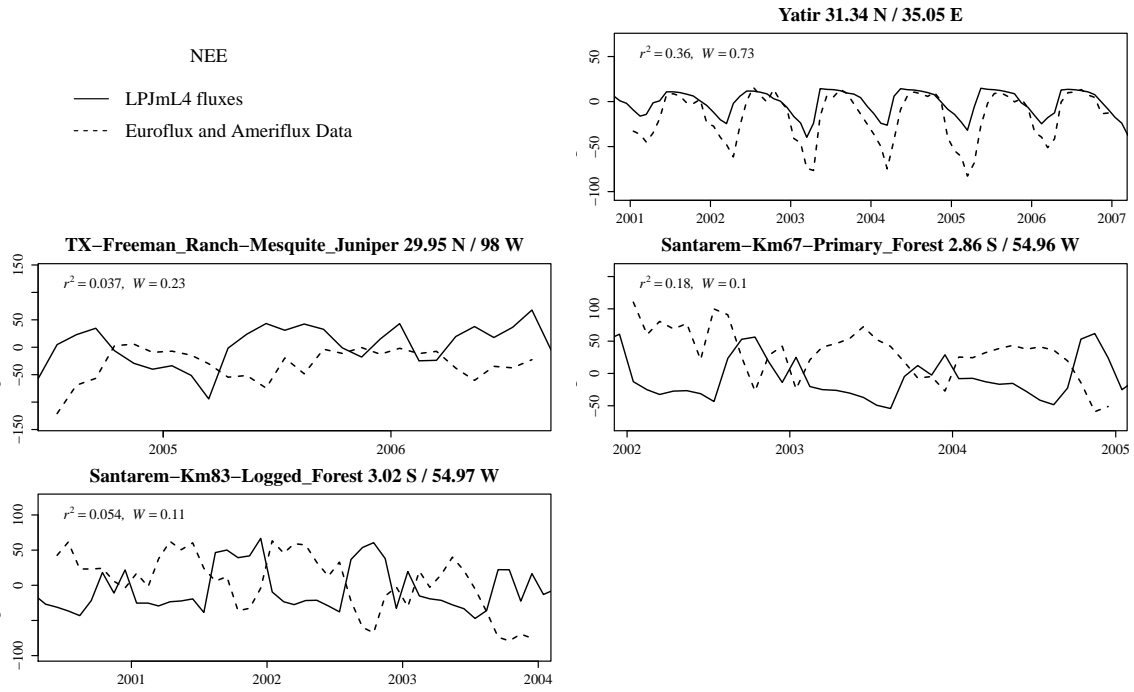


Figure 5. Comparison of NEE fluxes with EDDY-flux measurements.



**Figure 6.** Comparison of NEE fluxes with EDDY-flux measurements.



**Figure 7.** Comparison of NEE fluxes with EDDY-flux measurements.



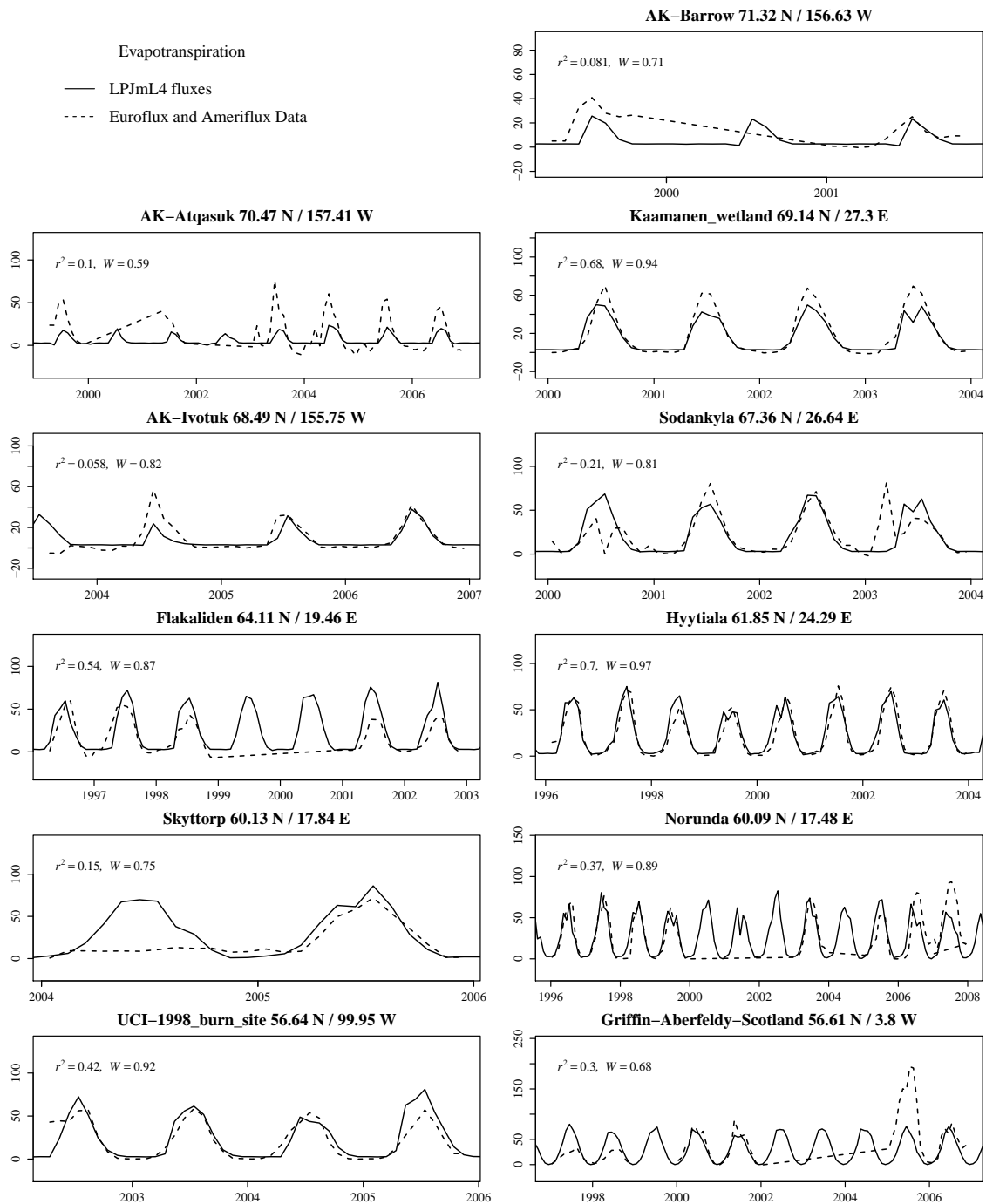


**Figure 8.** Comparison of Evapotranspiration fluxes with EDDY-flux measurements.

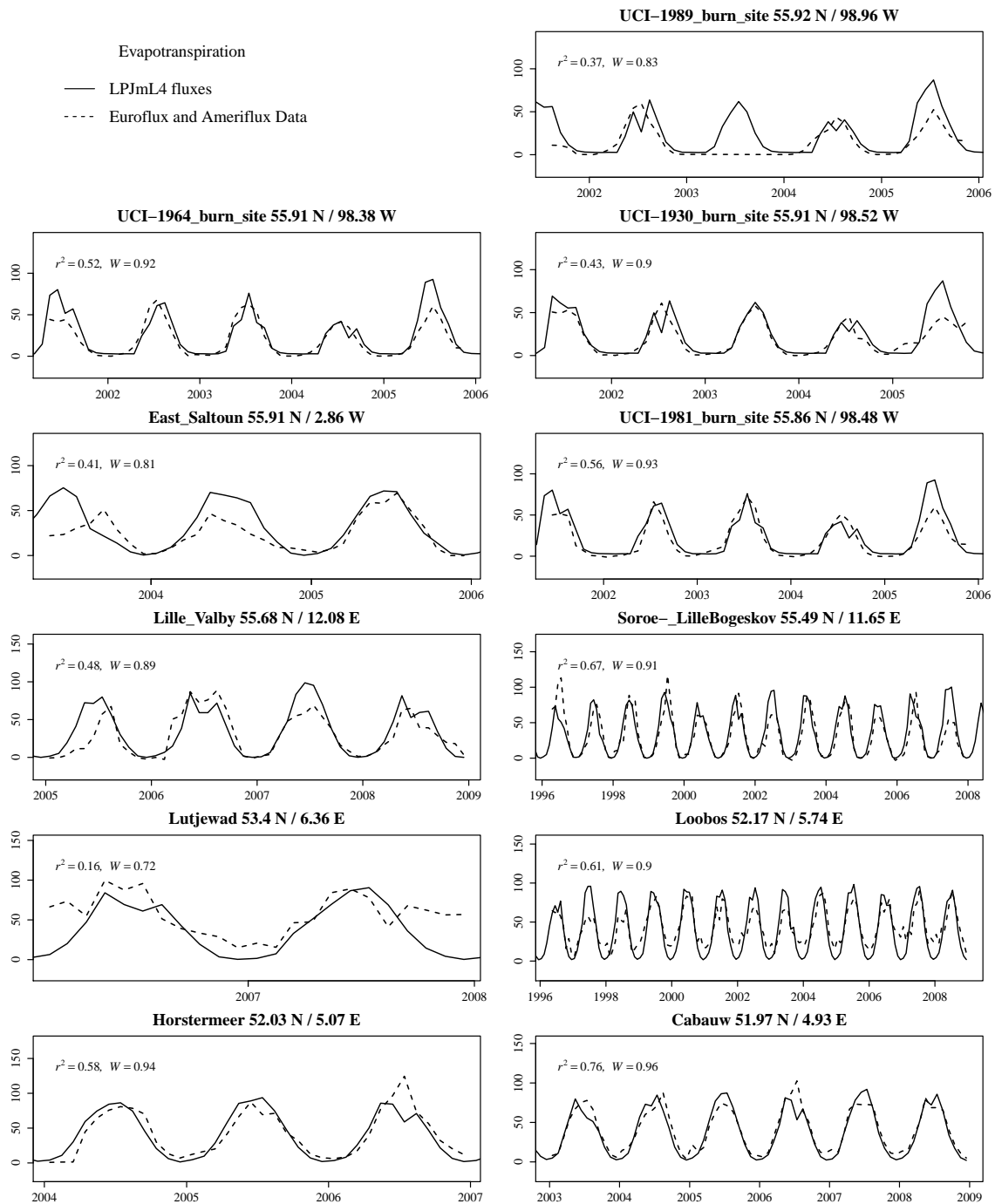


**Figure 9.** Comparison of Evapotranspiration fluxes with EDDY-flux measurements.

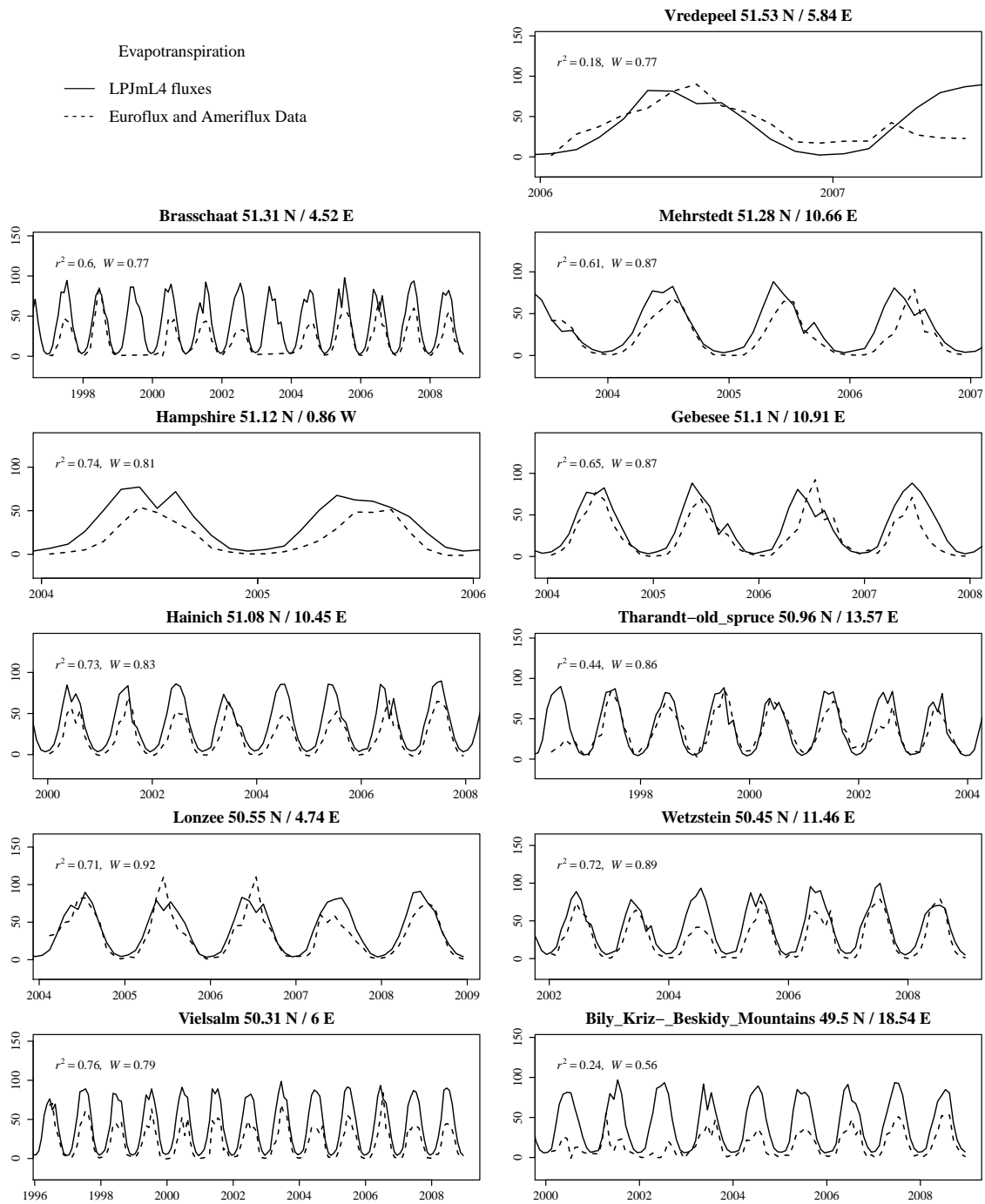


**Figure 10.** Comparison of Evapotranspiration fluxes with EDDY-flux measurements.

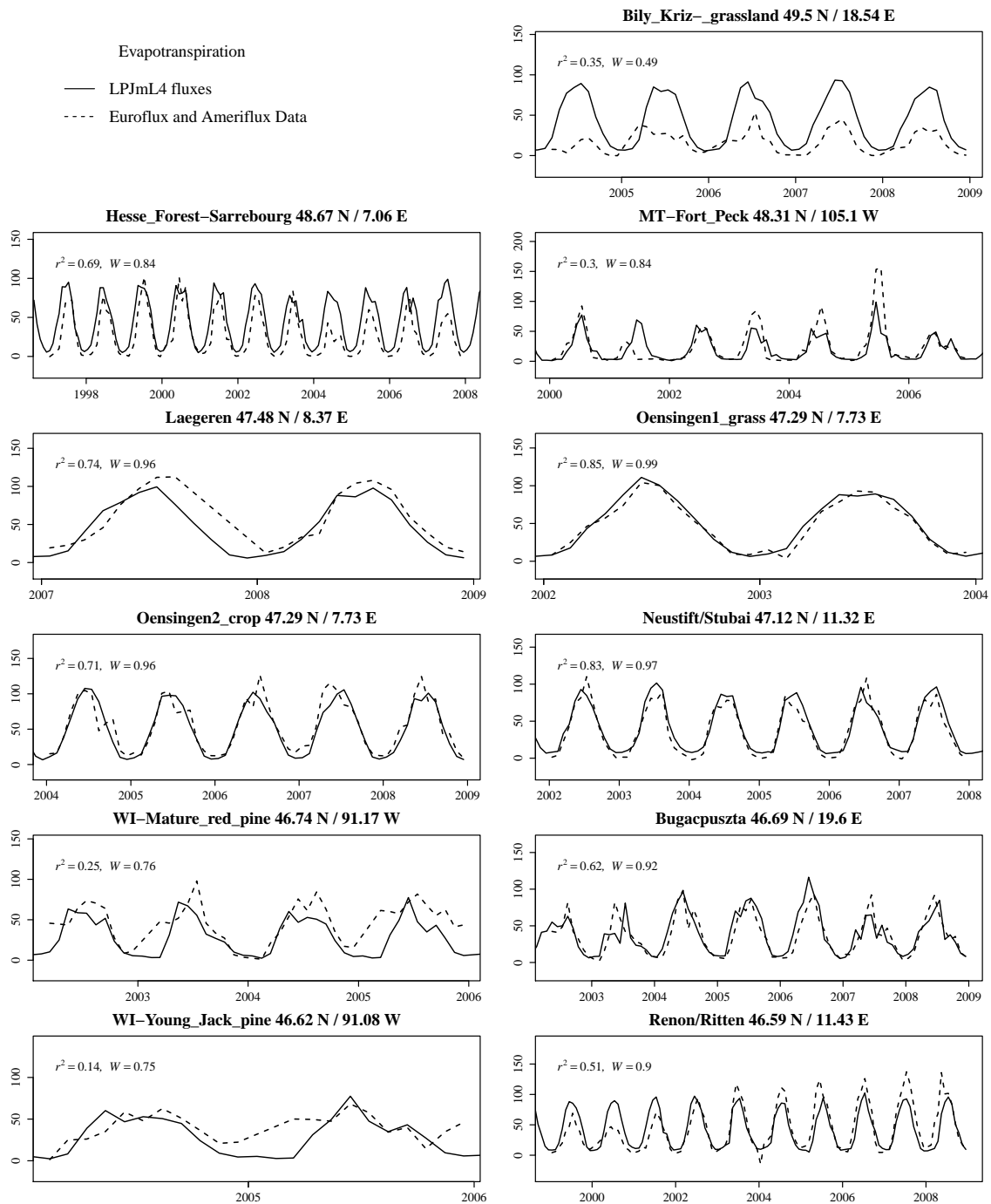


**Figure 11.** Comparison of Evapotranspiration fluxes with EDDY-flux measurements.

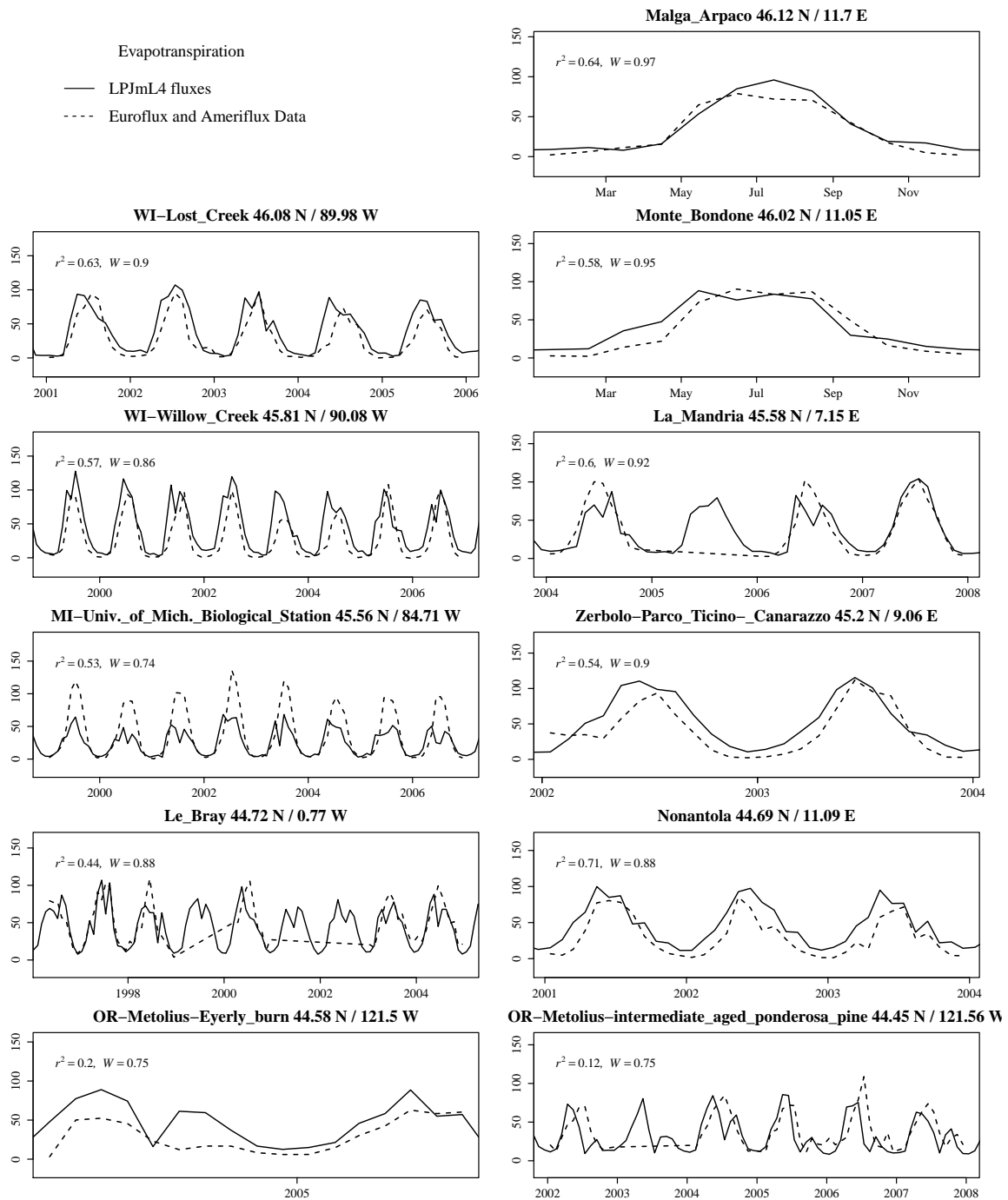


**Figure 12.** Comparison of Evapotranspiration fluxes with EDDY-flux measurements.

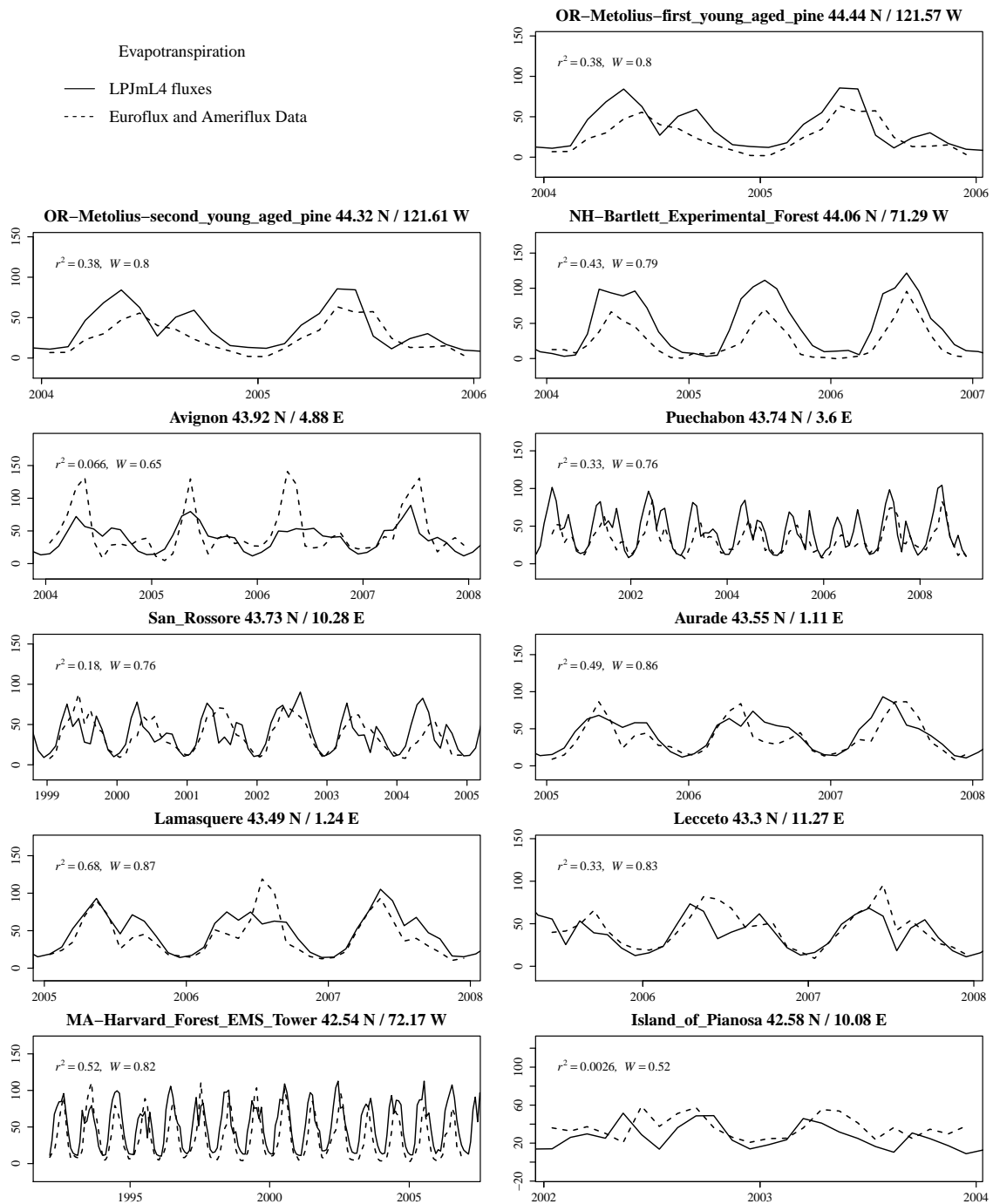


**Figure 13.** Comparison of Evapotranspiration fluxes with EDDY-flux measurements.

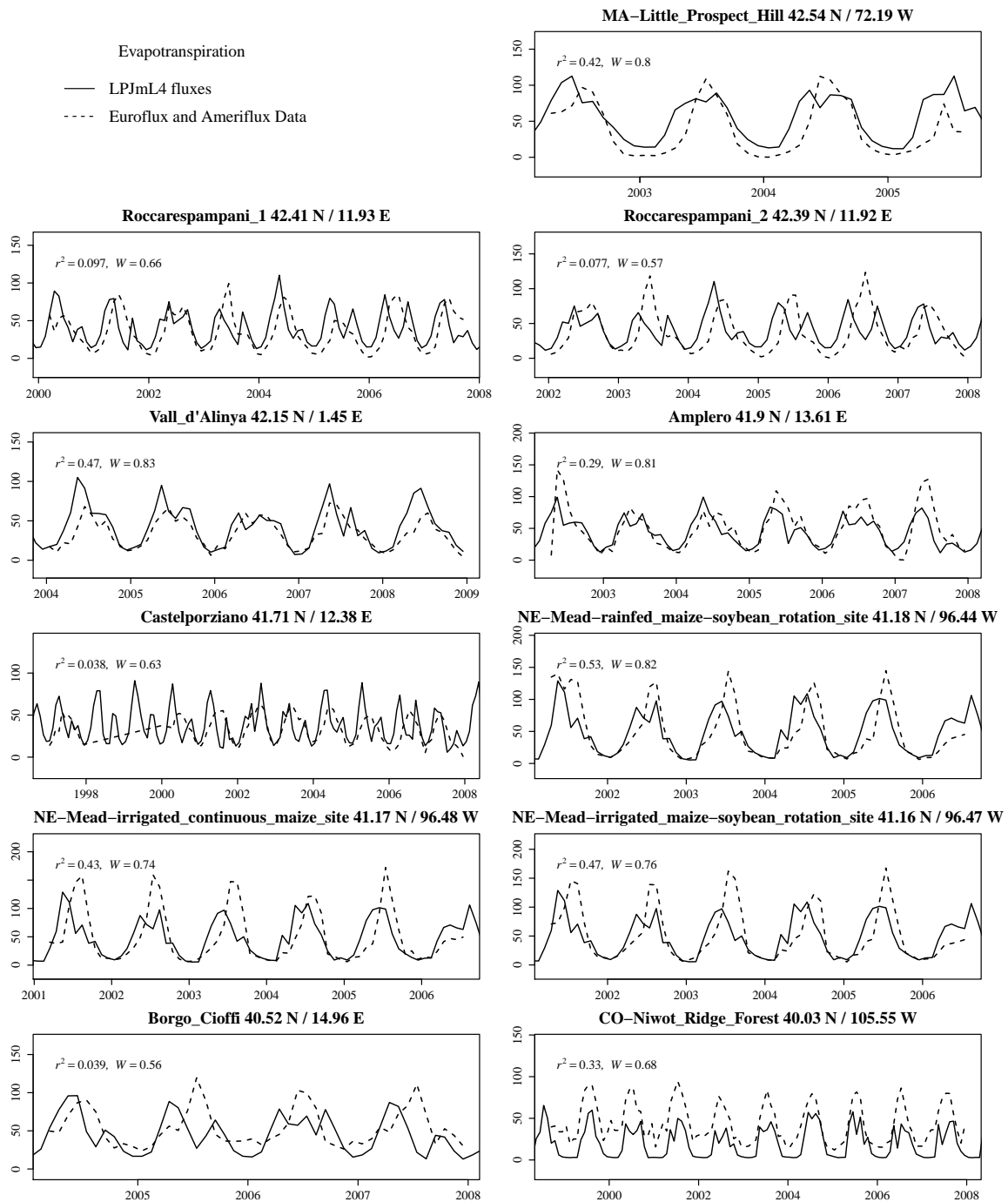


**Figure 14.** Comparison of Evapotranspiration fluxes with EDDY-flux measurements.

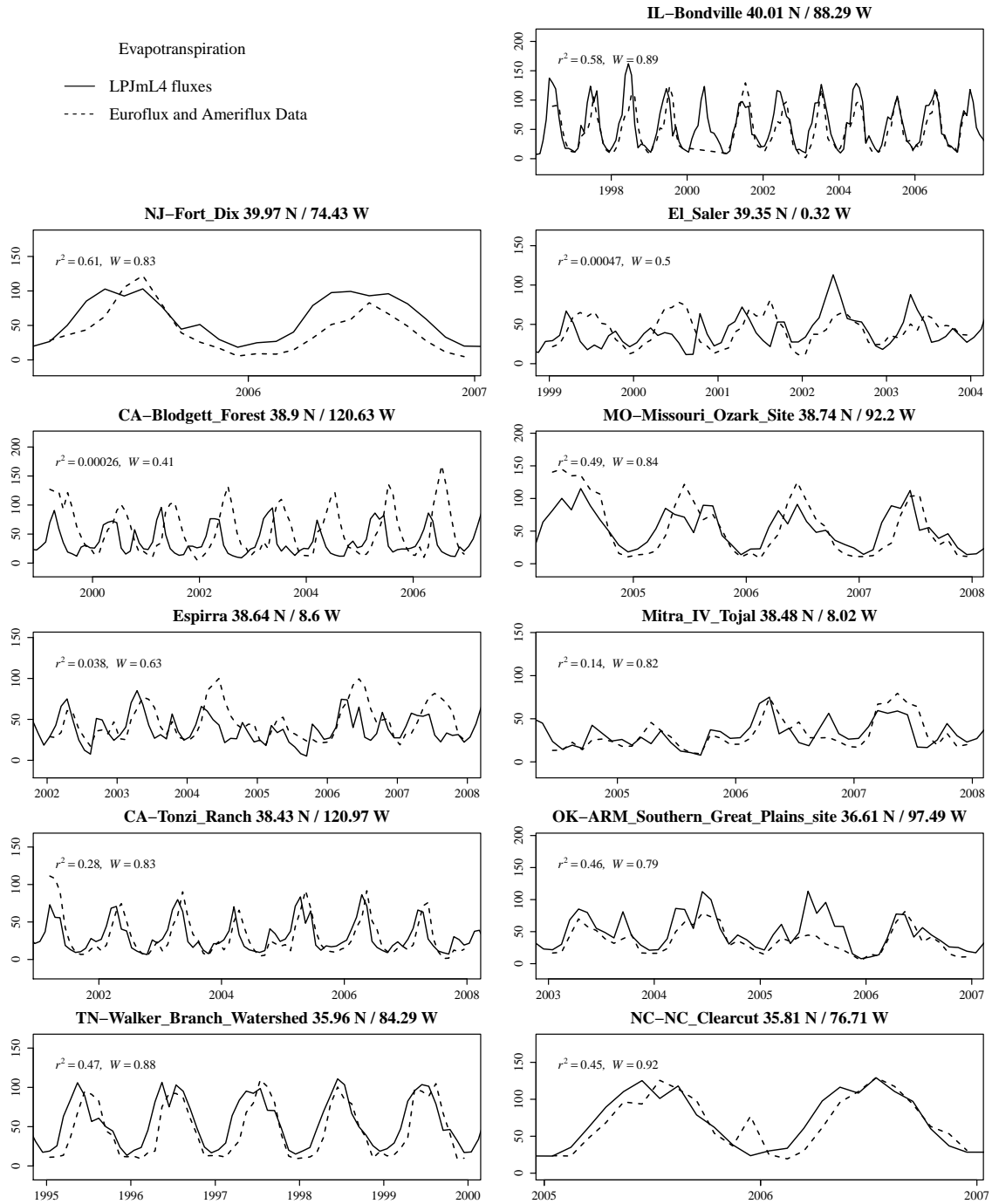
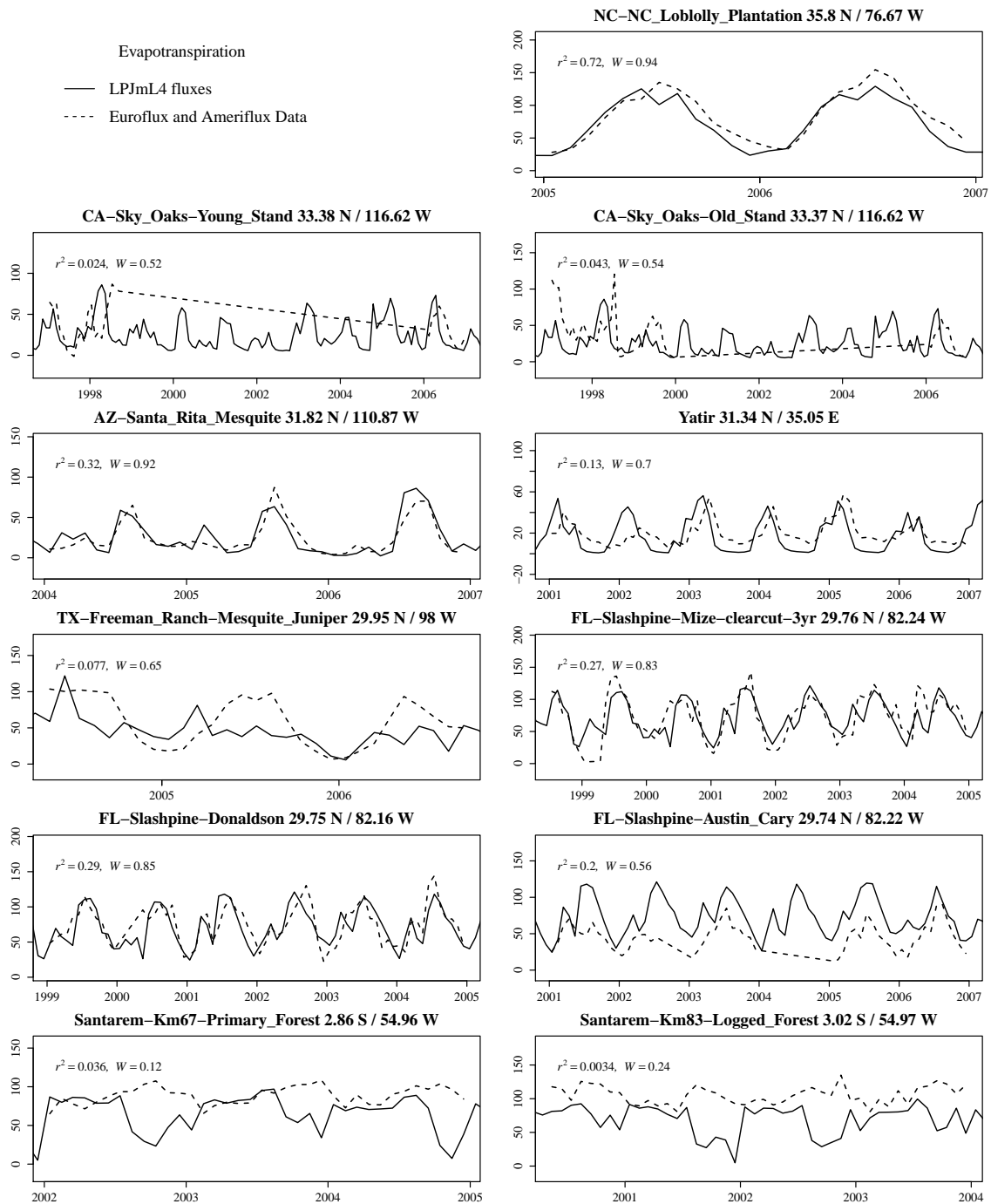


Figure 15. Comparison of Evapotranspiration fluxes with EDDY-flux measurements.





**Figure 16.** Comparison of Evapotranspiration fluxes with EDDY-flux measurements.

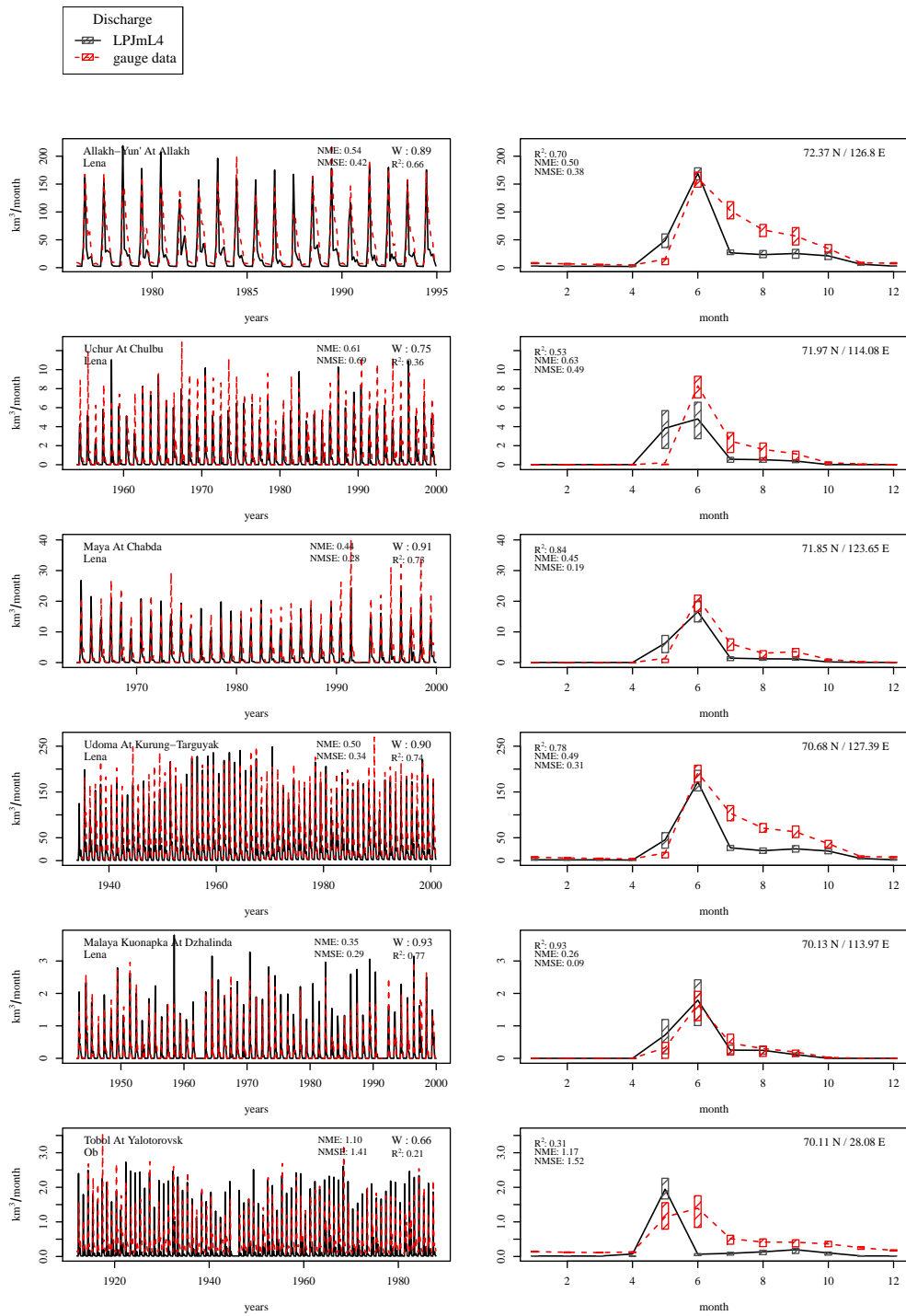


Figure 17. Evaluation of river discharge at gauging stations [1].

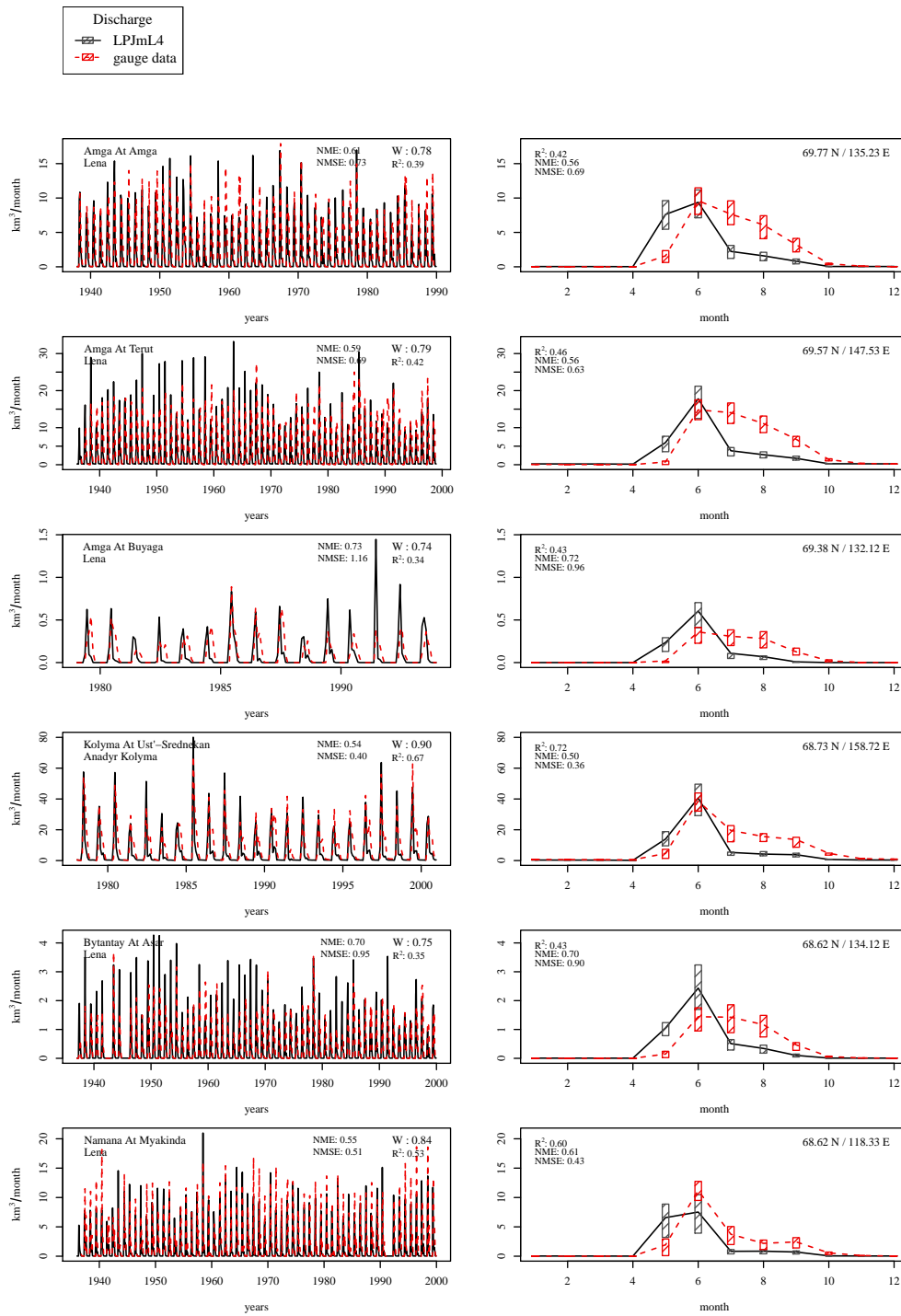


Figure 18. Evaluation of river discharge at gauging stations [2].

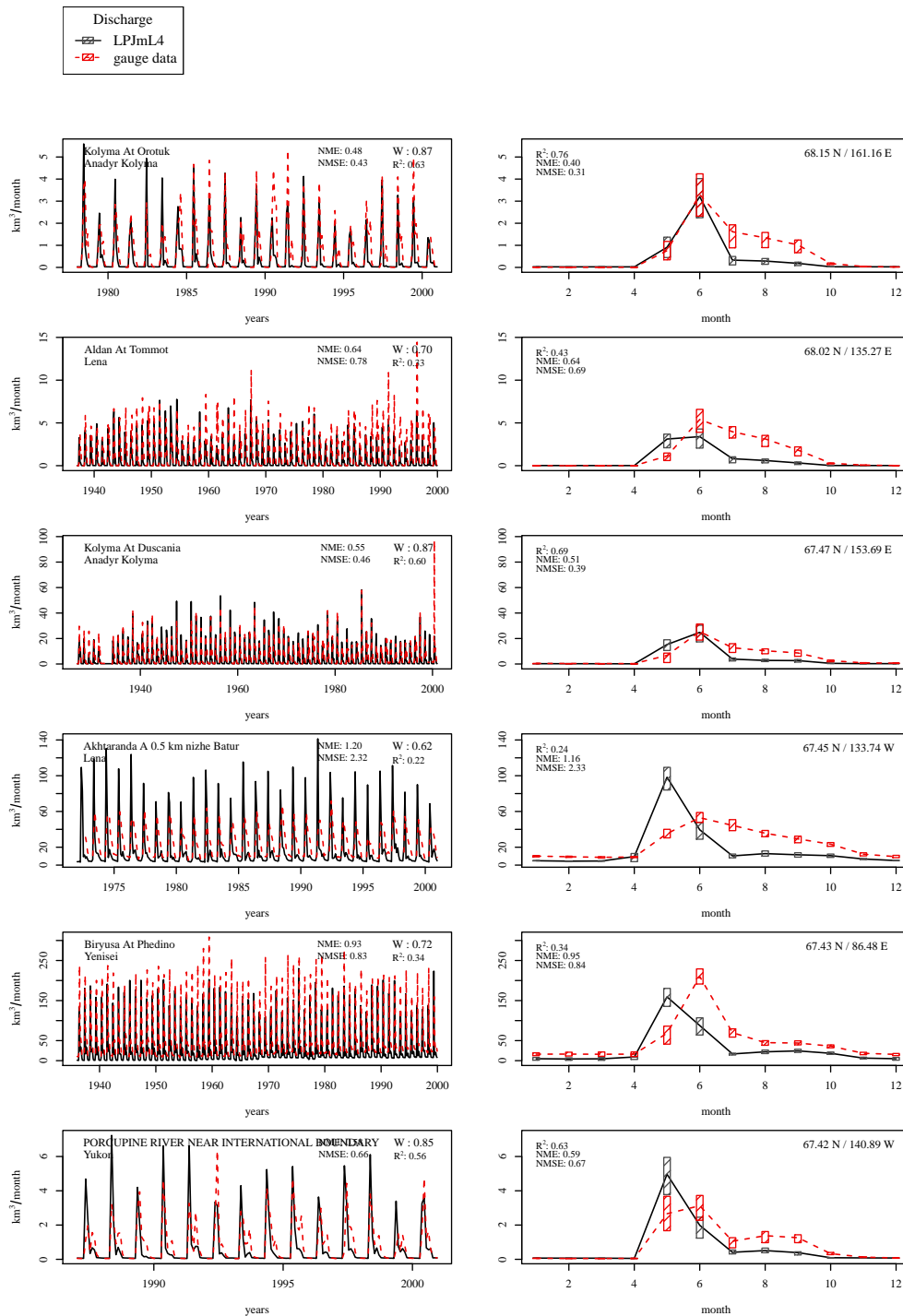


Figure 19. Evaluation of river discharge at gauging stations [3].

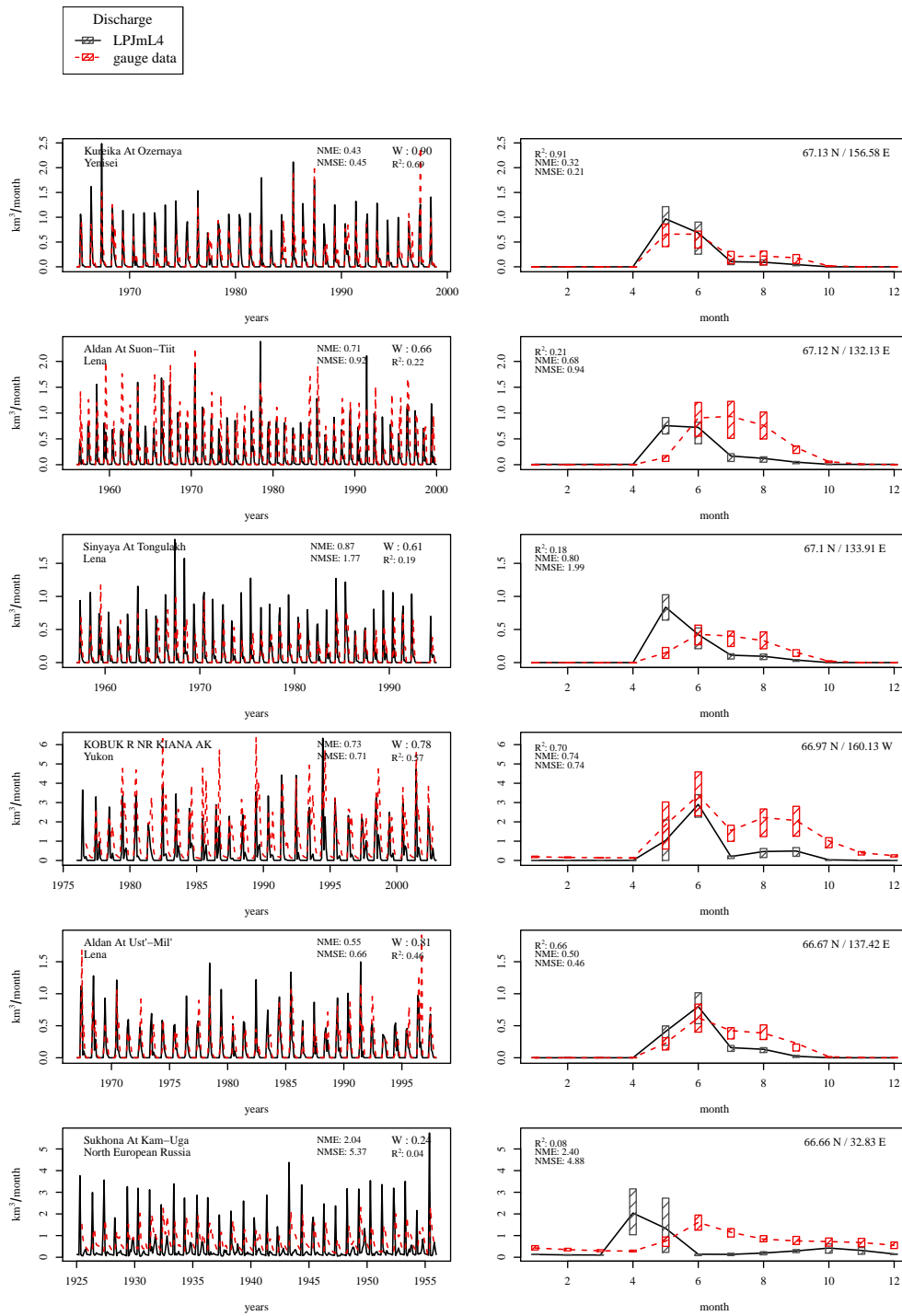


Figure 20. Evaluation of river discharge at gauging stations [4].

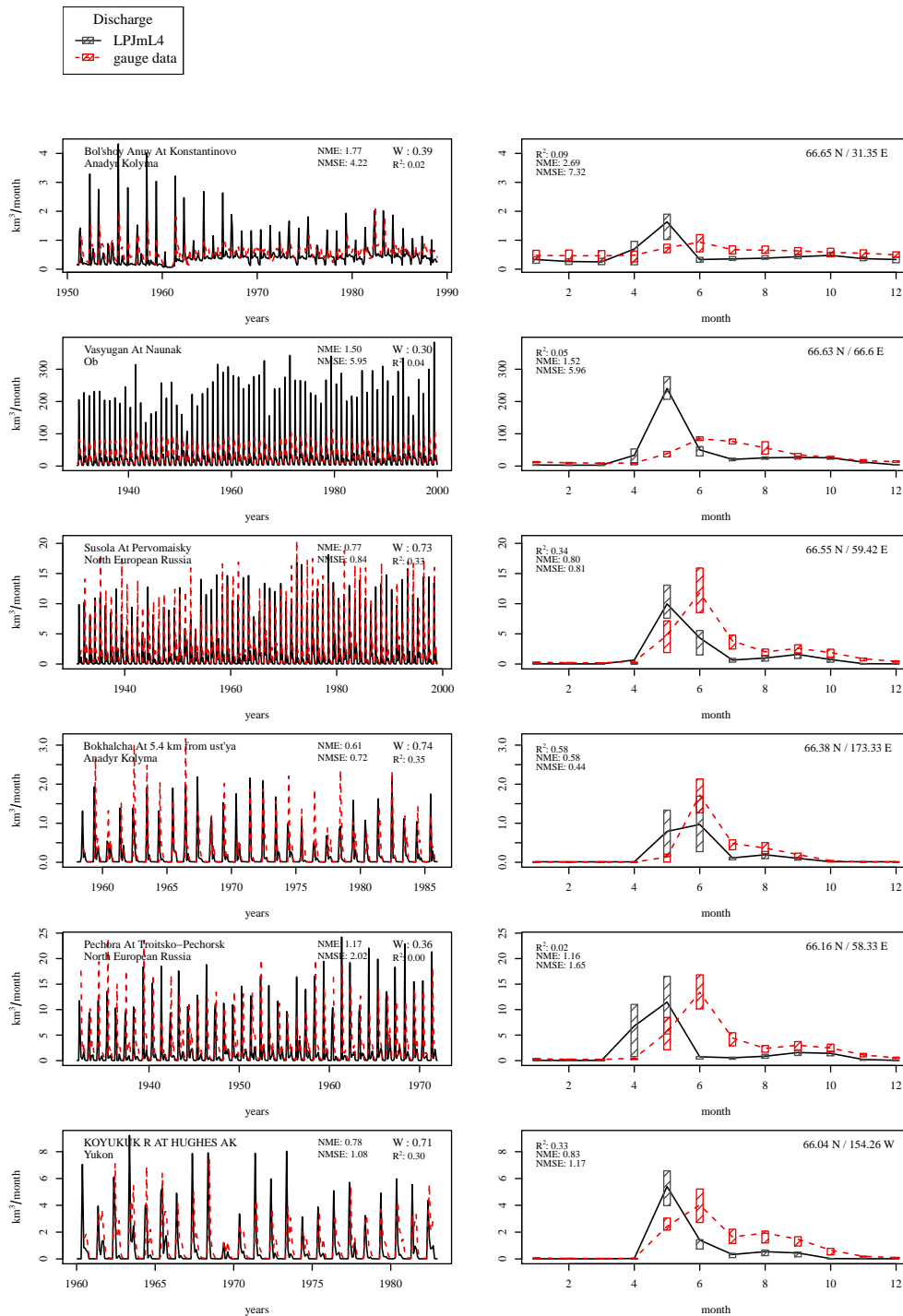


Figure 21. Evaluation of river discharge at gauging stations [5].

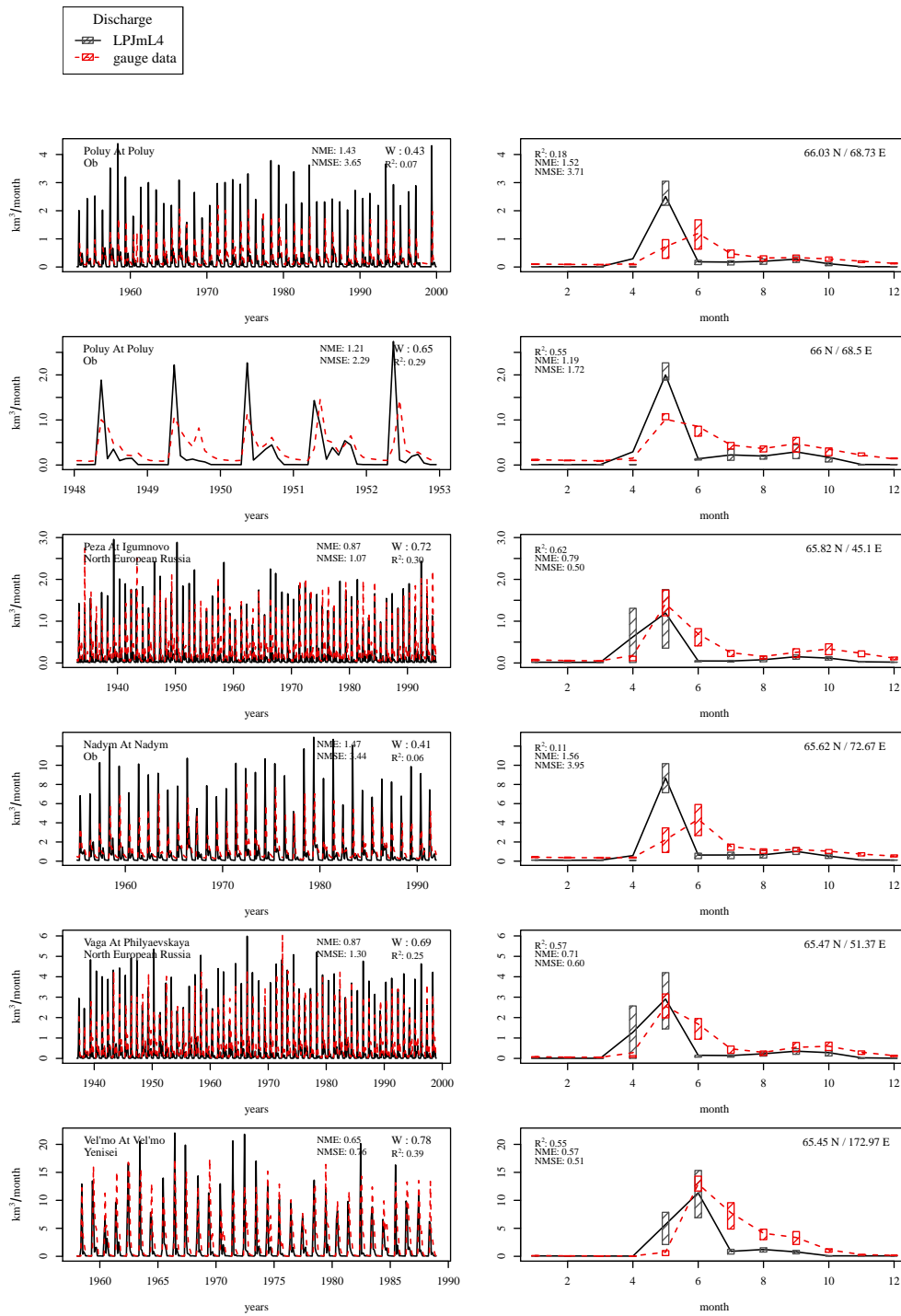


Figure 22. Evaluation of river discharge at gauging stations [6].

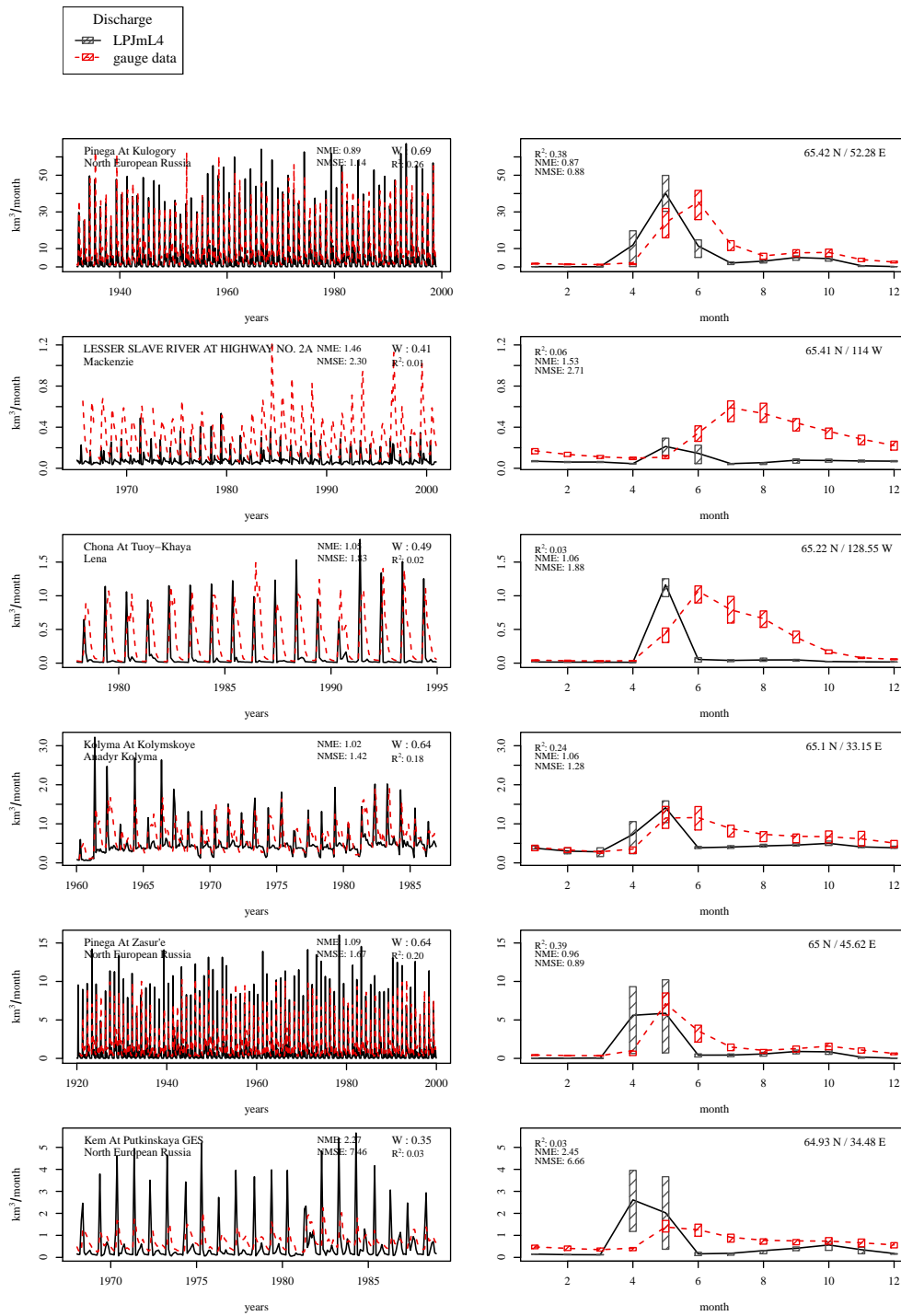


Figure 23. Evaluation of river discharge at gauging stations [7].



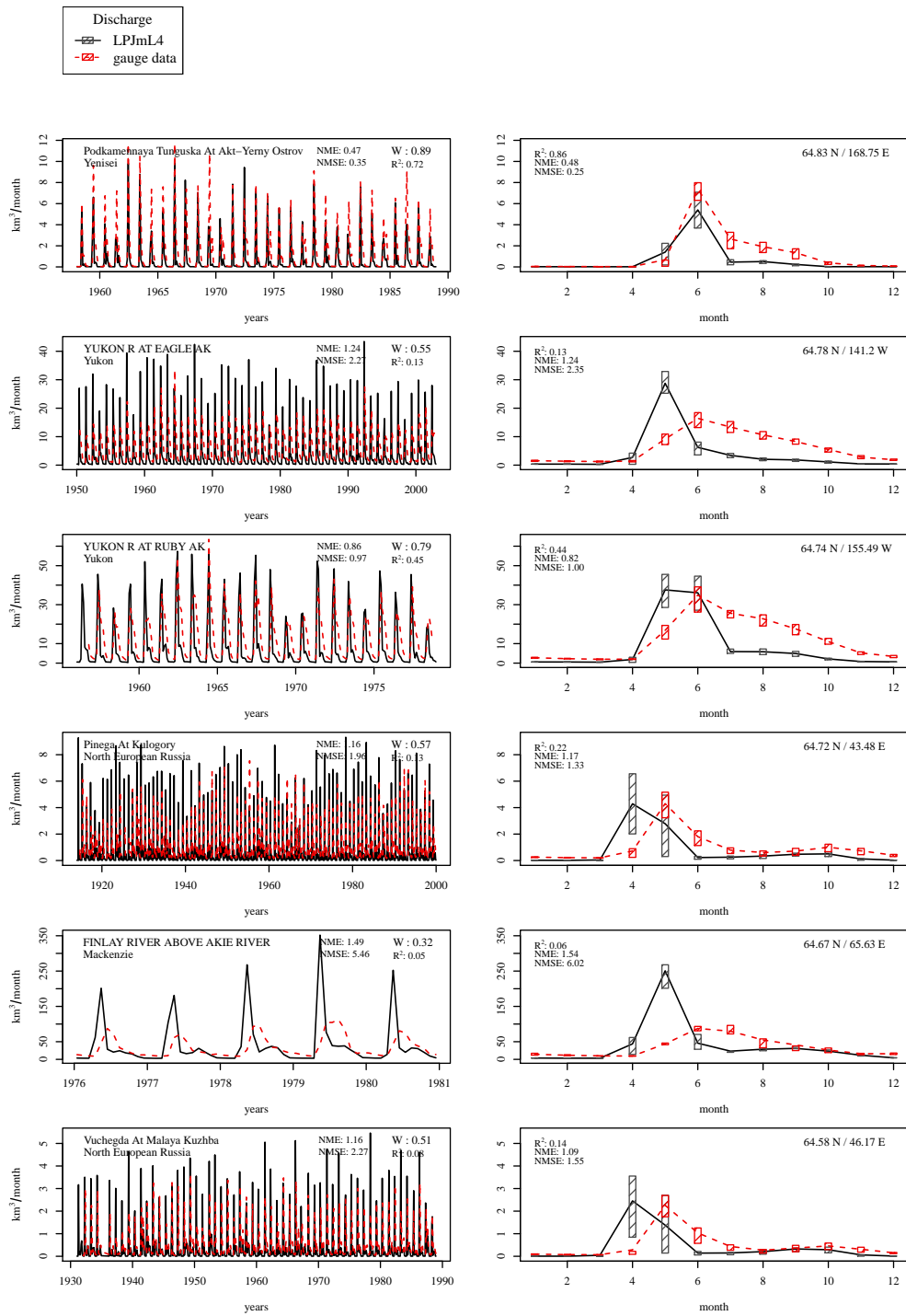


Figure 24. Evaluation of river discharge at gauging stations [8].

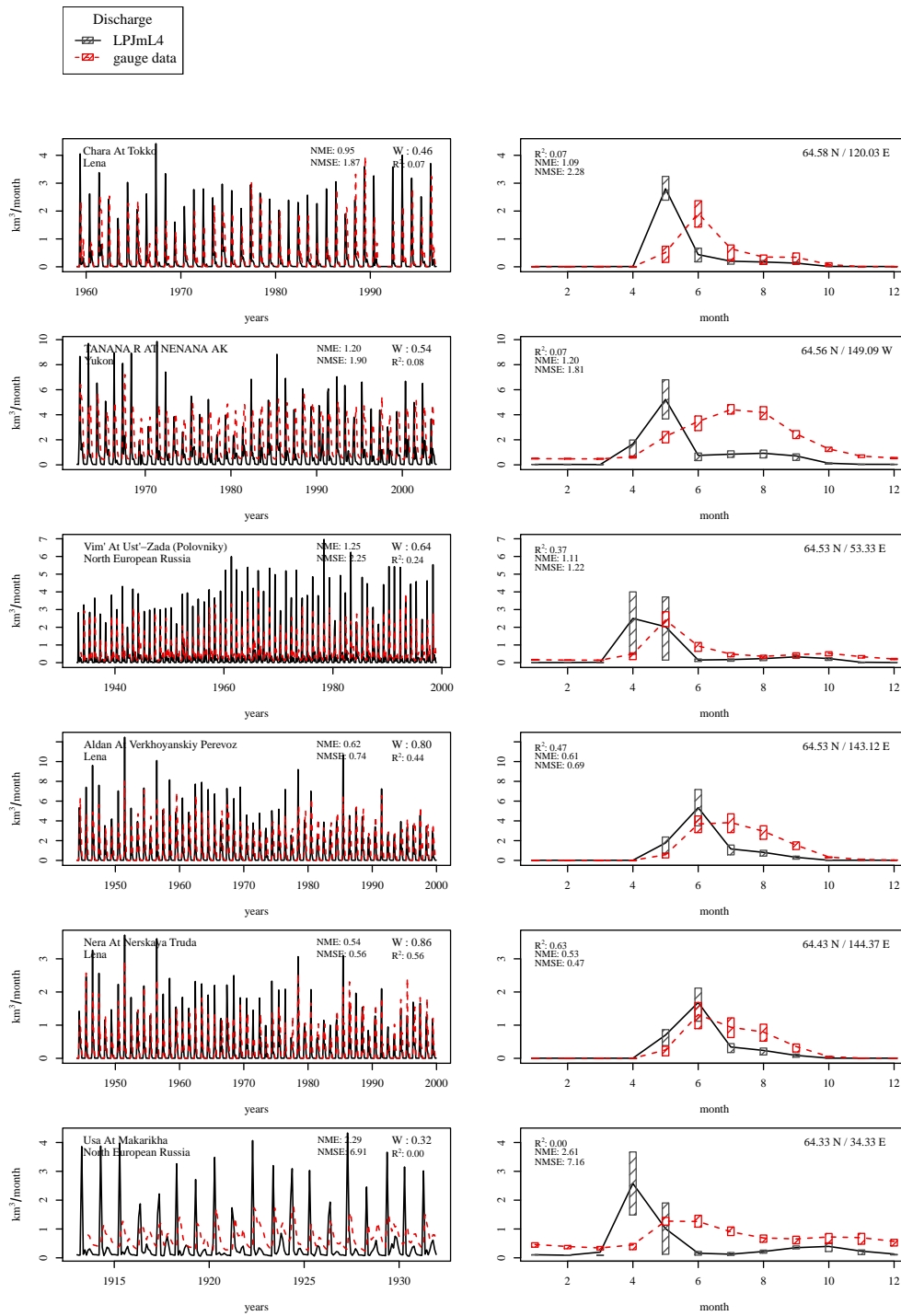


Figure 25. Evaluation of river discharge at gauging stations [9].

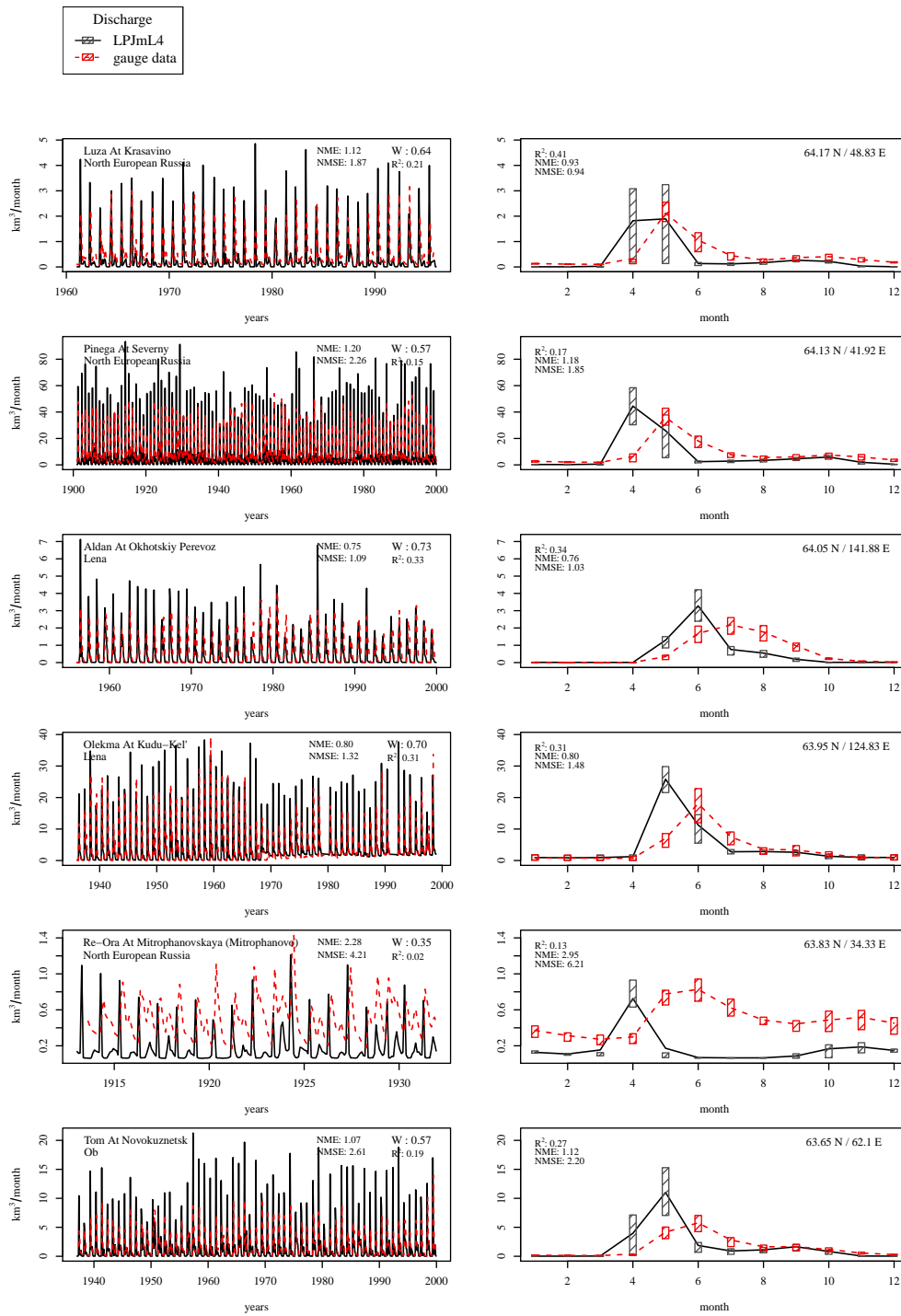


Figure 26. Evaluation of river discharge at gauging stations [10].



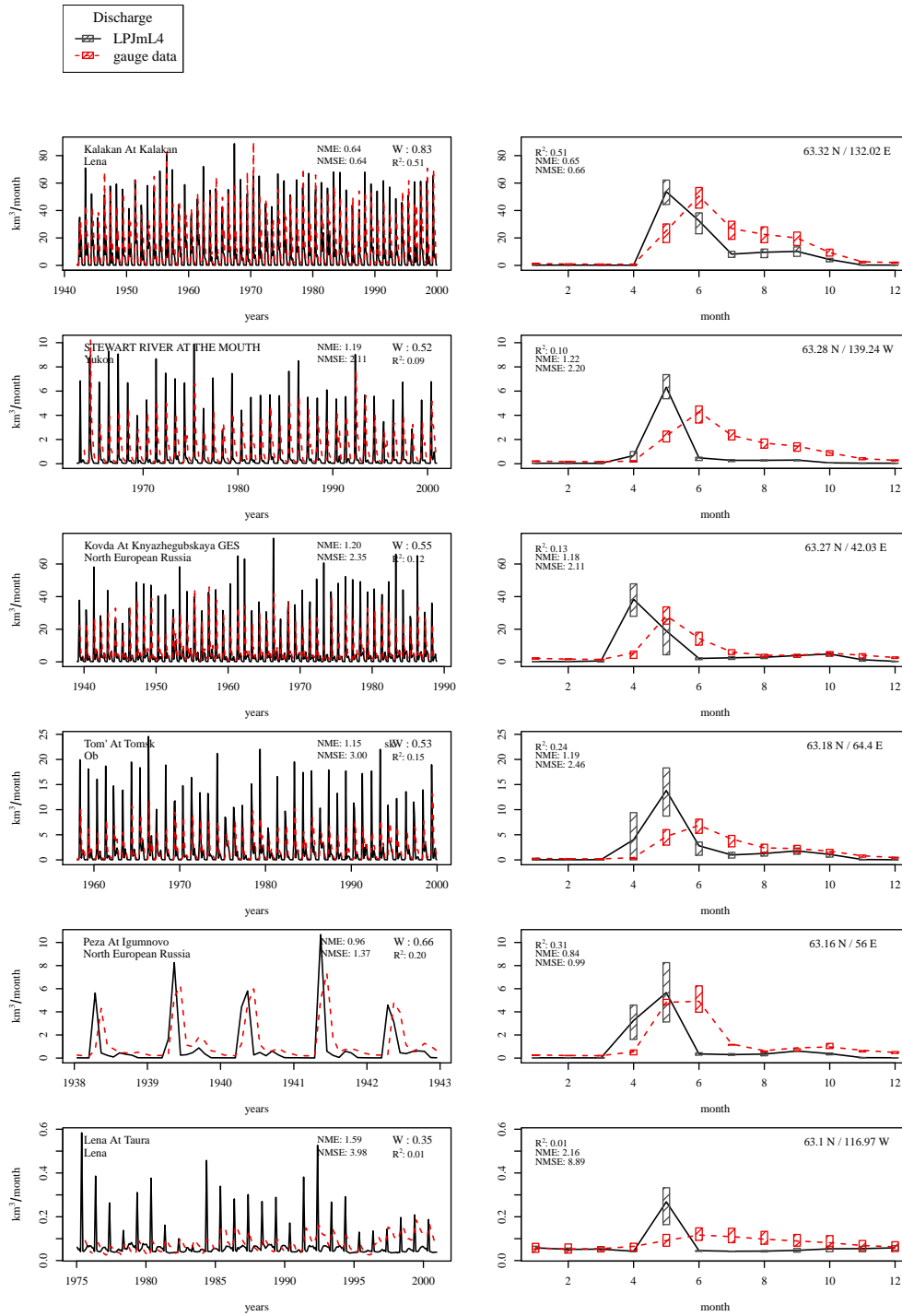


Figure 28. Evaluation of river discharge at gauging stations [12].

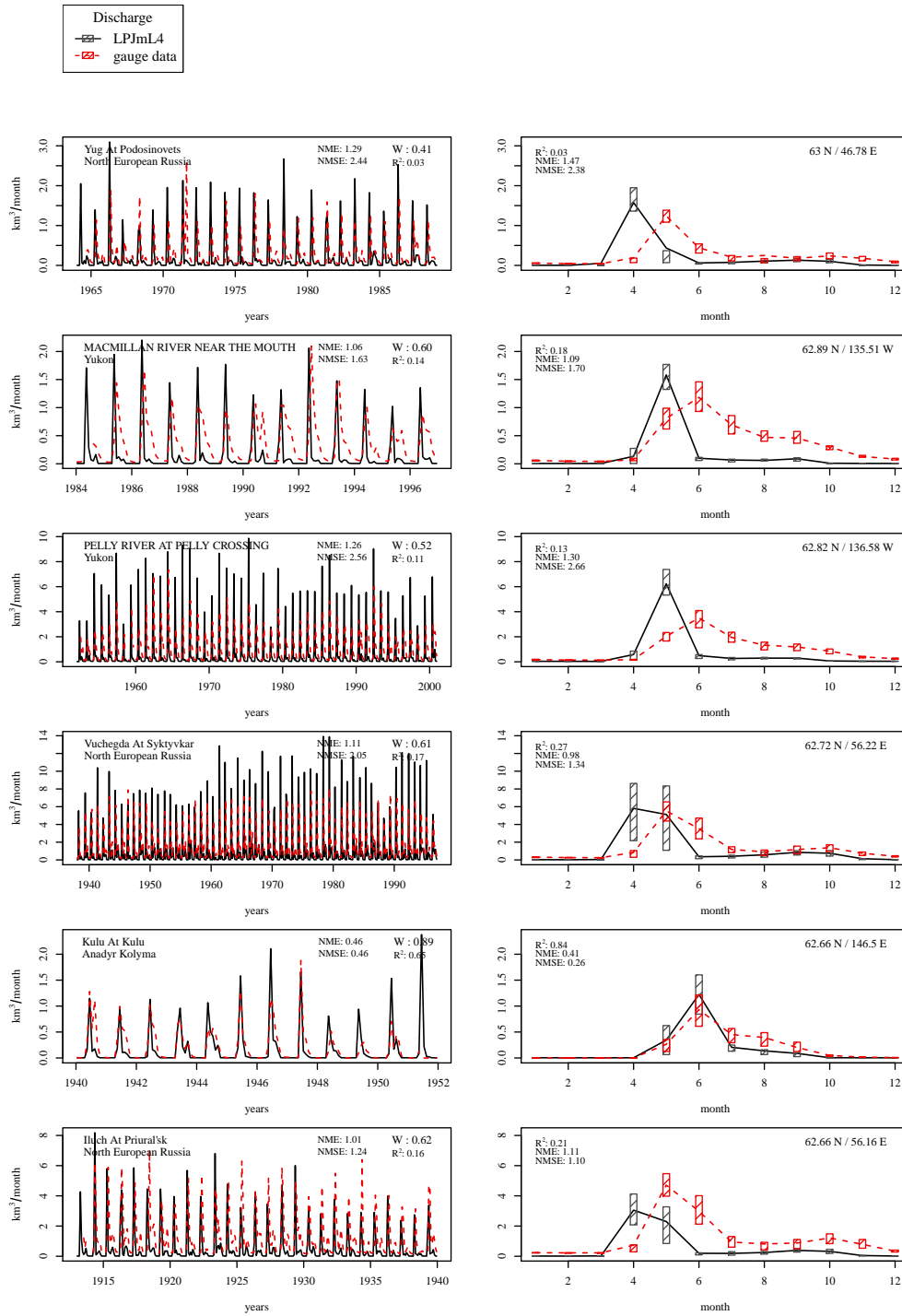


Figure 29. Evaluation of river discharge at gauging stations [13].

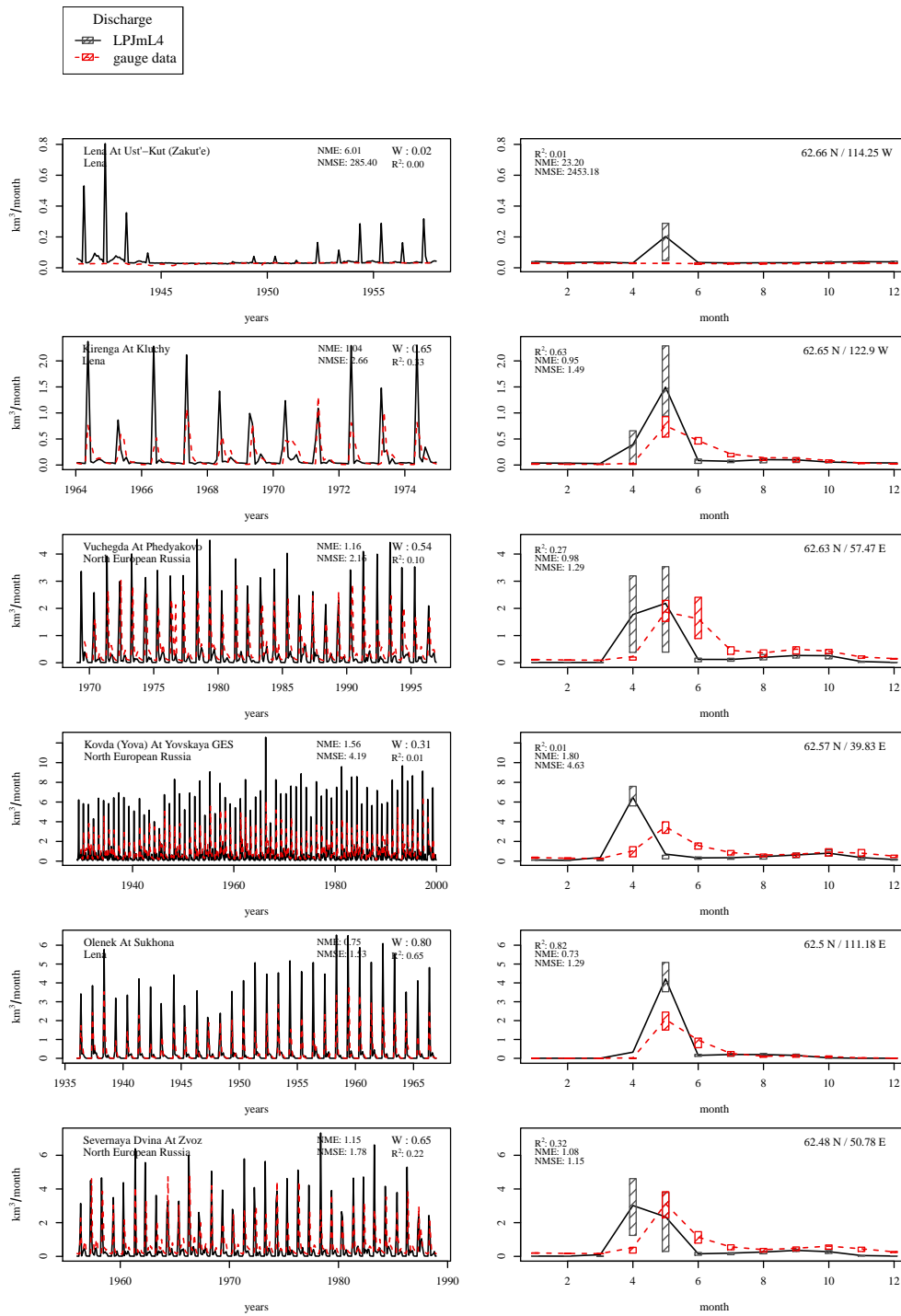


Figure 30. Evaluation of river discharge at gauging stations [14].

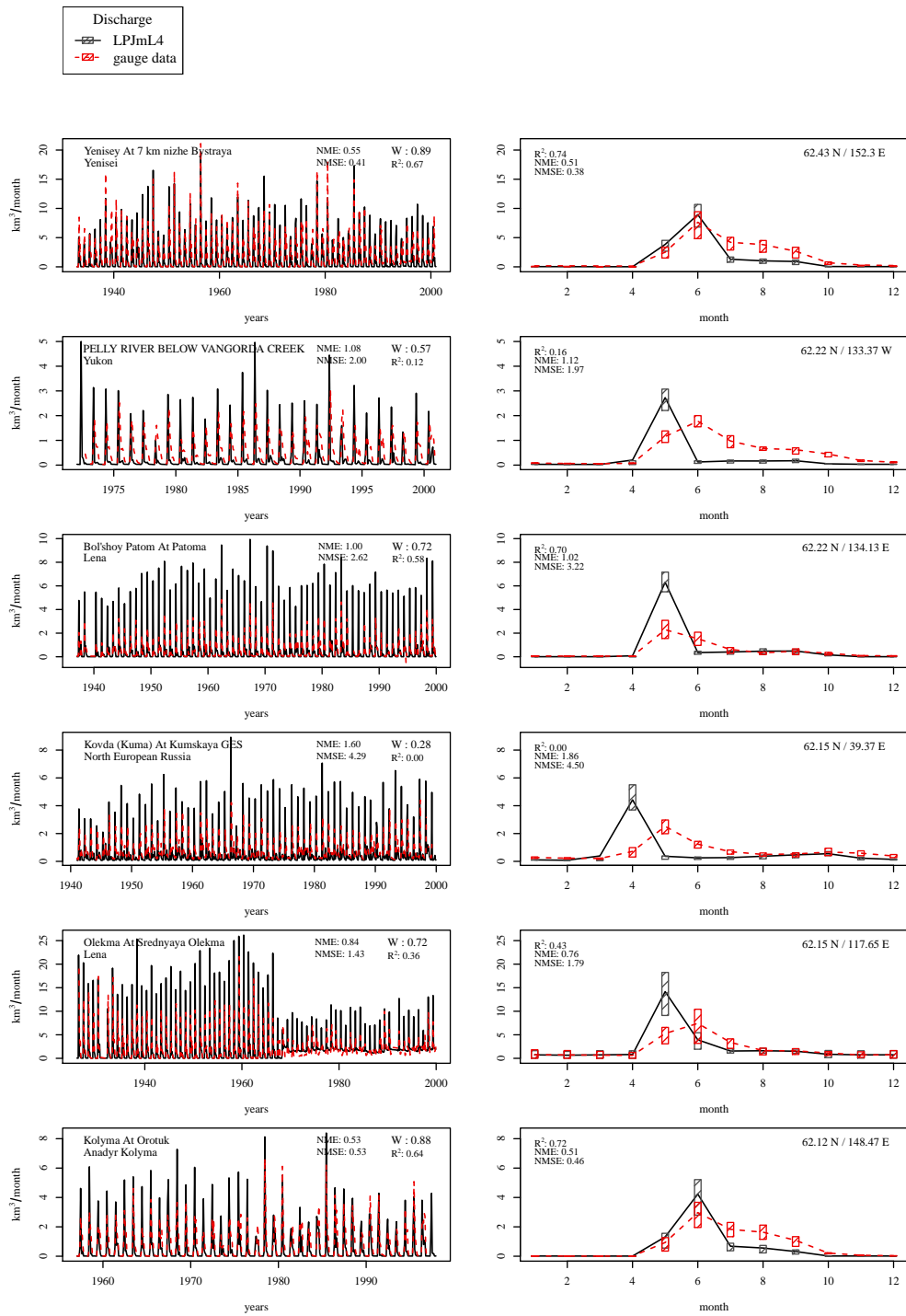


Figure 31. Evaluation of river discharge at gauging stations [15].



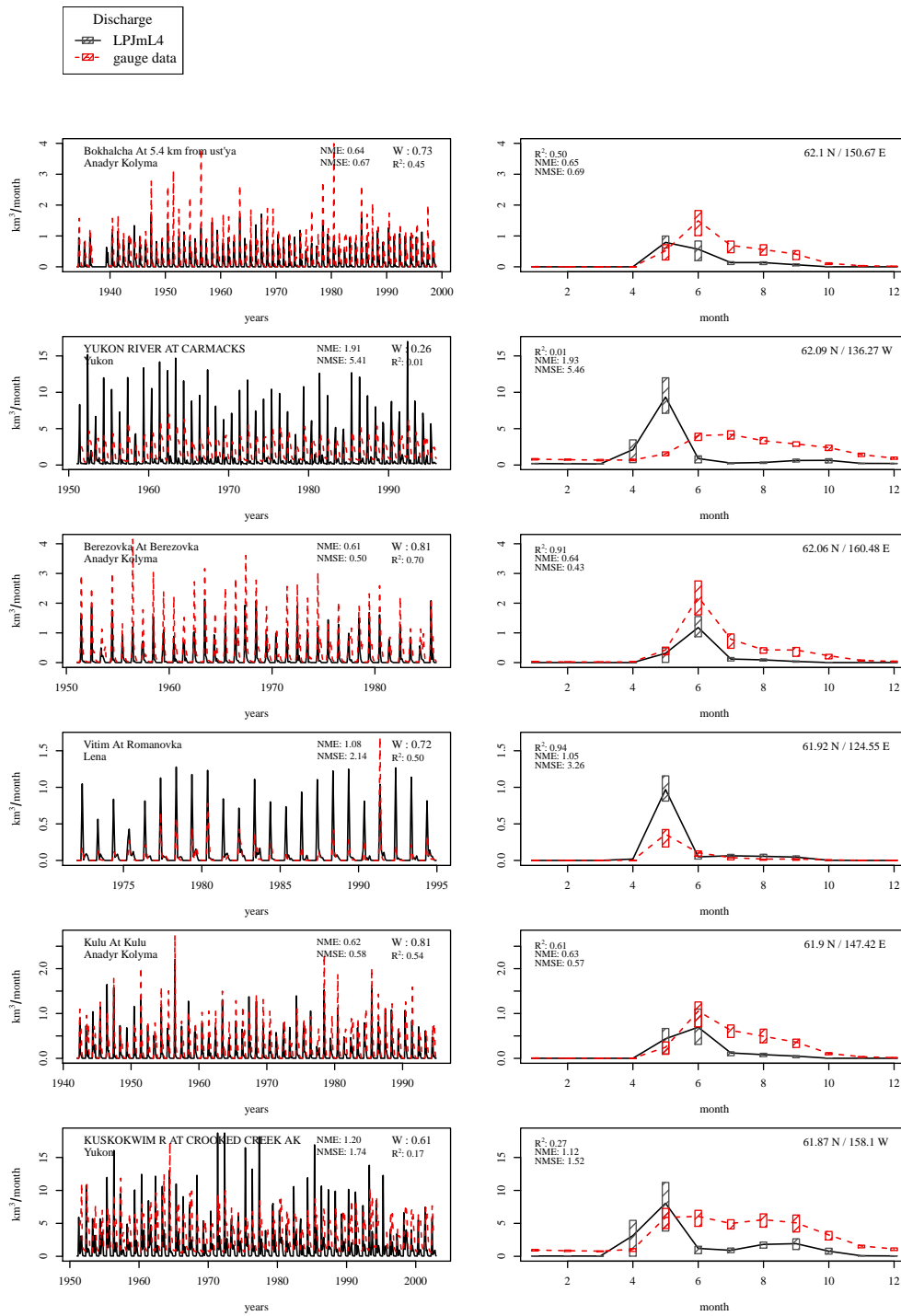


Figure 32. Evaluation of river discharge at gauging stations [16].

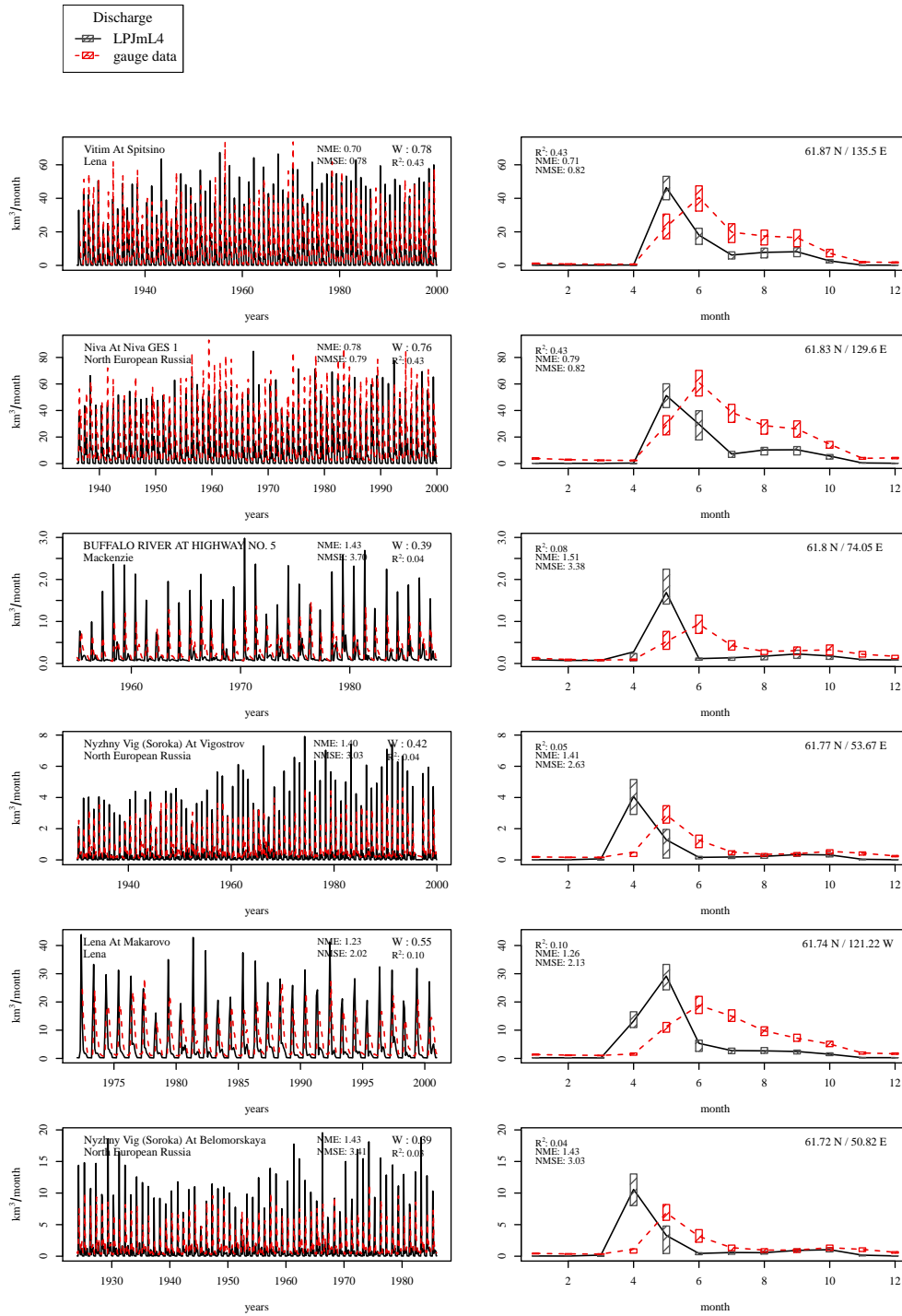


Figure 33. Evaluation of river discharge at gauging stations [17].

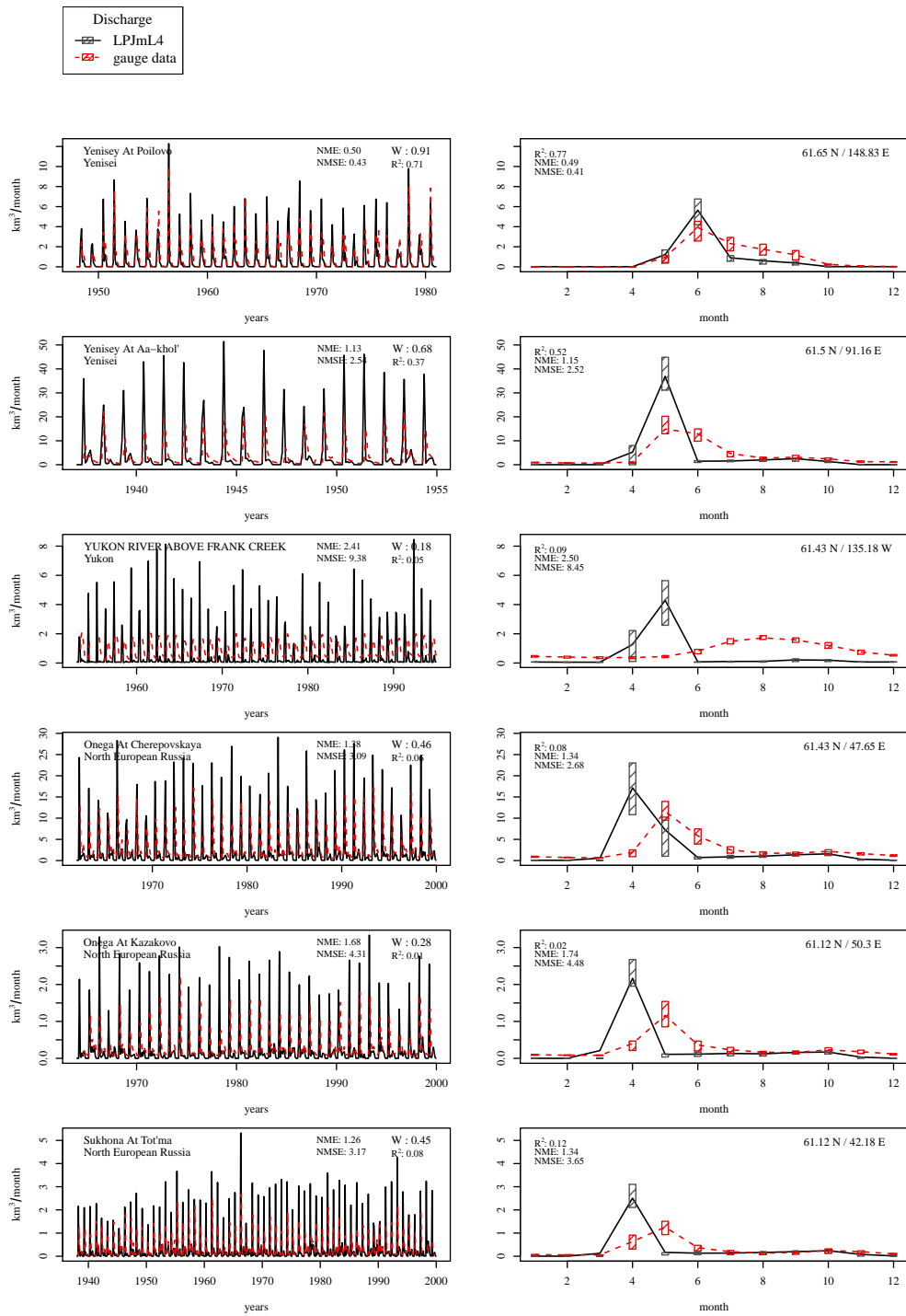


Figure 34. Evaluation of river discharge at gauging stations [18].

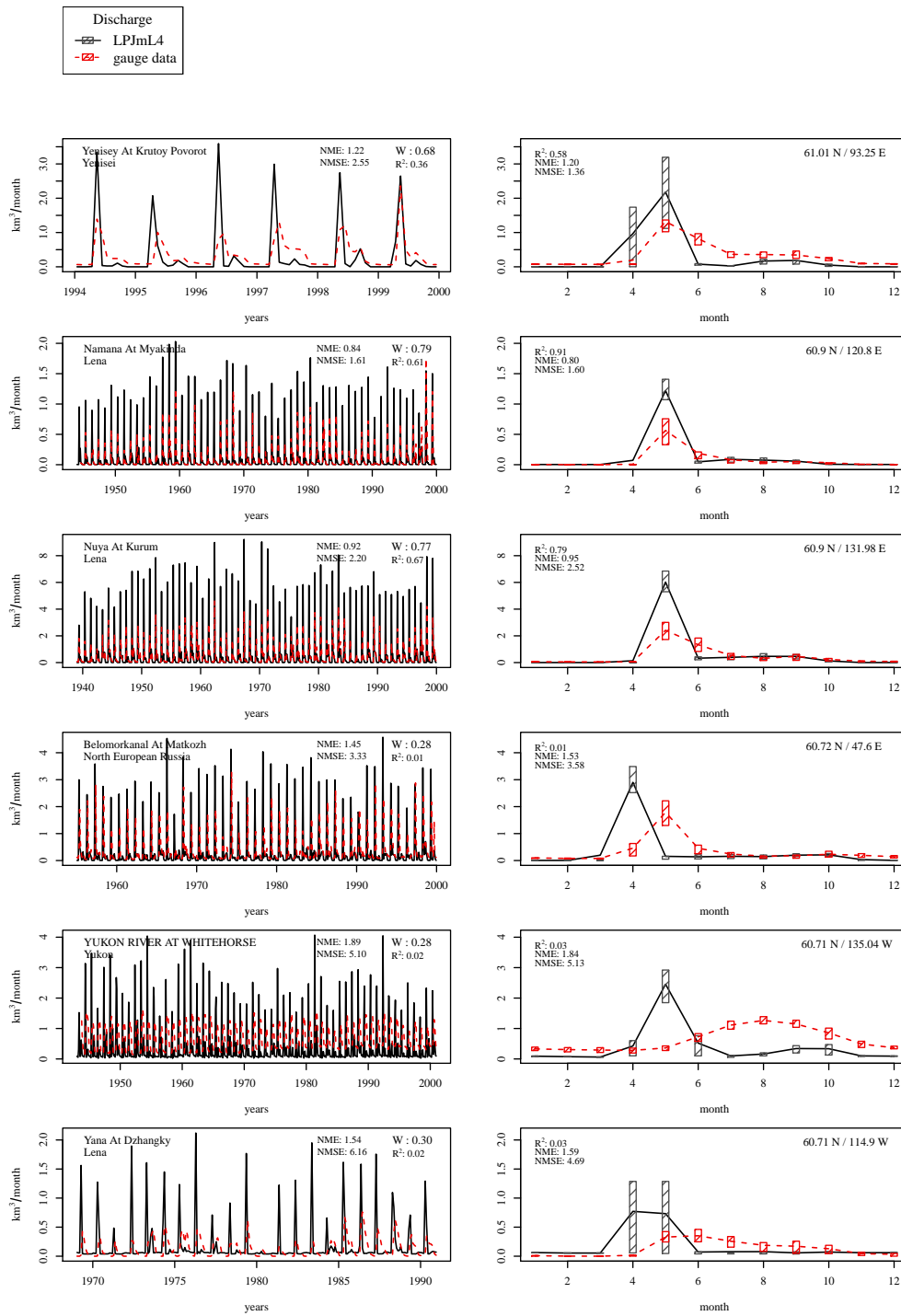


Figure 35. Evaluation of river discharge at gauging stations [19].

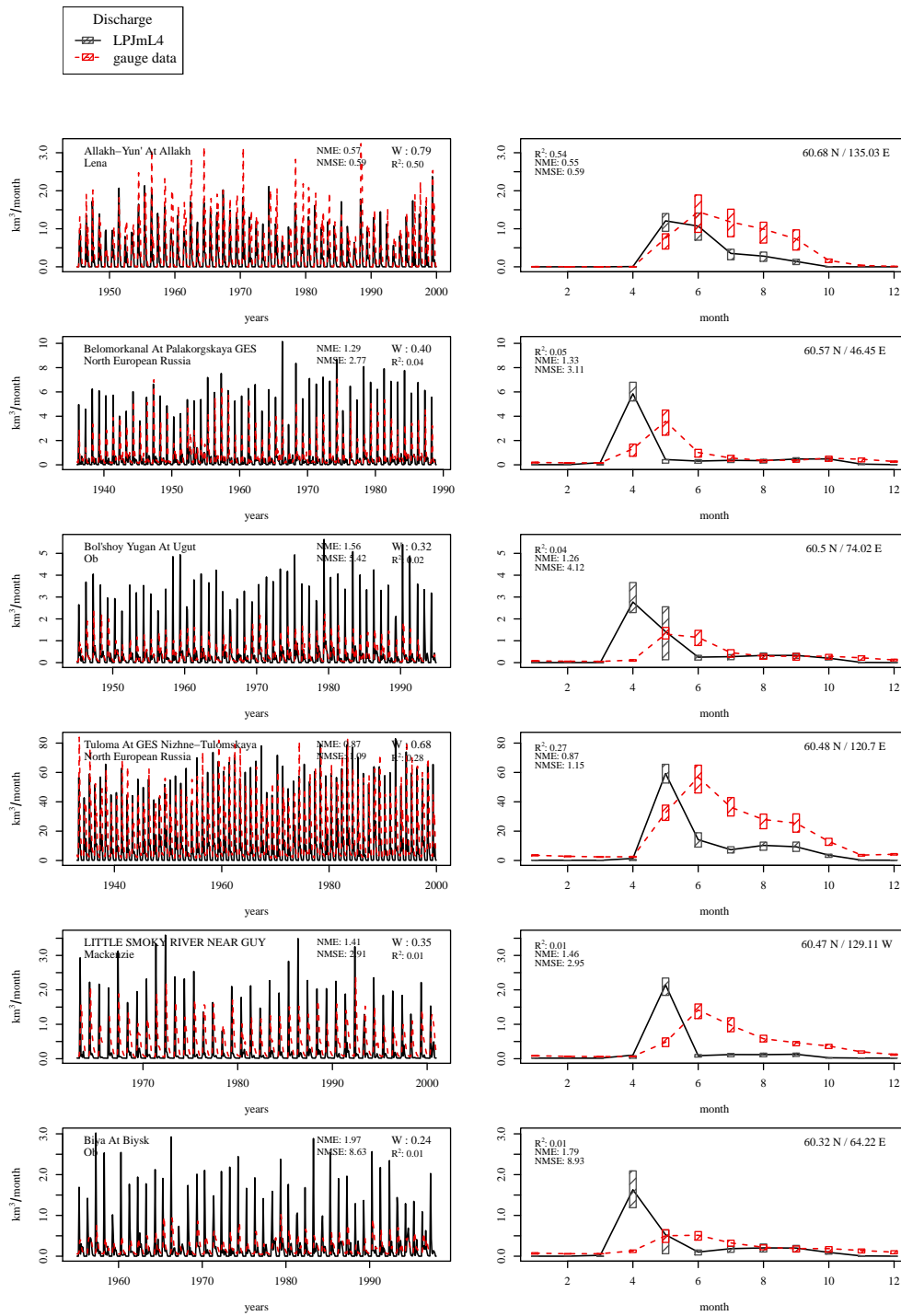


Figure 36. Evaluation of river discharge at gauging stations [20].

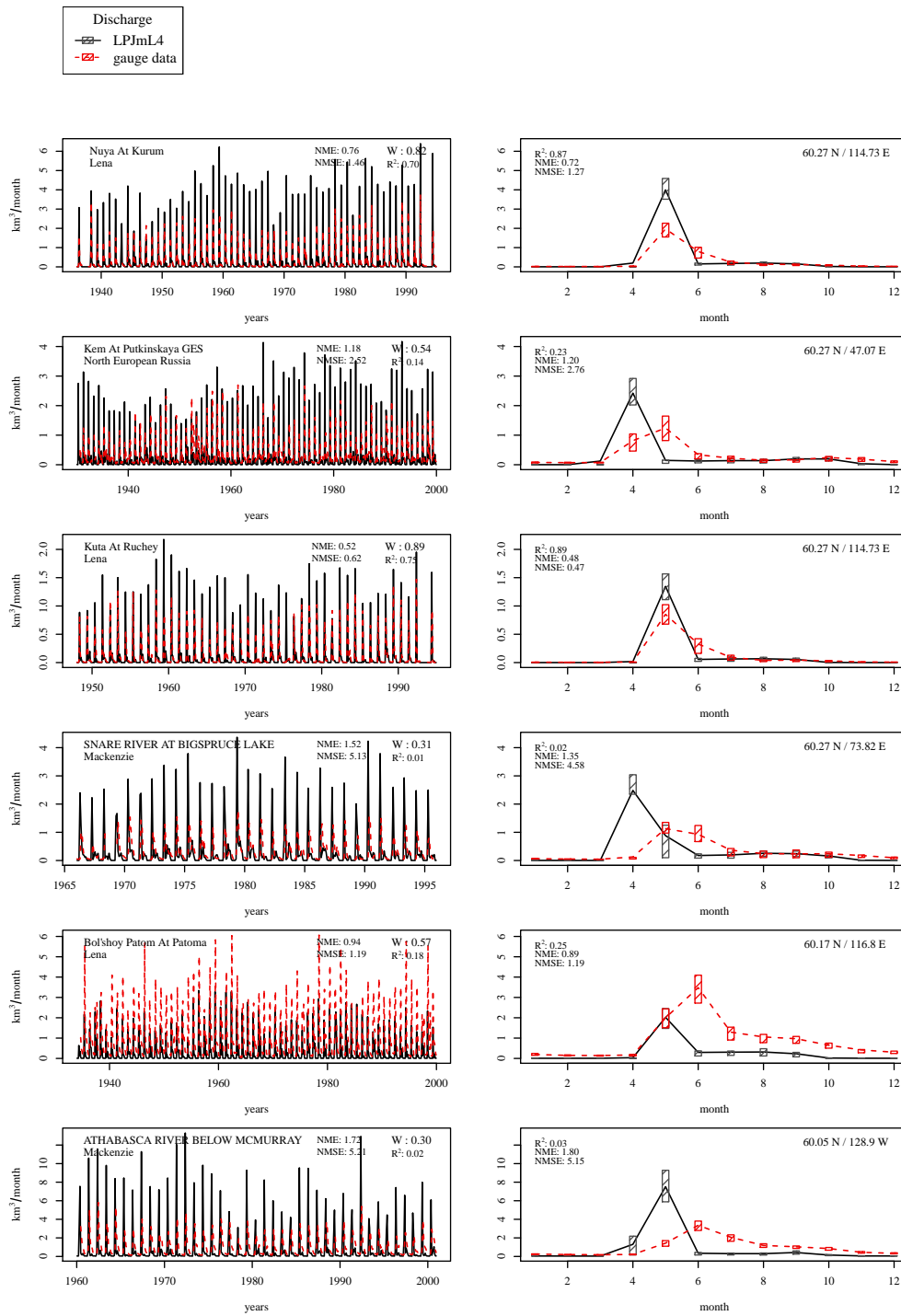


Figure 37. Evaluation of river discharge at gauging stations [21].

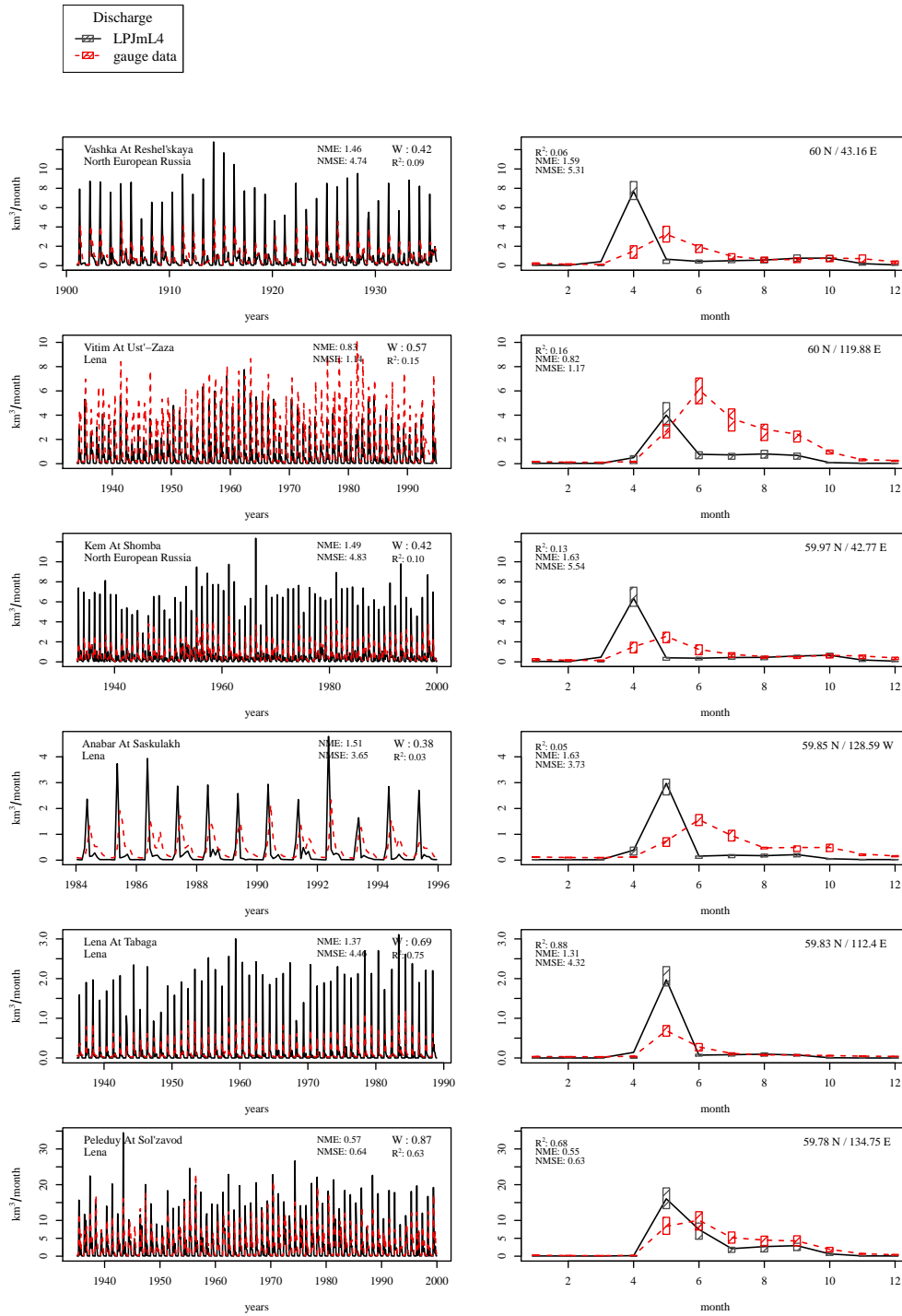


Figure 38. Evaluation of river discharge at gauging stations [22].

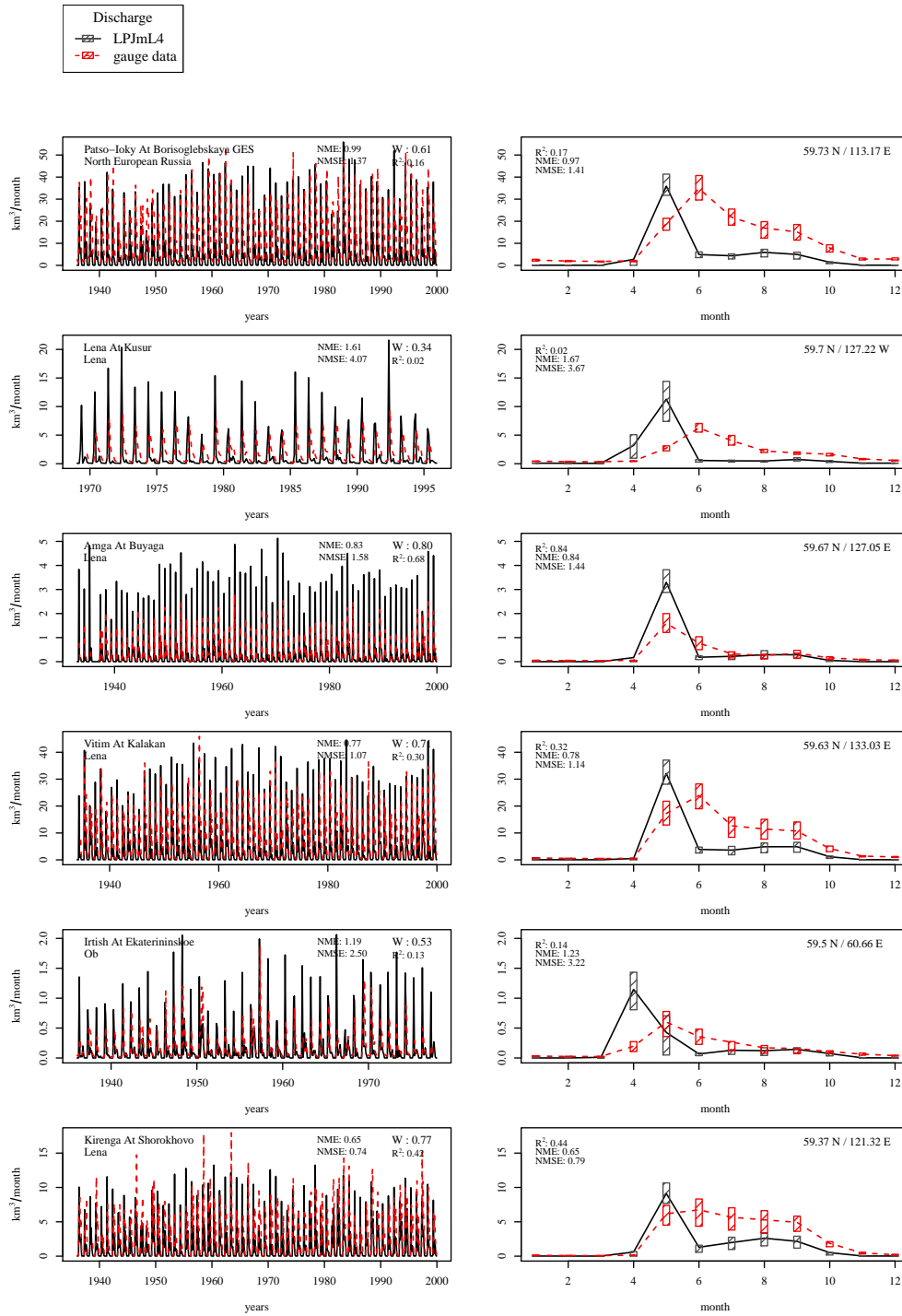


Figure 39. Evaluation of river discharge at gauging stations [23].



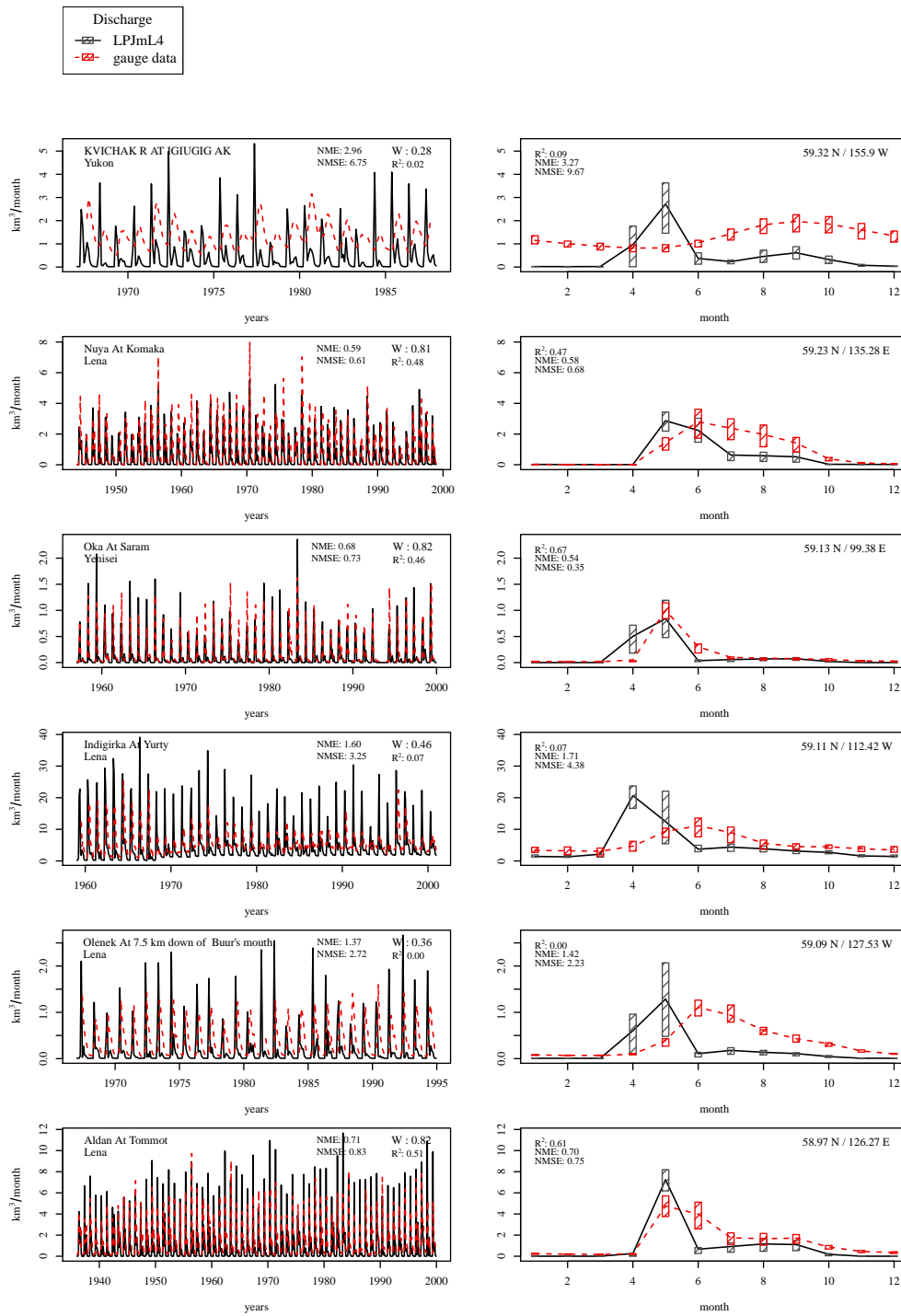


Figure 40. Evaluation of river discharge at gauging stations [24].

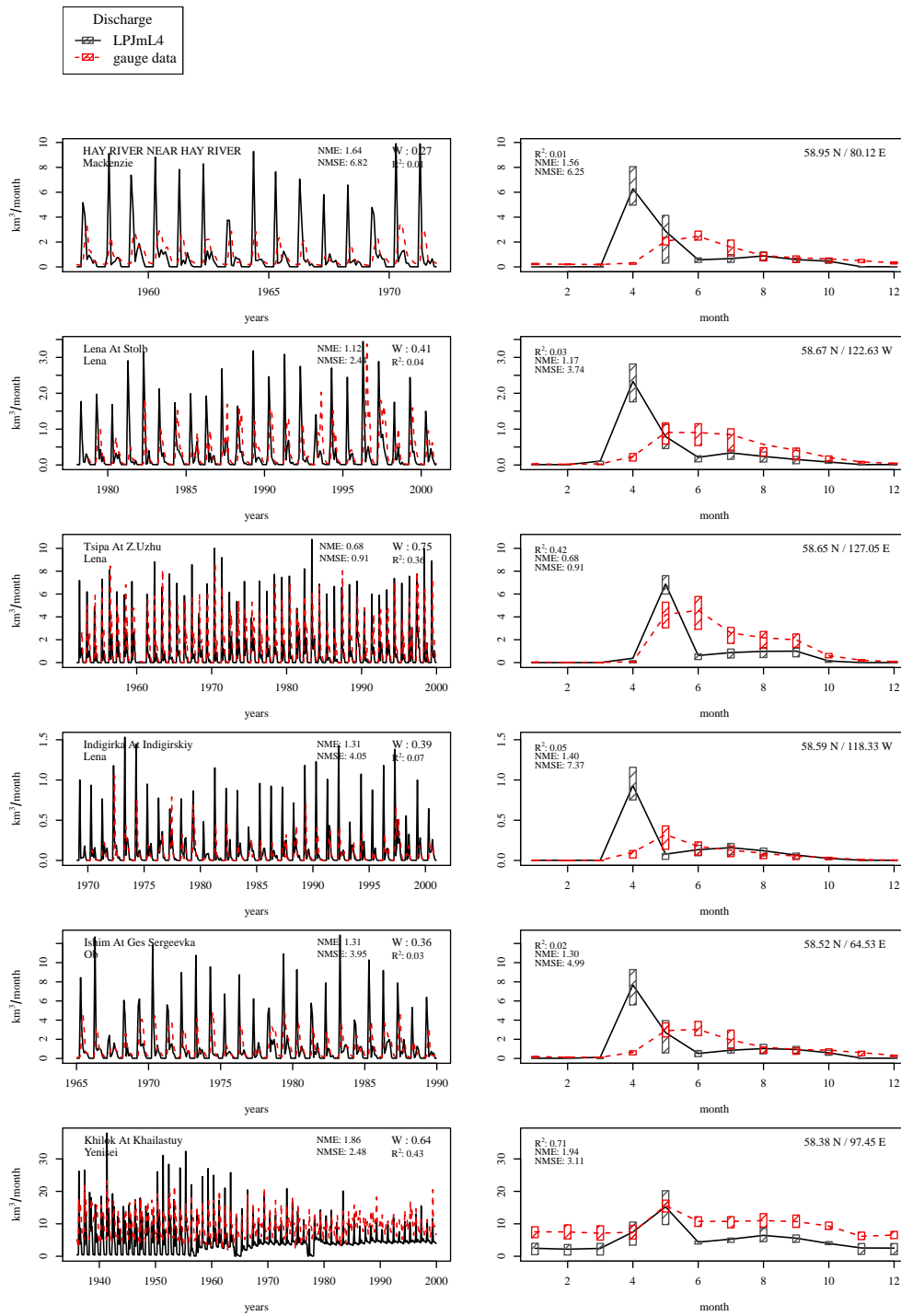


Figure 41. Evaluation of river discharge at gauging stations [25].

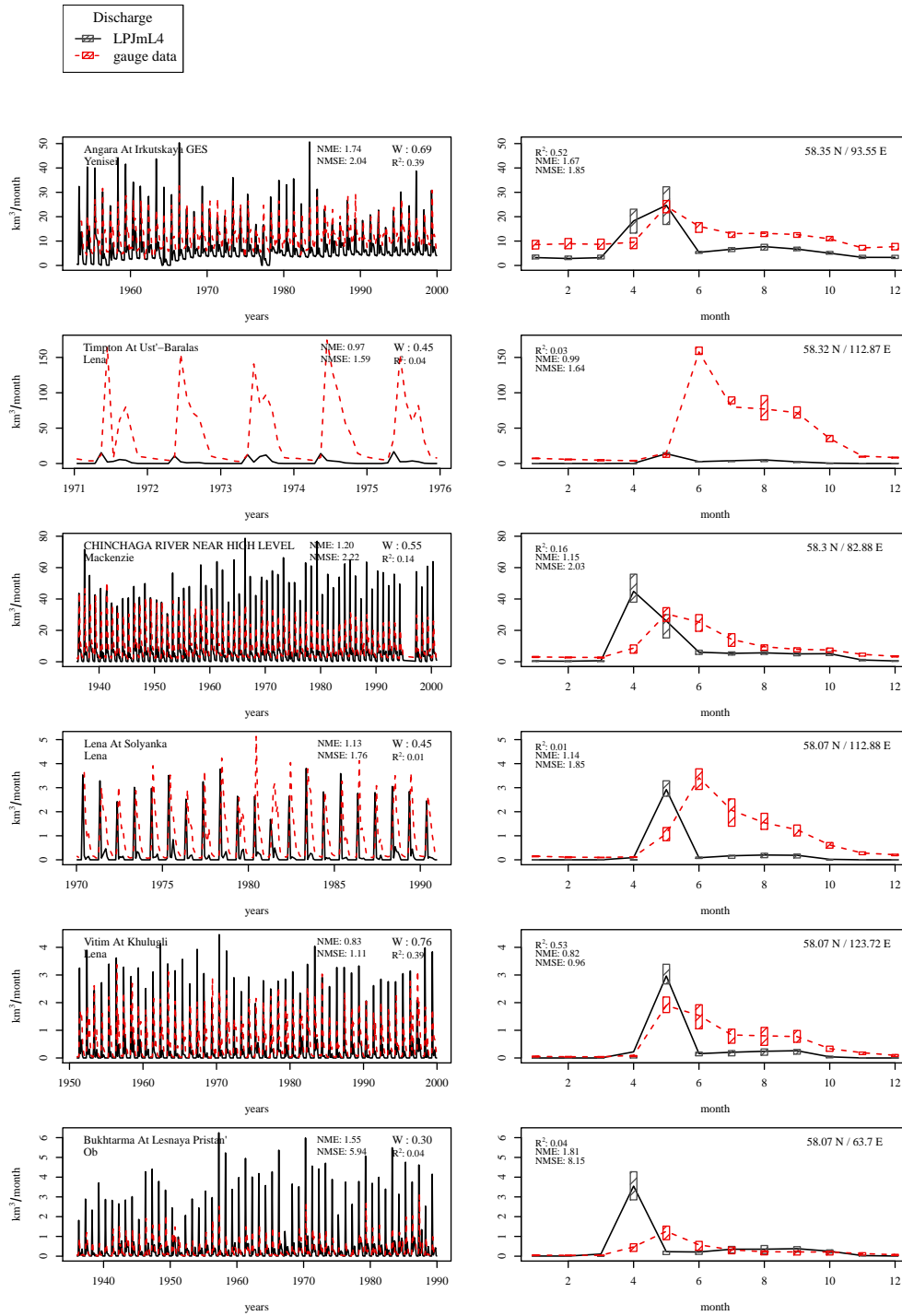


Figure 42. Evaluation of river discharge at gauging stations [26].

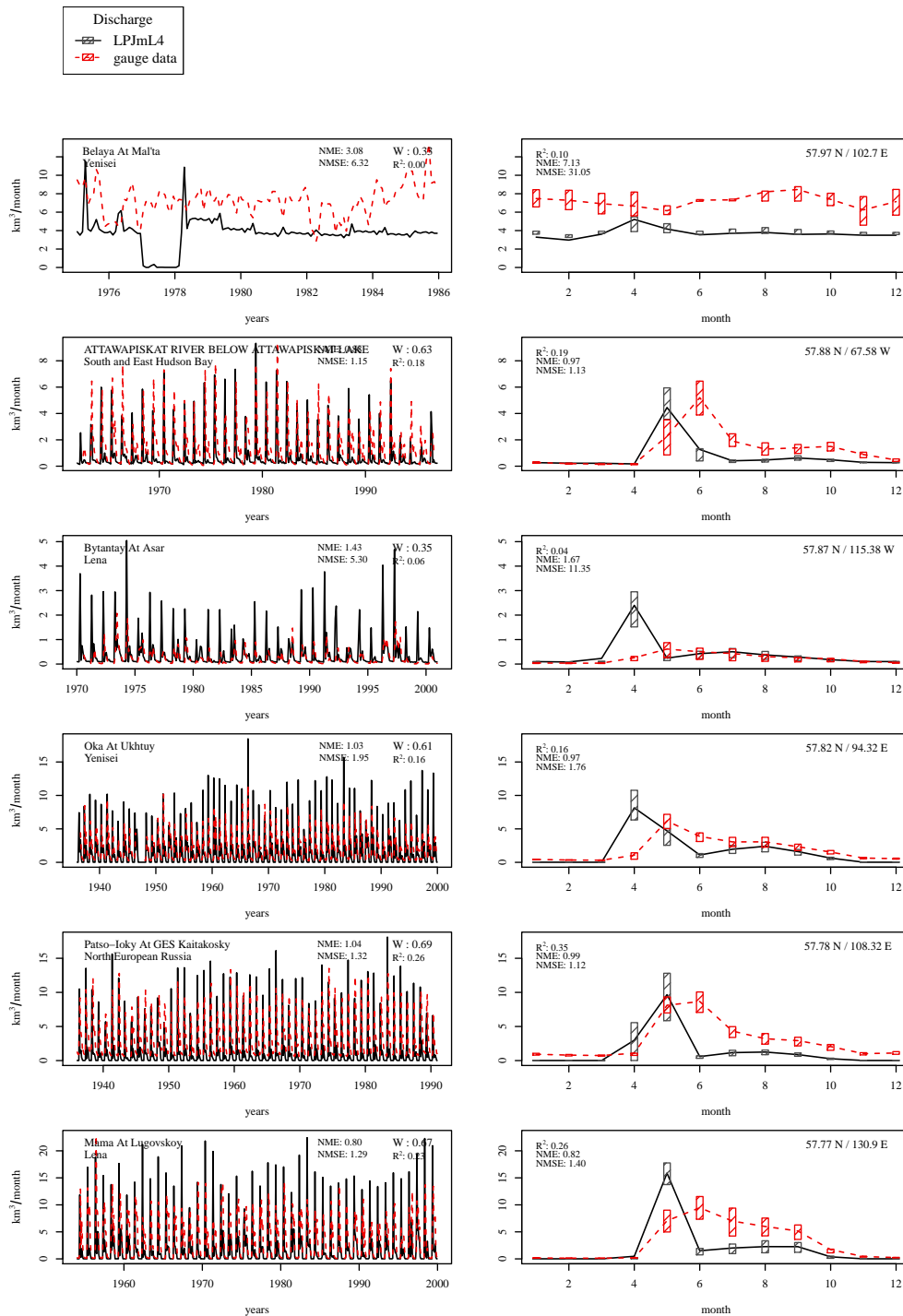


Figure 43. Evaluation of river discharge at gauging stations [27].

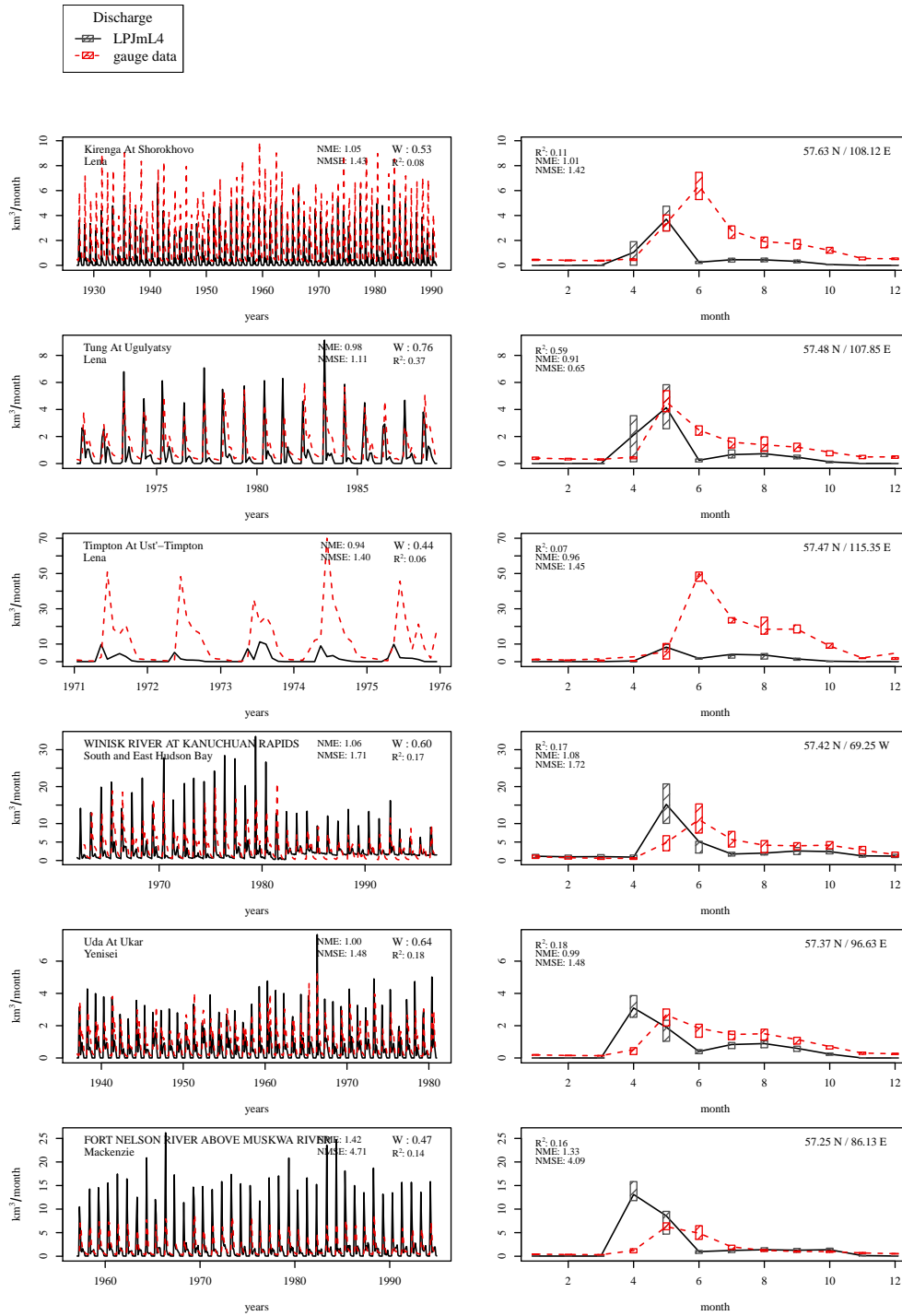


Figure 44. Evaluation of river discharge at gauging stations [28].

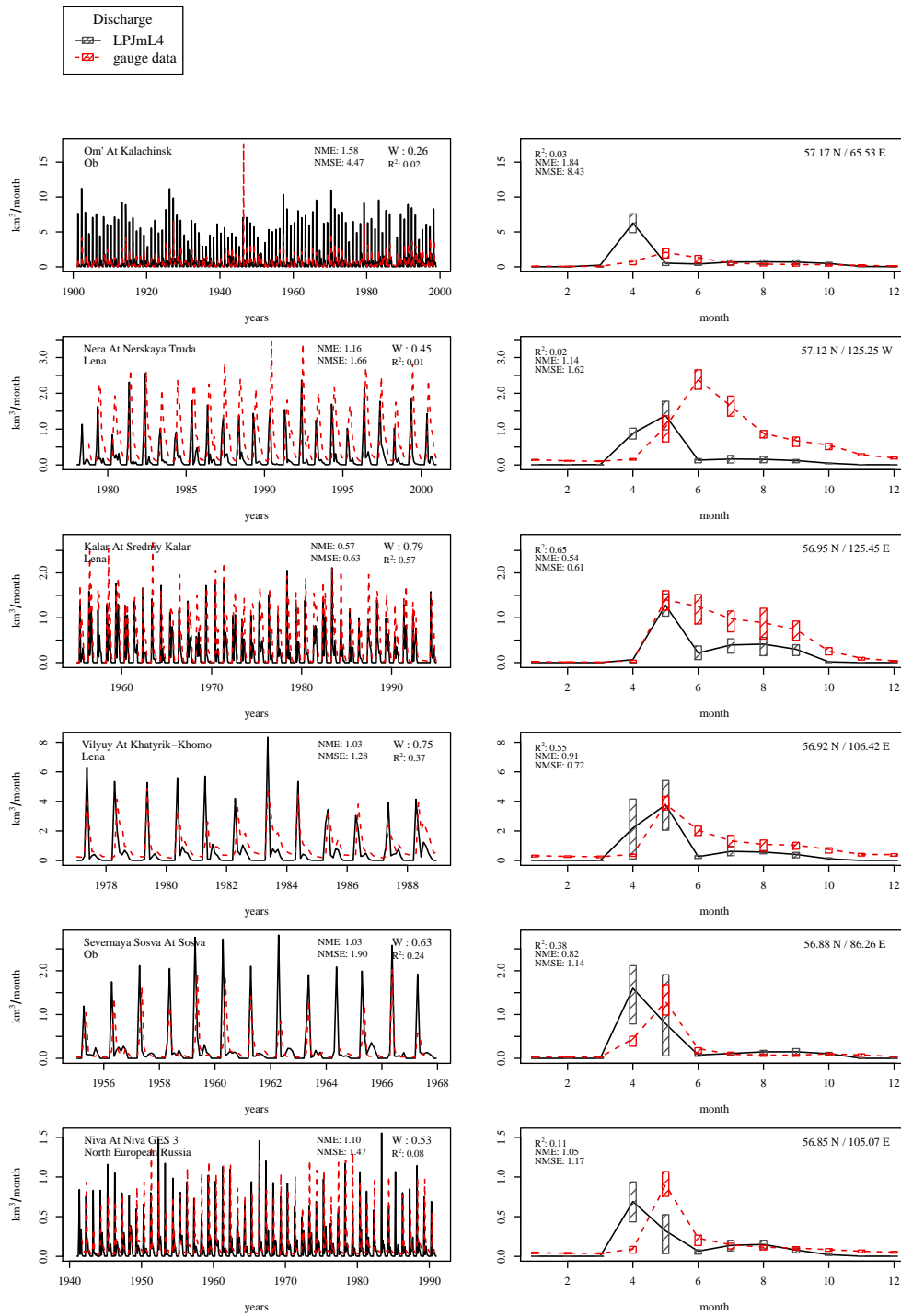


Figure 45. Evaluation of river discharge at gauging stations [29].

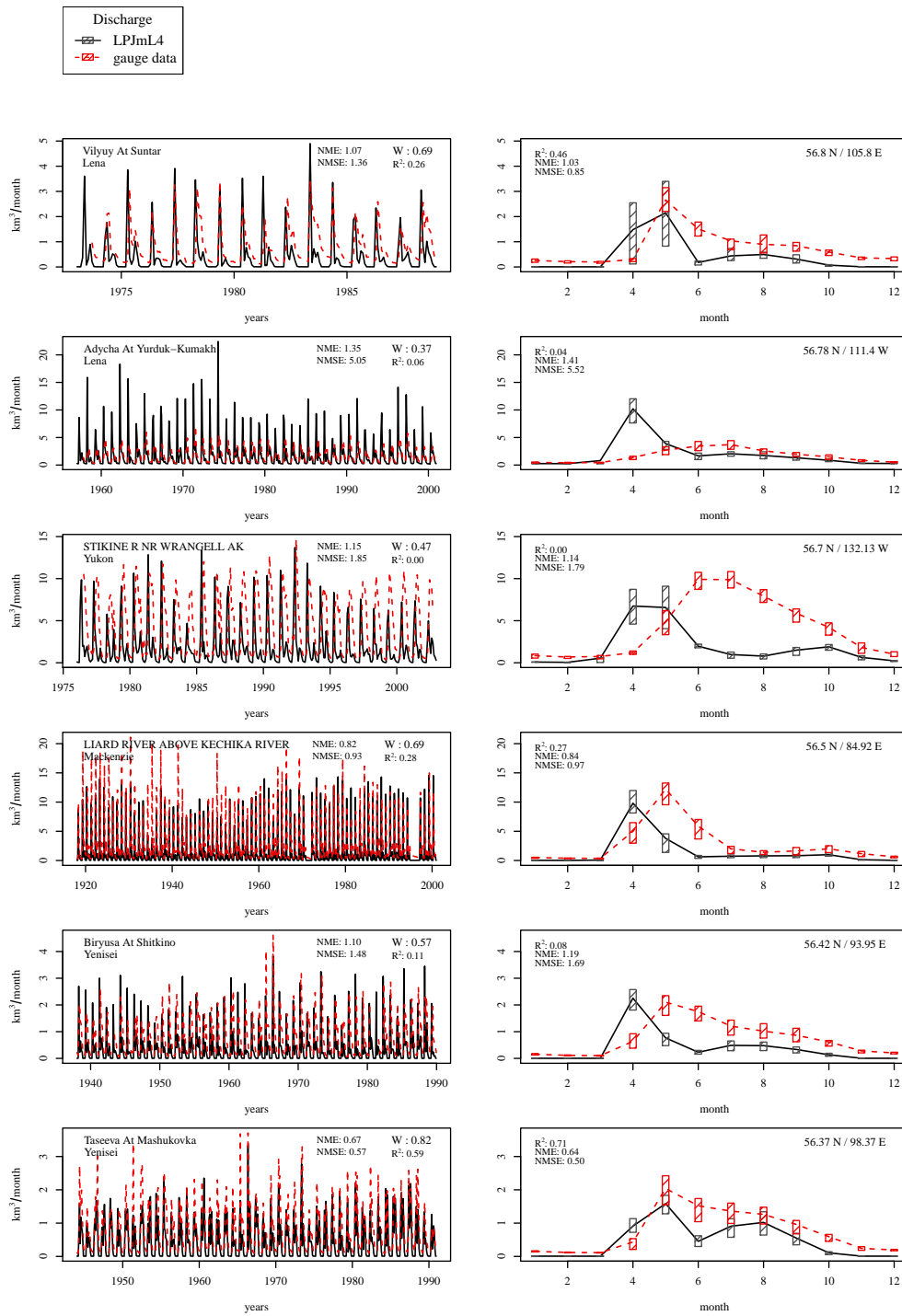


Figure 46. Evaluation of river discharge at gauging stations [30].

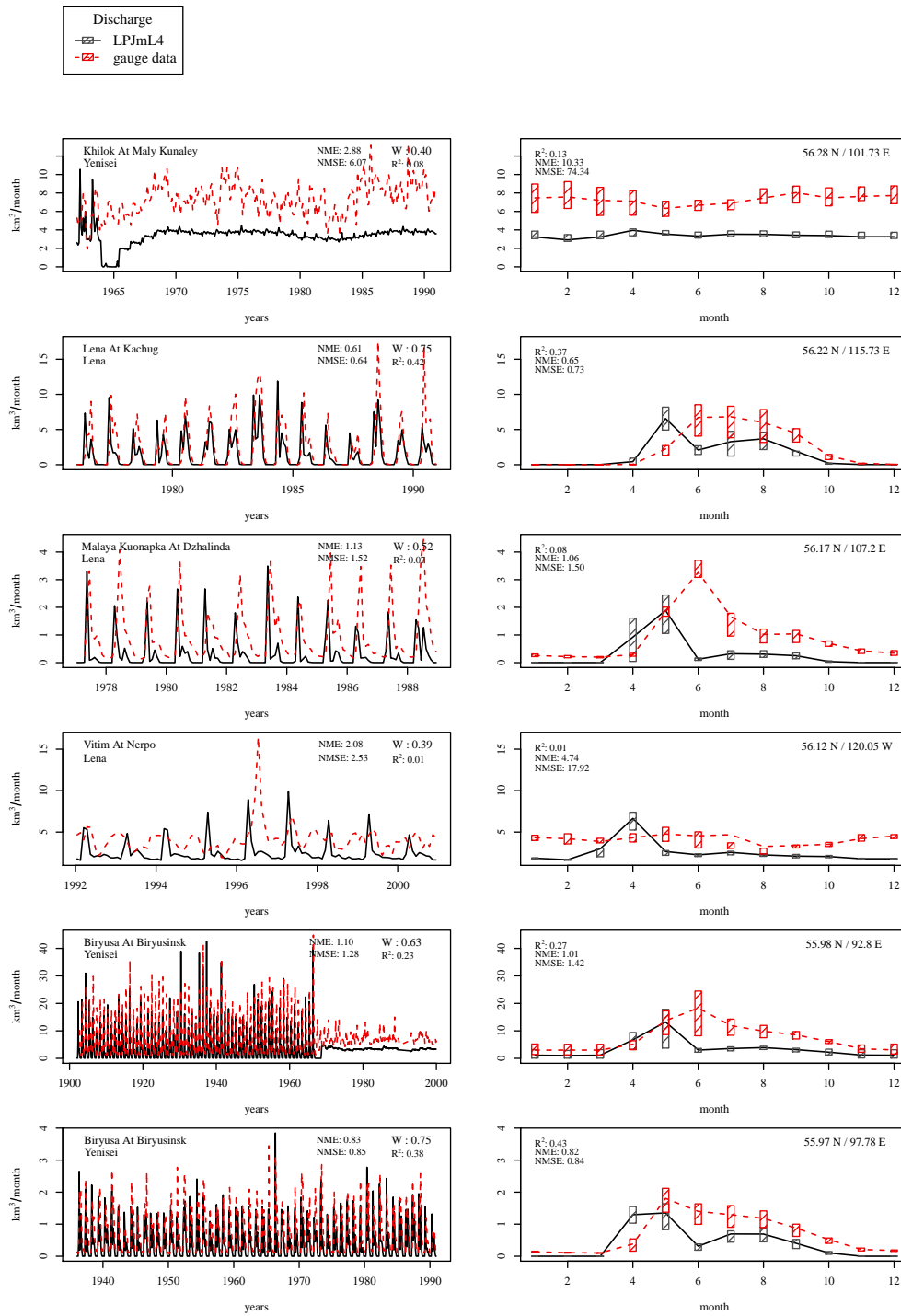


Figure 47. Evaluation of river discharge at gauging stations [31].



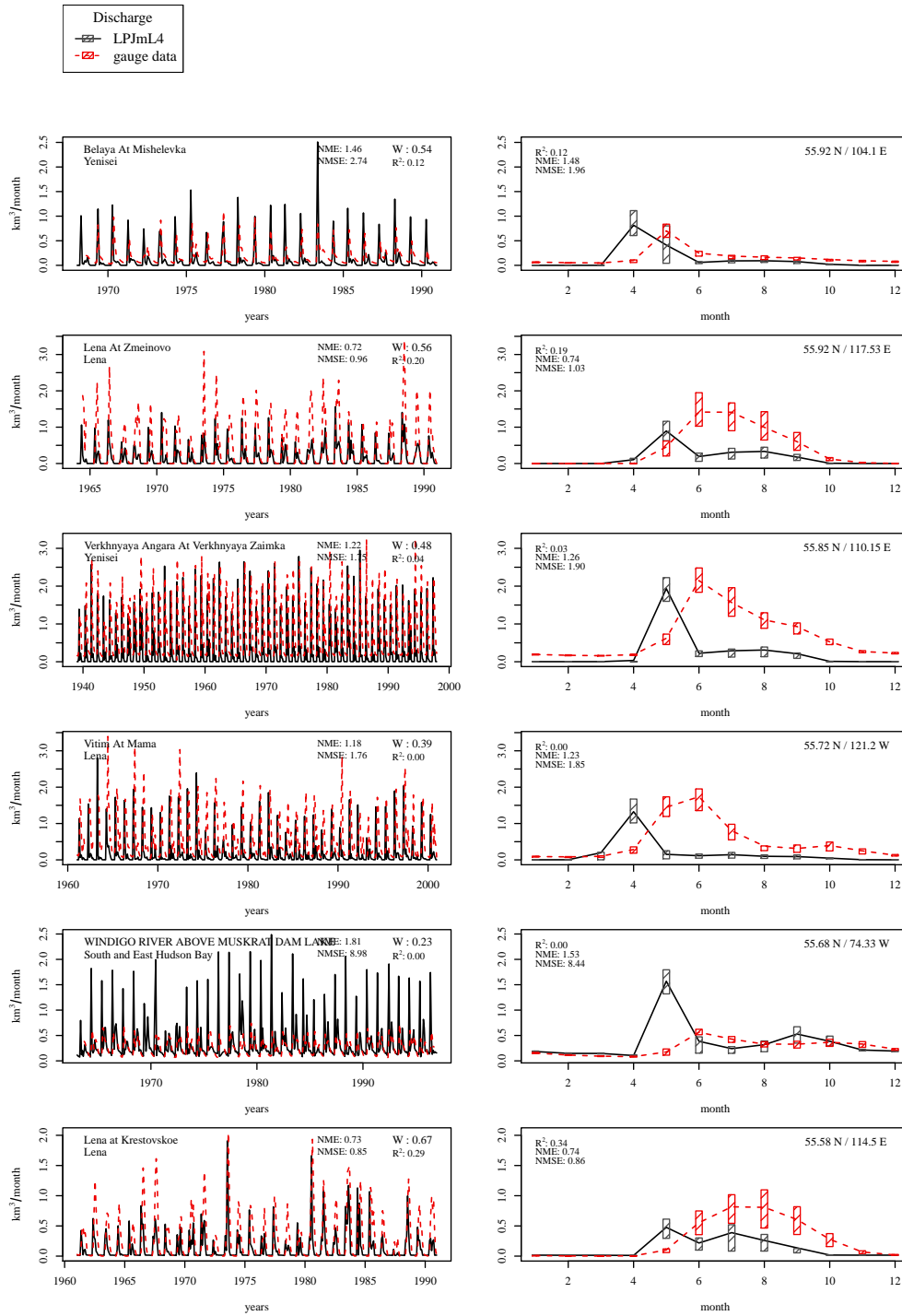


Figure 48. Evaluation of river discharge at gauging stations [32].

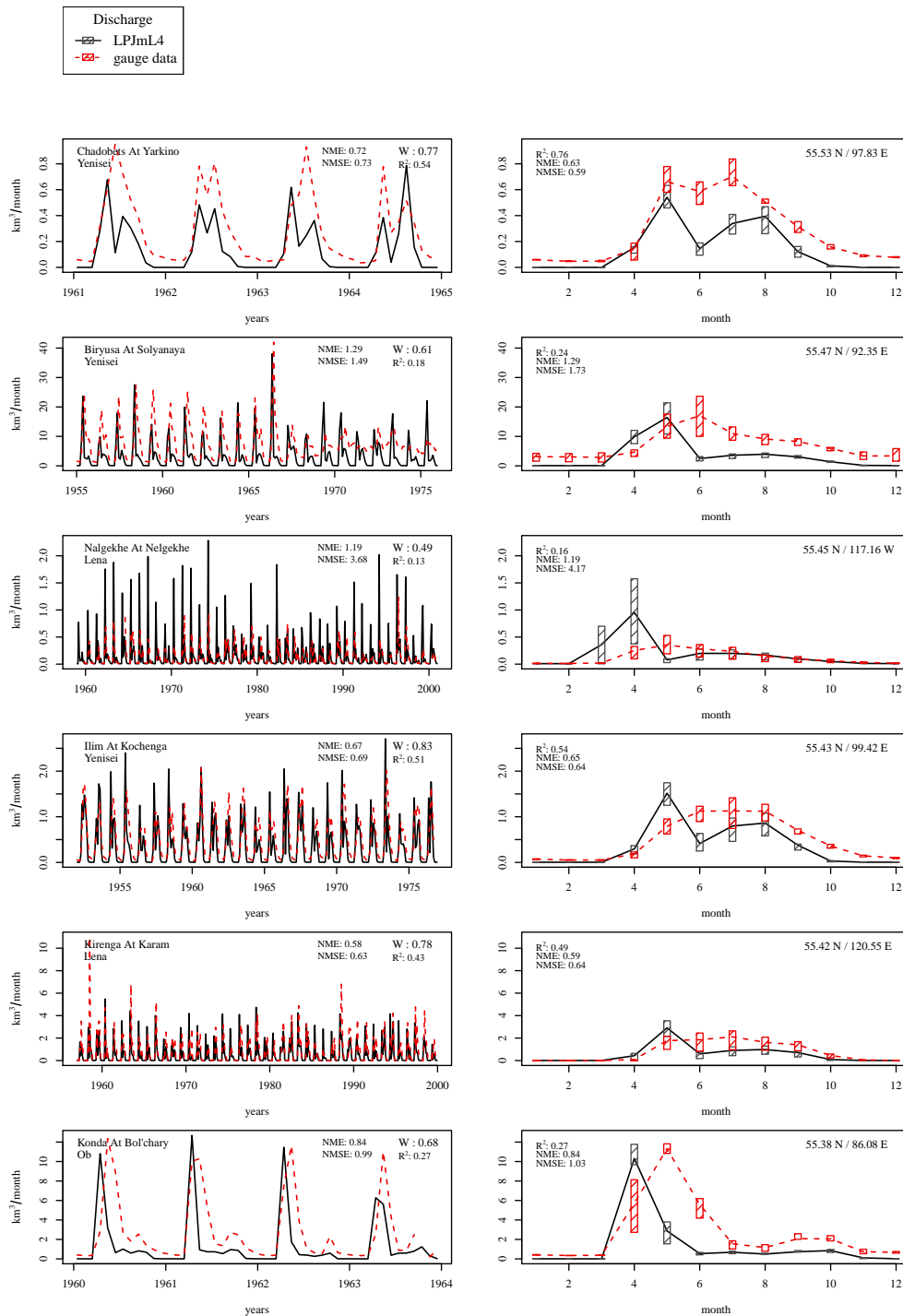


Figure 49. Evaluation of river discharge at gauging stations [33].

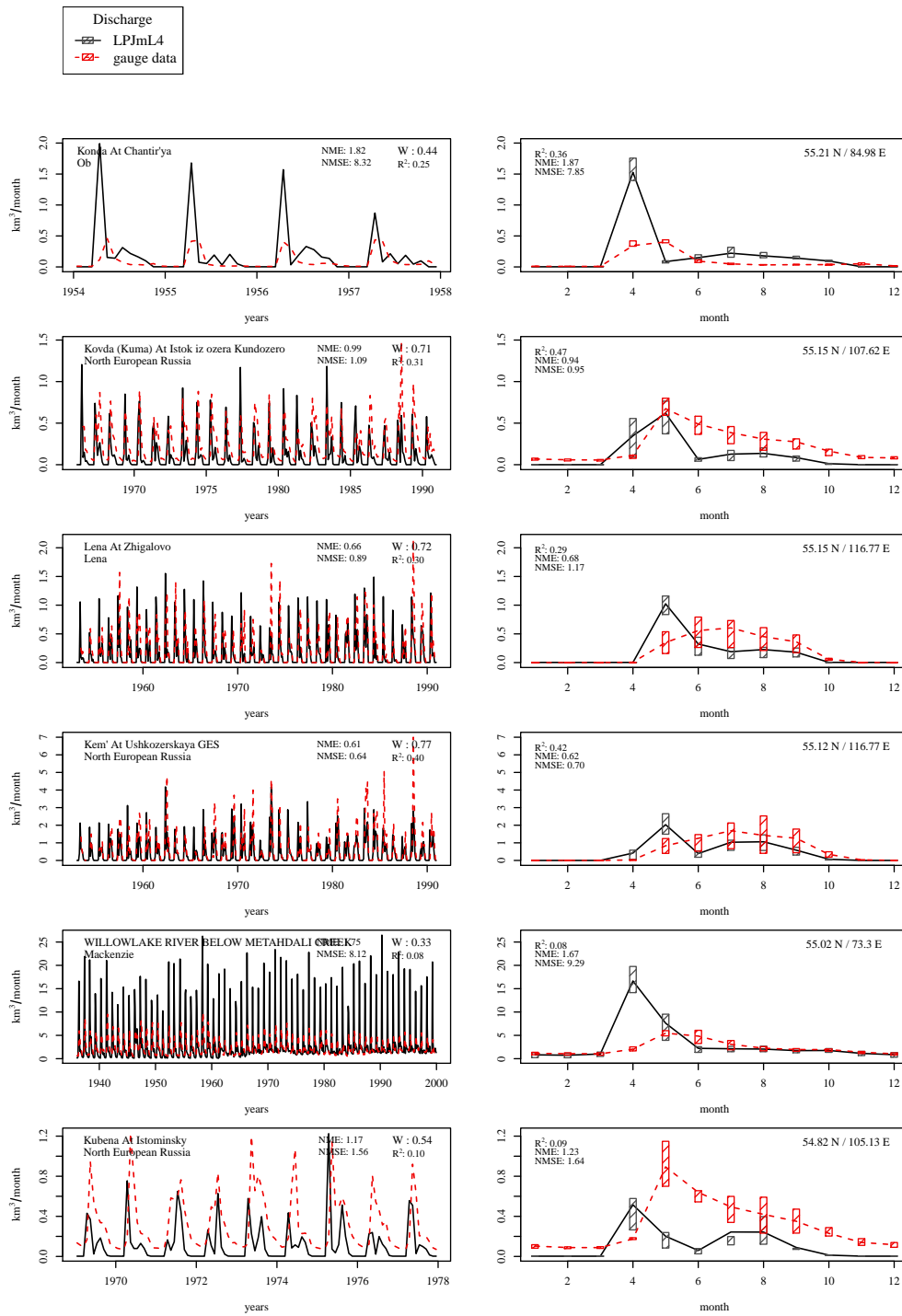


Figure 50. Evaluation of river discharge at gauging stations [34].

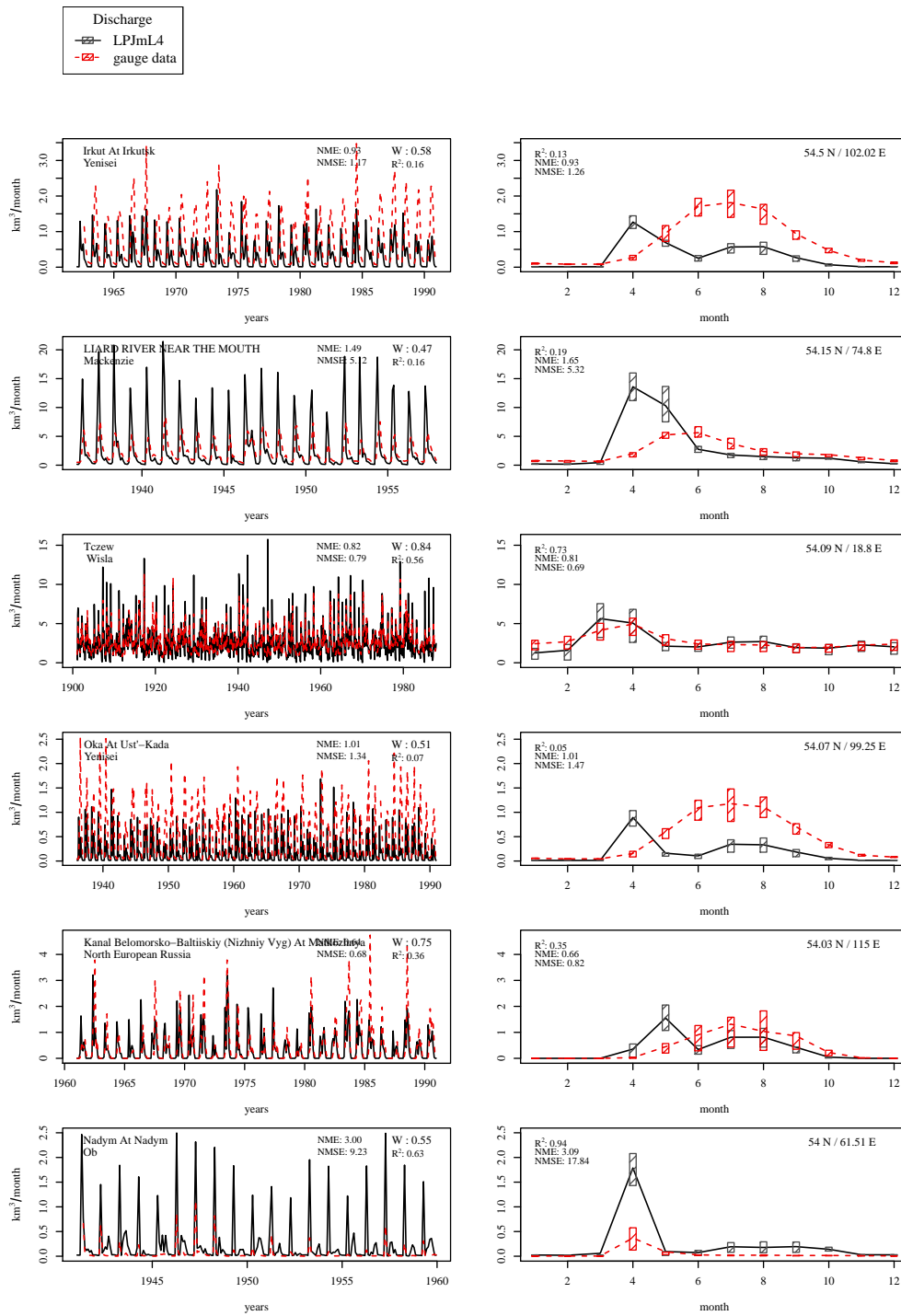


Figure 51. Evaluation of river discharge at gauging stations [35].

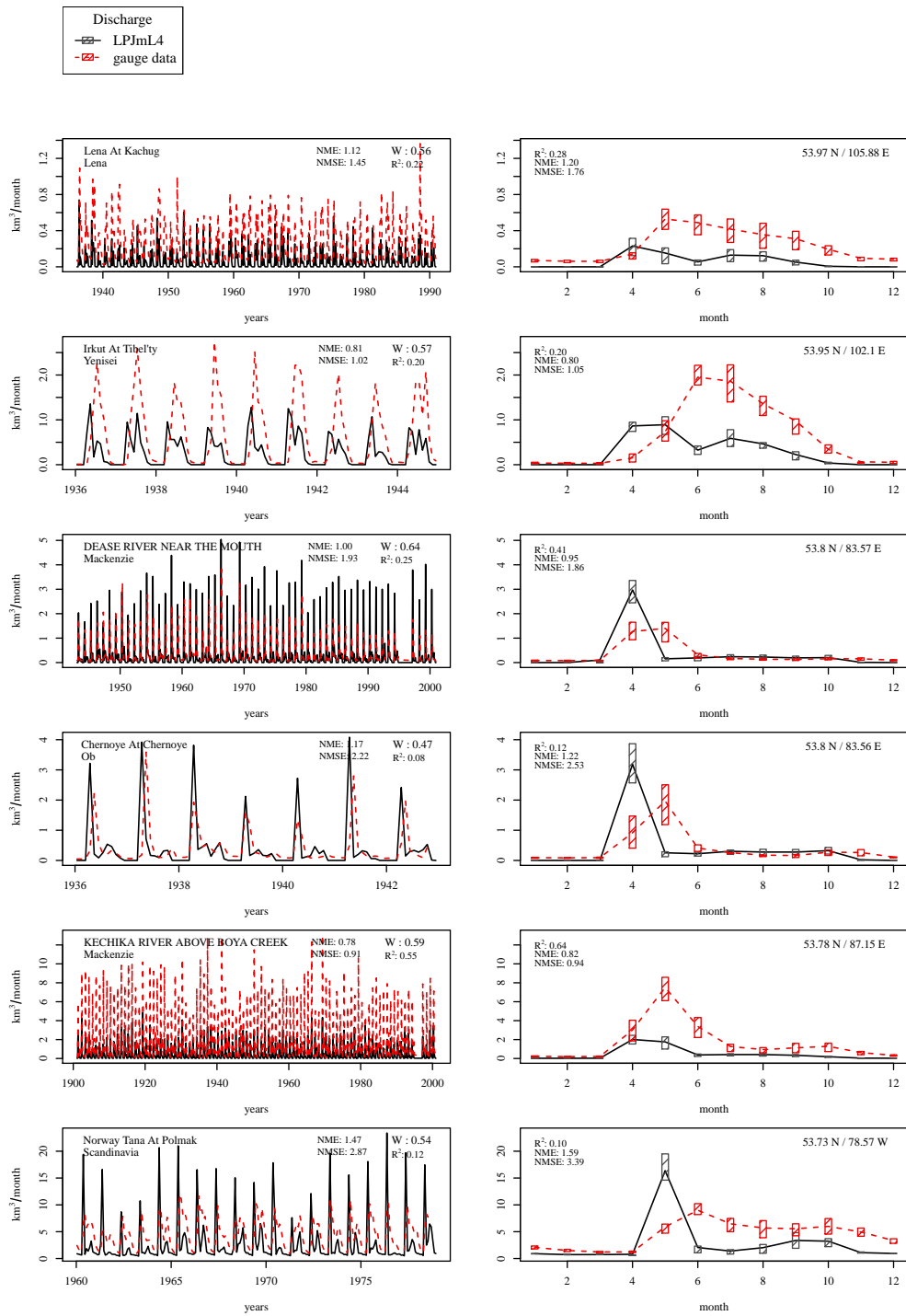


Figure 52. Evaluation of river discharge at gauging stations [36].

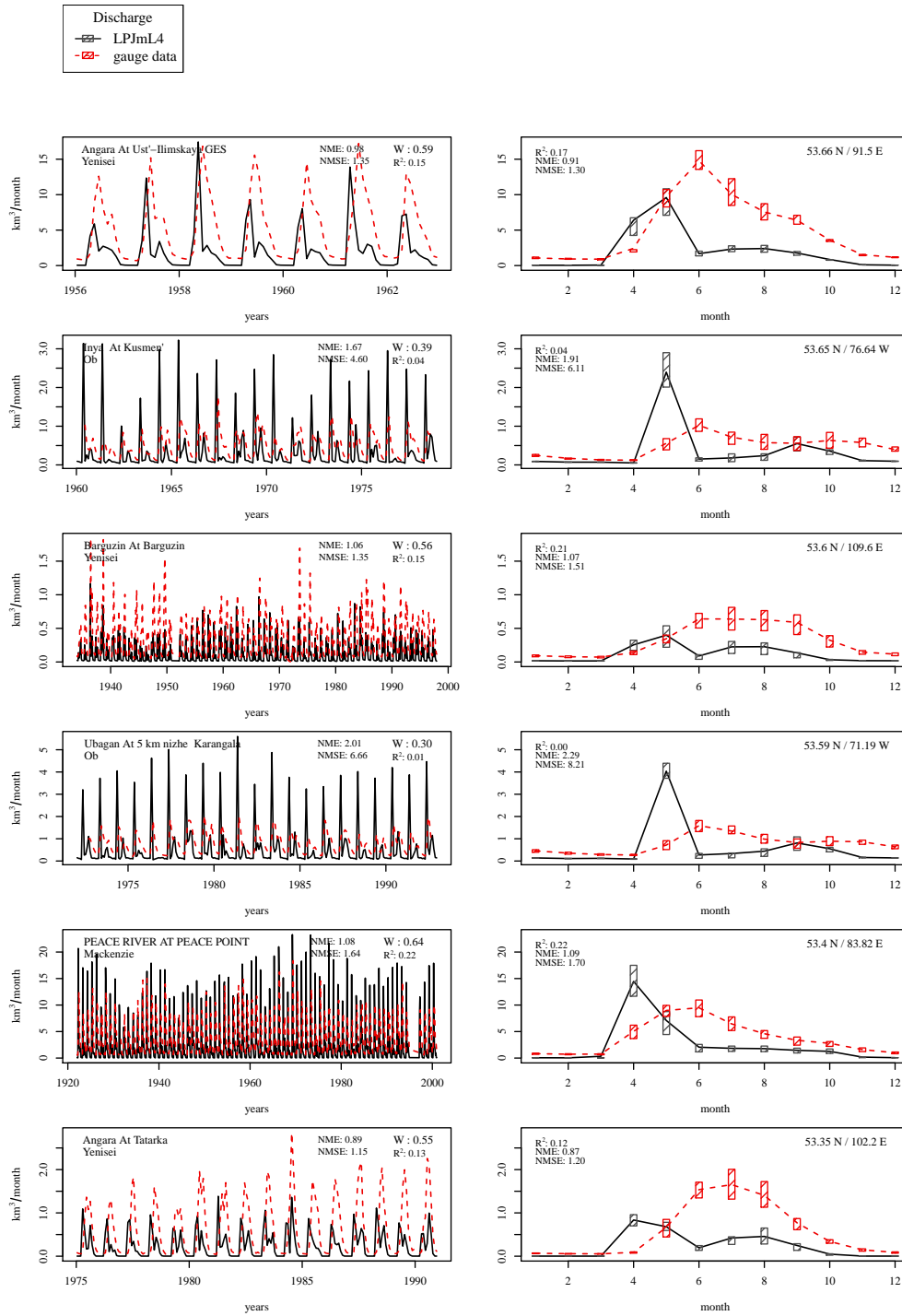


Figure 53. Evaluation of river discharge at gauging stations [37].

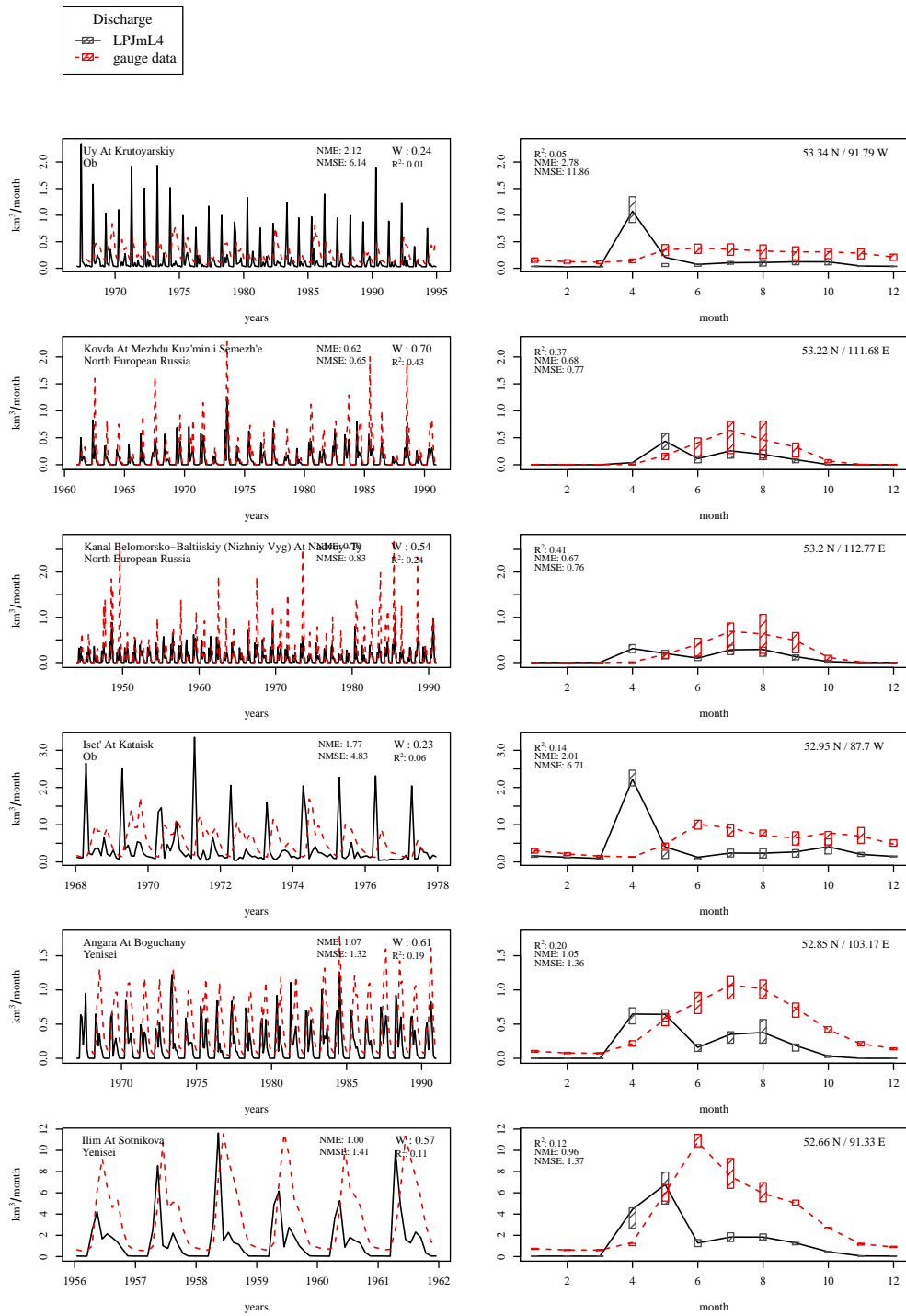


Figure 54. Evaluation of river discharge at gauging stations [38].

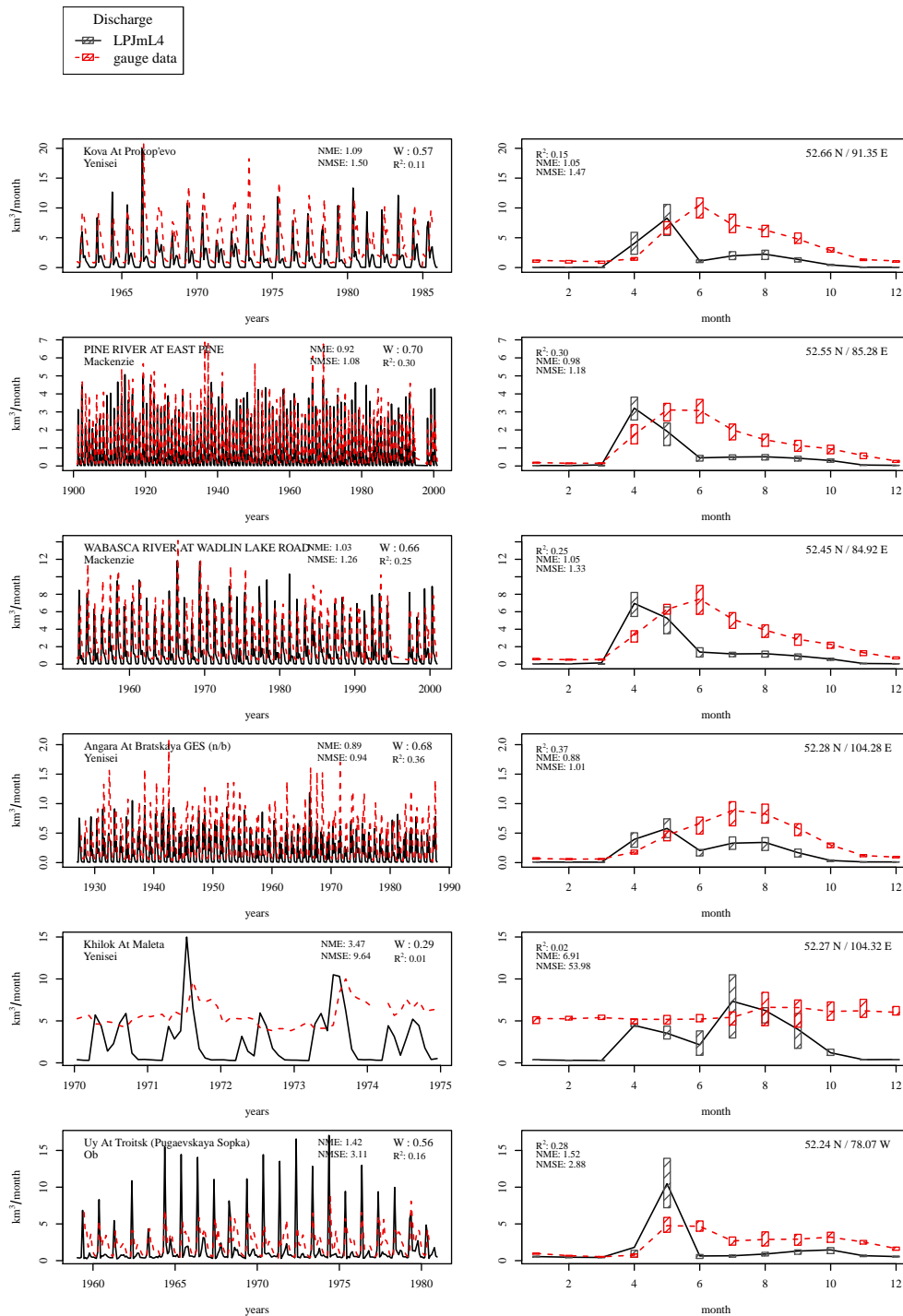


Figure 55. Evaluation of river discharge at gauging stations [39].



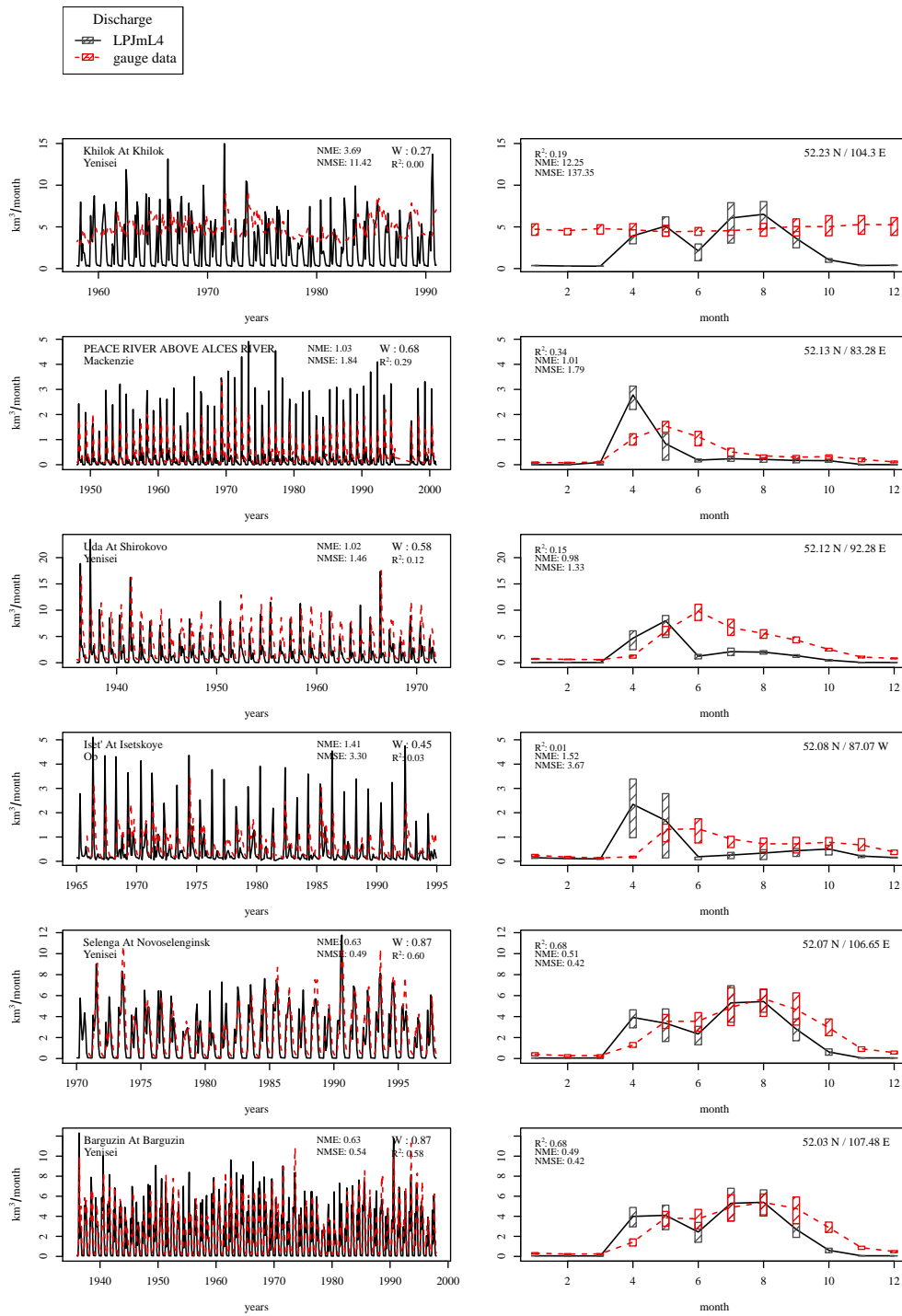


Figure 56. Evaluation of river discharge at gauging stations [40].

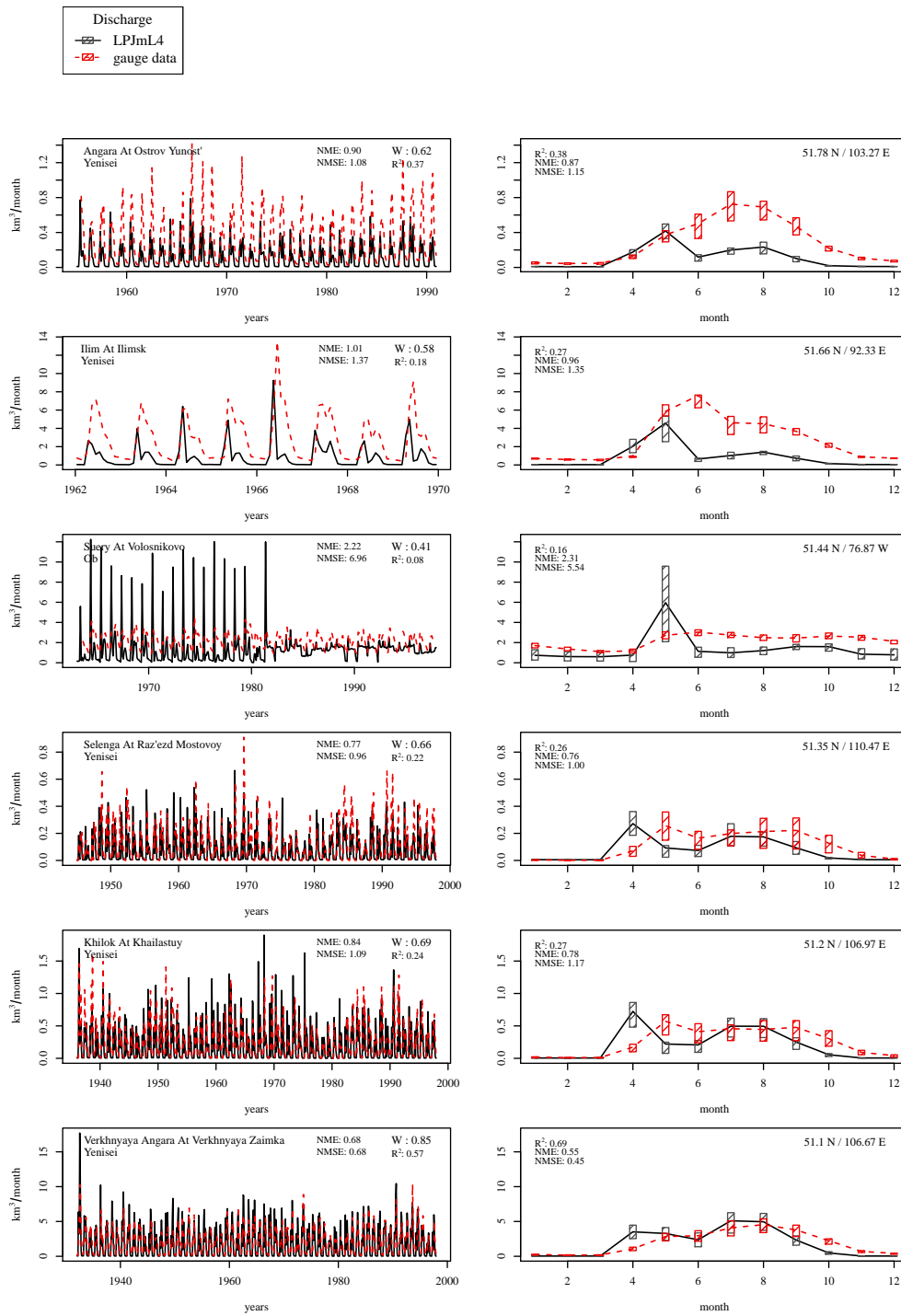


Figure 57. Evaluation of river discharge at gauging stations [41].

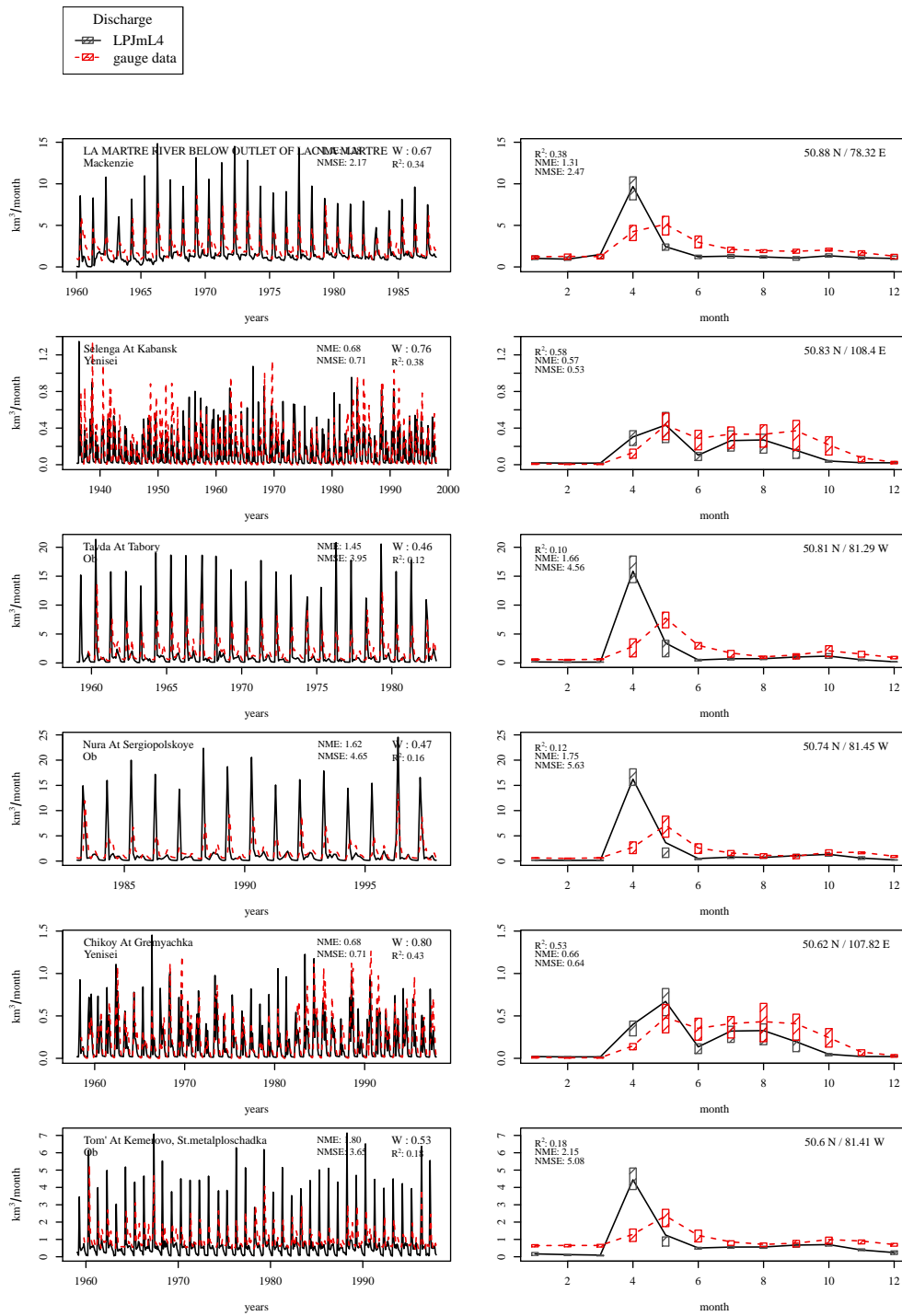


Figure 58. Evaluation of river discharge at gauging stations [42].

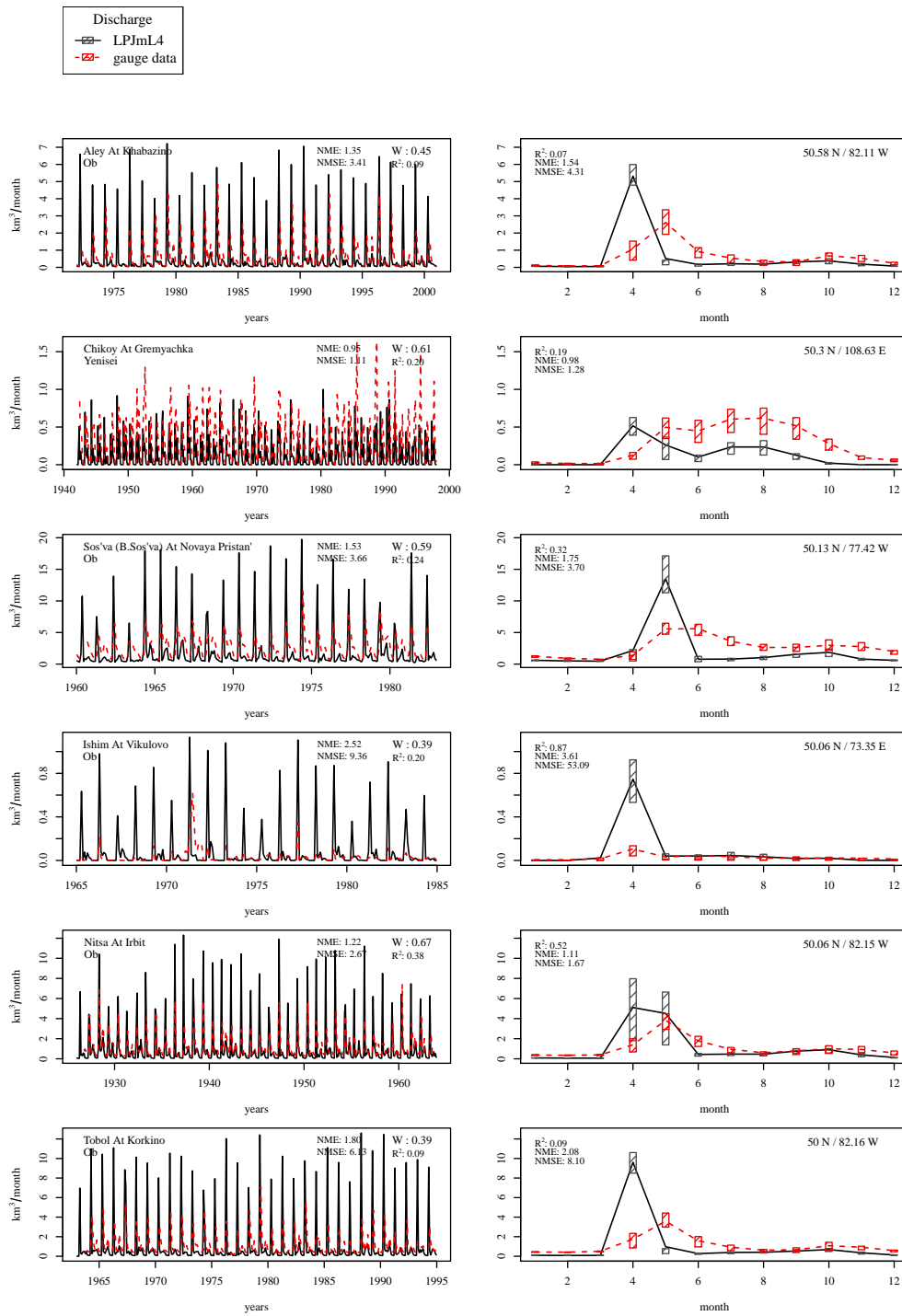


Figure 59. Evaluation of river discharge at gauging stations [43].

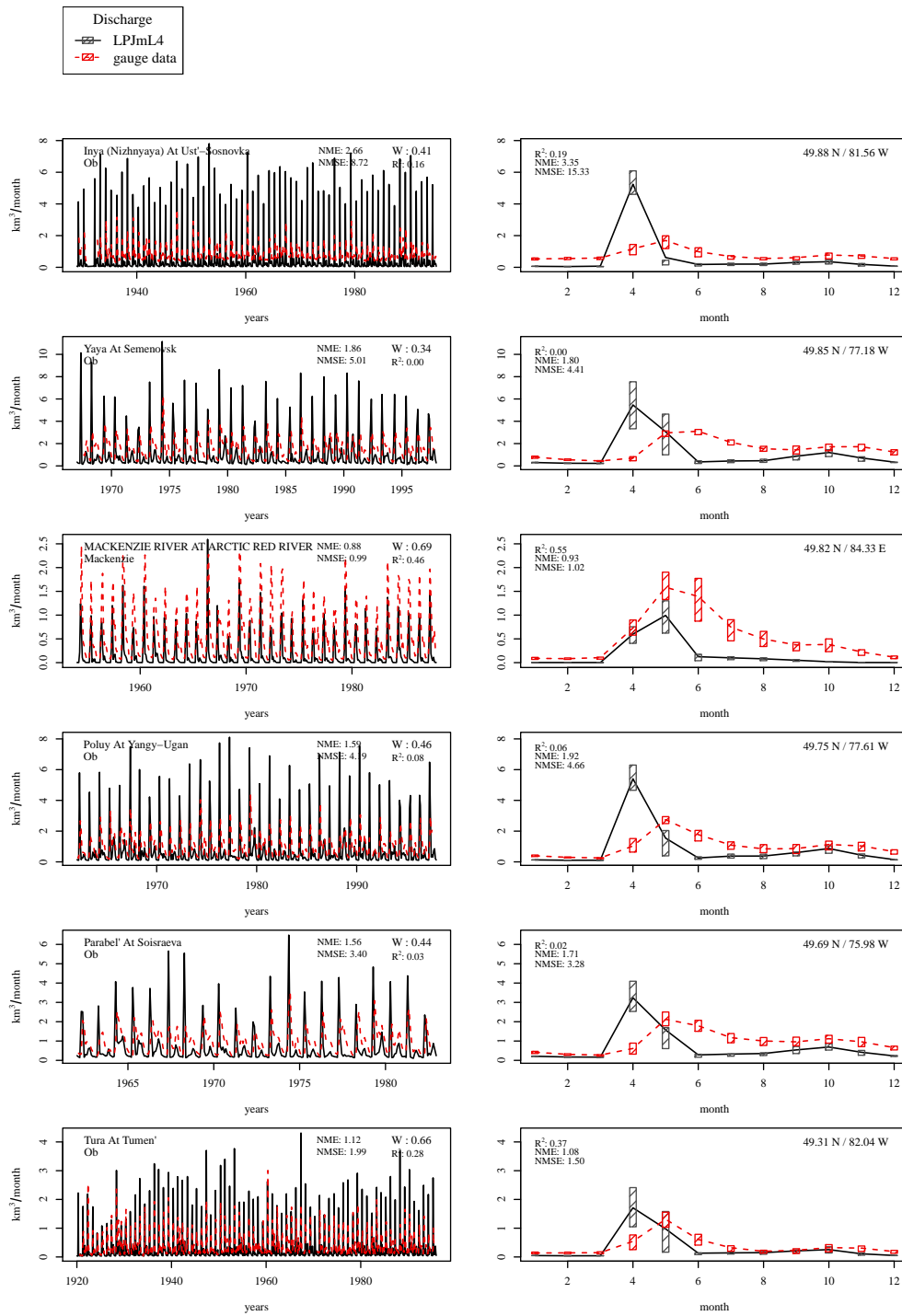


Figure 60. Evaluation of river discharge at gauging stations [44].

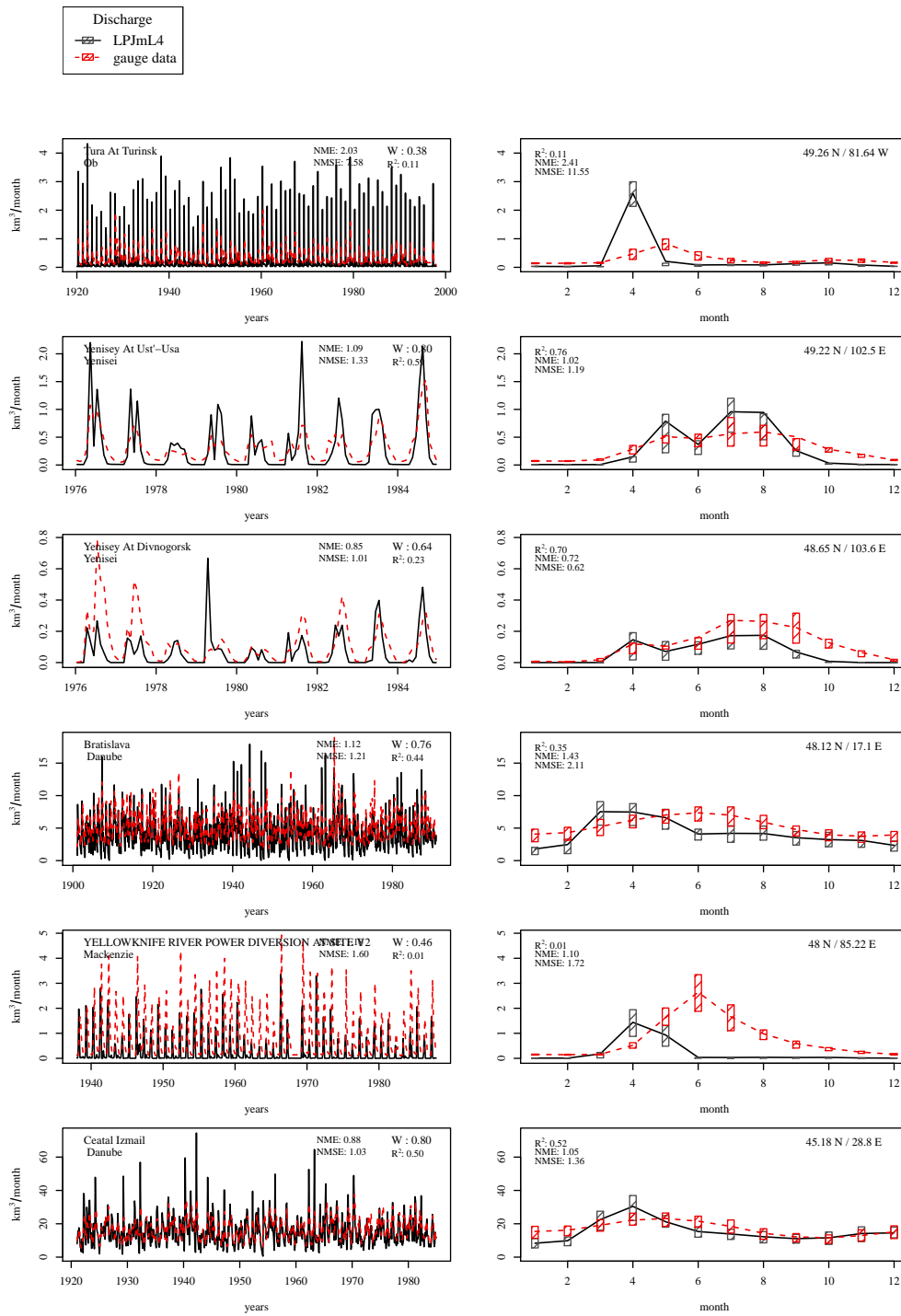


Figure 61. Evaluation of river discharge at gauging stations [45].

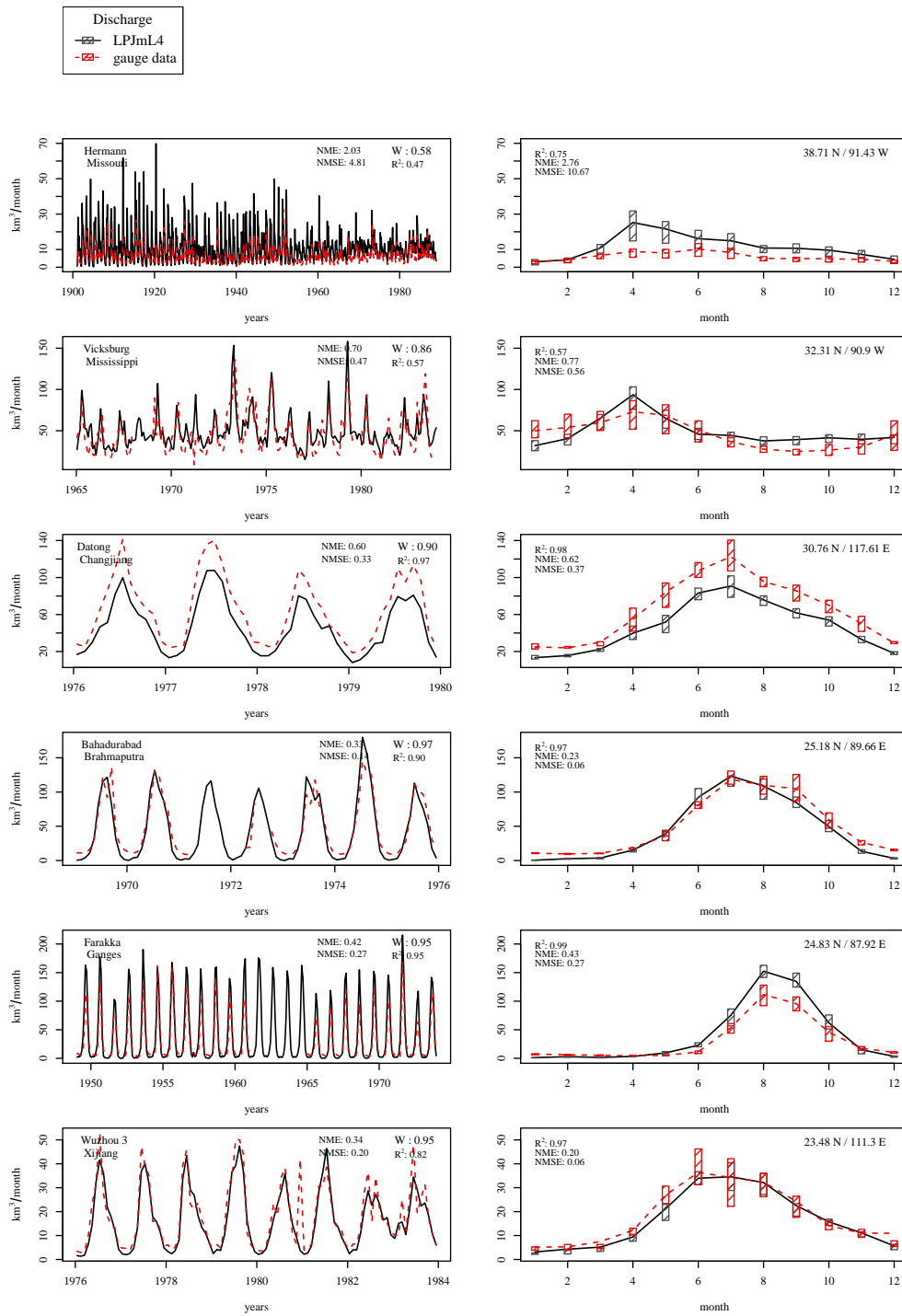


Figure 62. Evaluation of river discharge at gauging stations [46].

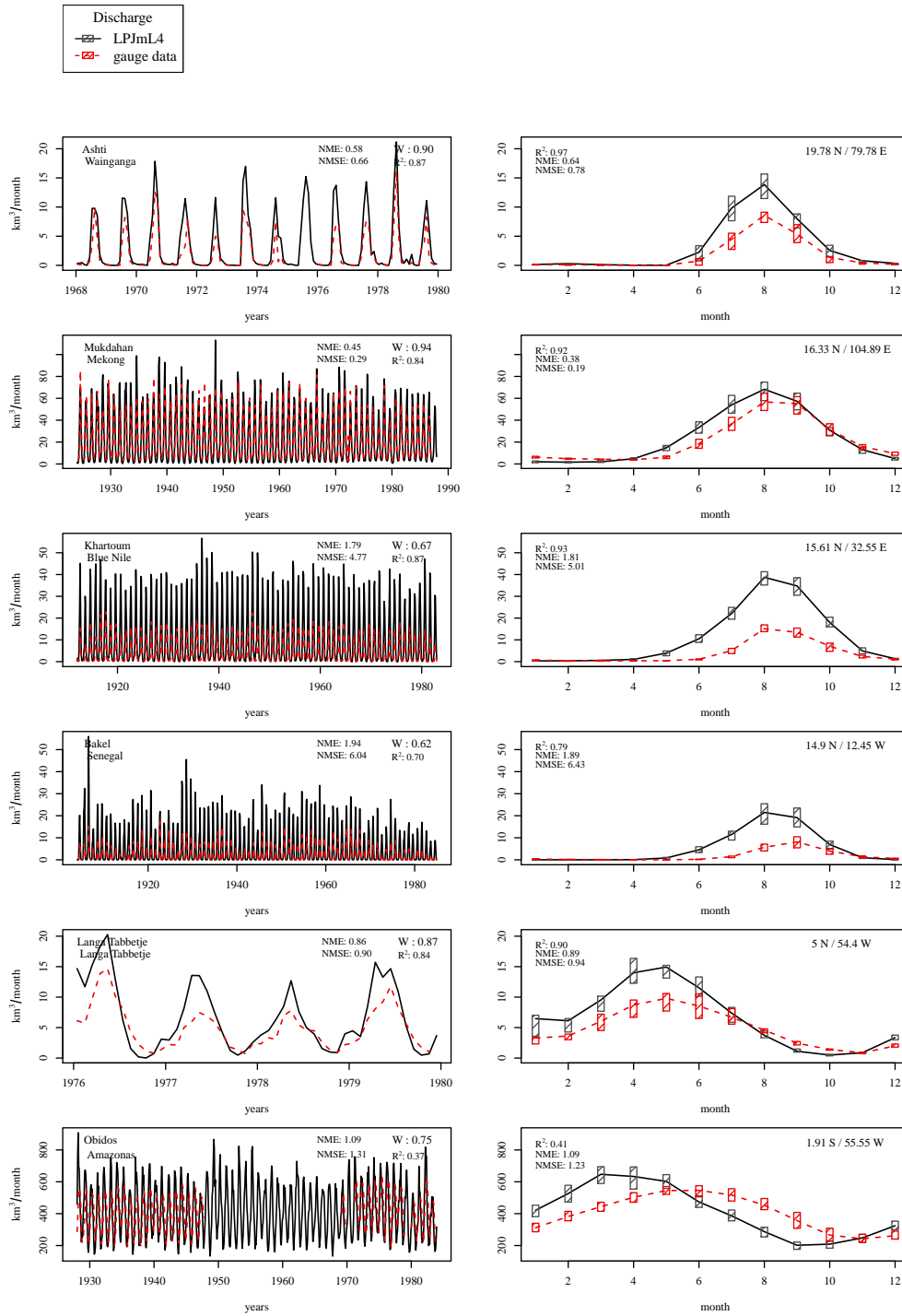


Figure 63. Evaluation of river discharge at gauging stations [47].



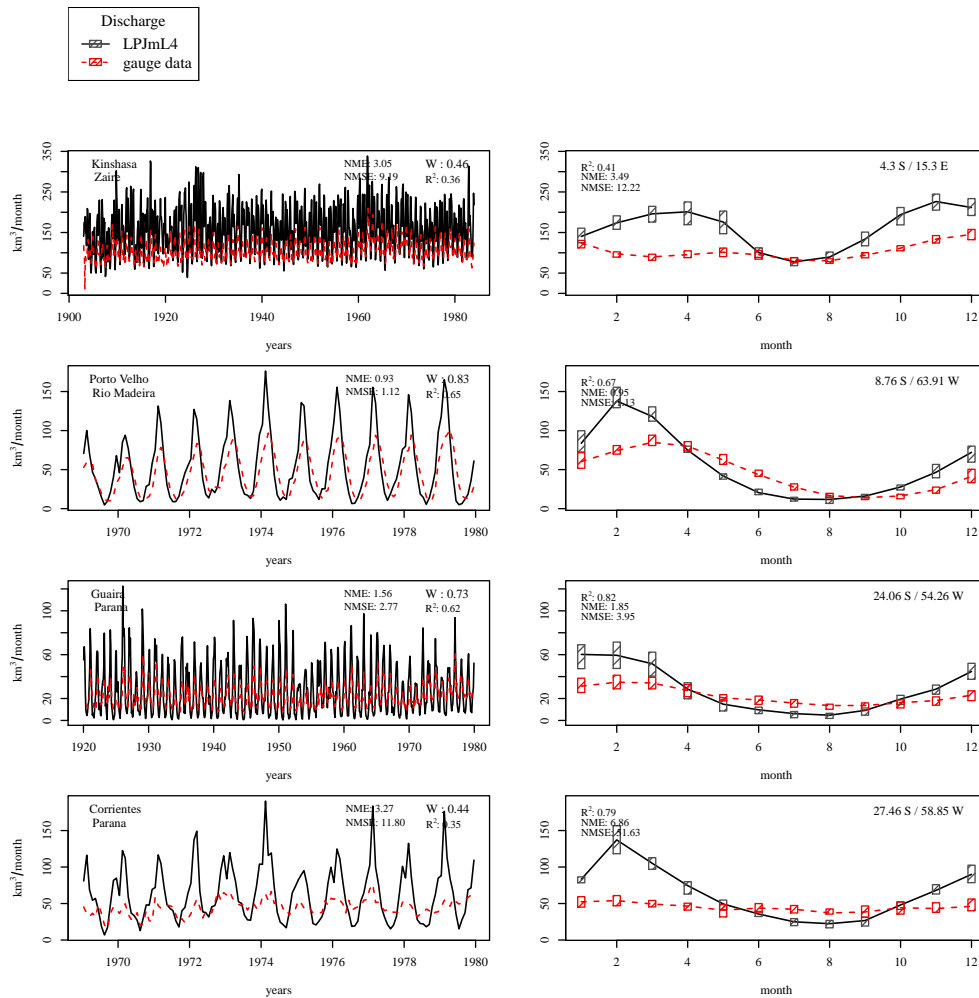
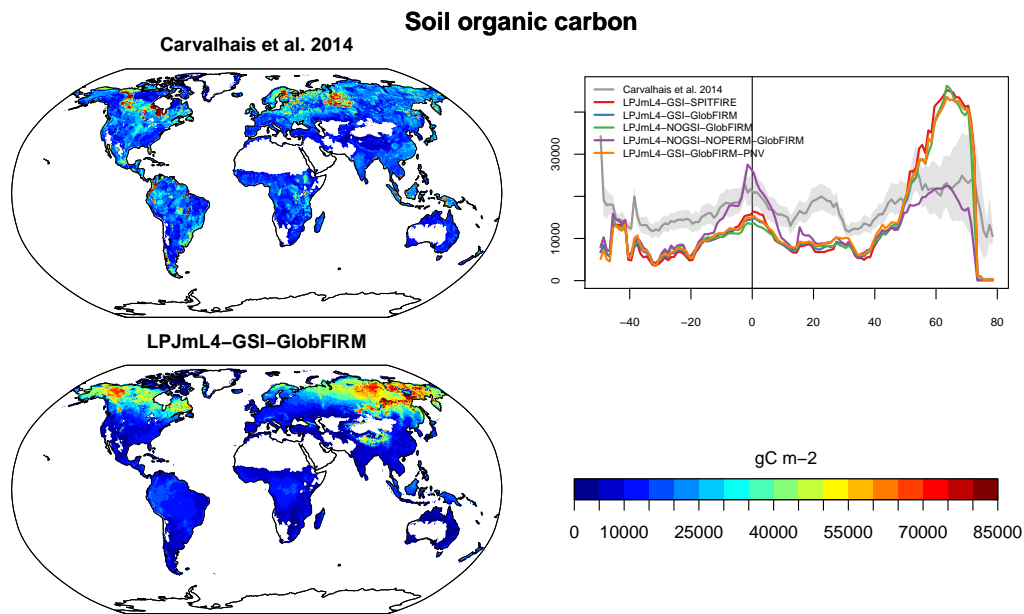
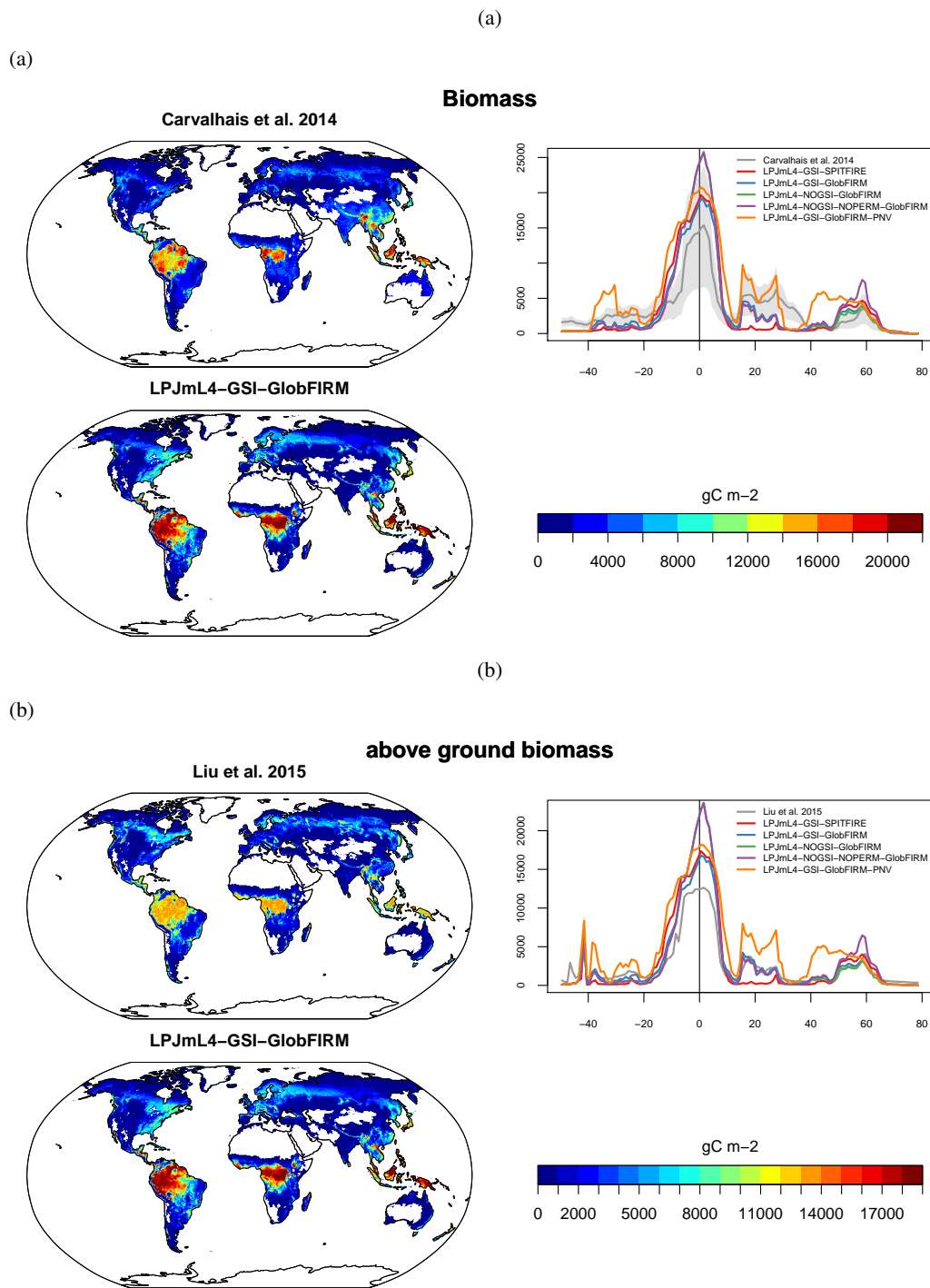


Figure 64. Evaluation of river discharge at gauging stations [48].



**Figure 65.** The maps (left side) show the spatial pattern of soil organic carbon [ $\text{gC m}^{-2}$ ] distribution from the standard LPJmL4 simulation against data from Carvalhais et al. (2014). The graph on the right side shows the latitudinal pattern of vegetation biomass distribution simulated by the different versions of LPJmL4 against data from Carvalhais et al. (2014).



**Figure 66.** (a) The maps (left side) show the spatial pattern of vegetation biomass [ $\text{gC m}^{-2}$ ] distribution from the standard LPJmL4 simulation against data from Carvalhois et al. (2014). The graph on the right side shows the latitudinal pattern of vegetation biomass distribution simulated by the different versions of LPJmL4 against data from Carvalhois et al. (2014). (b) Similar as above but for aboveground biomass [ $\text{gC m}^{-2}$ ] from Liu et al. (2015).

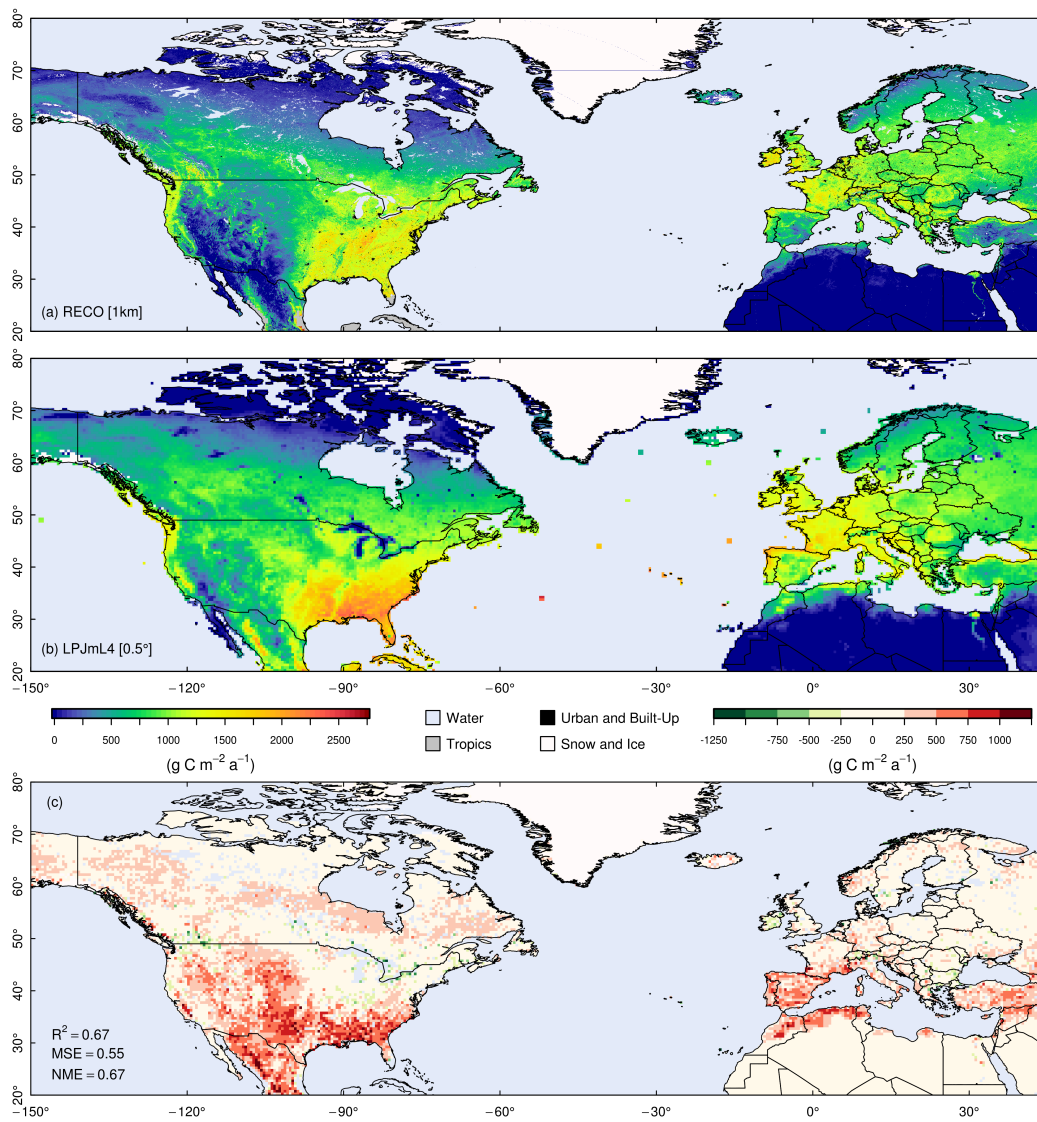


**Figure 67.** Evaluation of ecosystem respiration [ $\text{gC m}^{-2} \text{a}^{-1}$ ] comparing LPJm4 with satellite-derived ecosystem respiration (Jägermeyr et al., 2014).

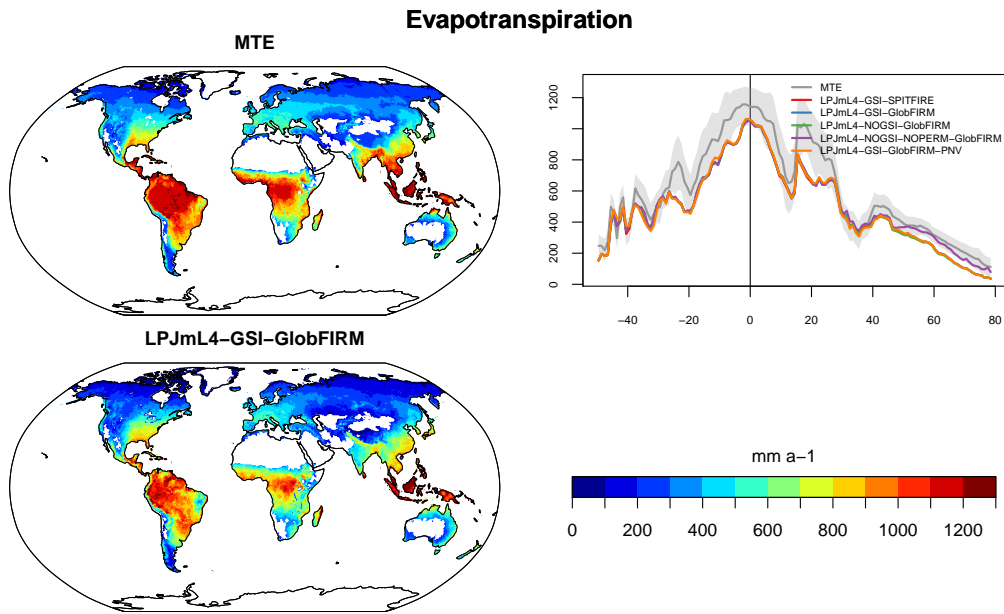


**Figure 68.** The maps (left side) show the spatial pattern of evapotranspiration [ $\text{mm a}^{-1}$ ] distribution from the standard LPJmL4 simulation against the MTE data (Jung et al., 2011). The graph on the right side shows the latitudinal pattern of evapotranspiration distribution simulated by the different versions of LPJmL4 against data from Jung et al. (2011).

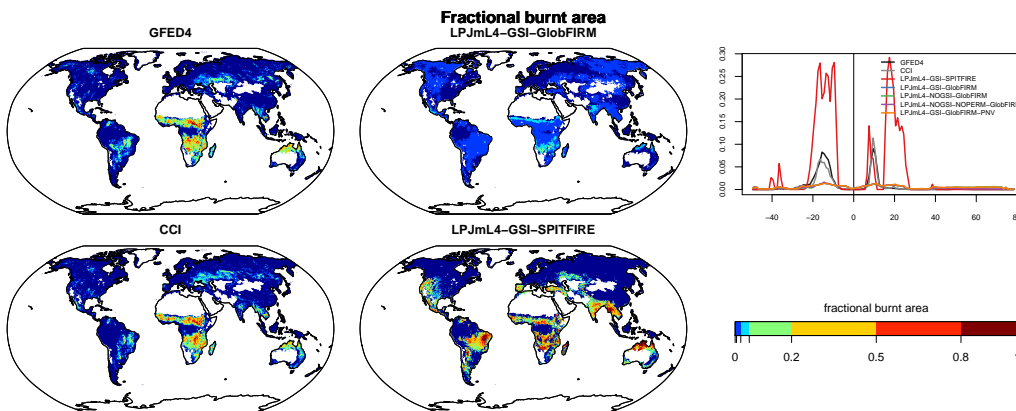


**Figure 69.** Observed and simulated estimations of fractional area burnt. Observed estimation both are based on remote sensing data (GFED4: <http://www.globalfiredata.org/> and CCI Fire Version 4.1: <http://cci.esa.int/data>).

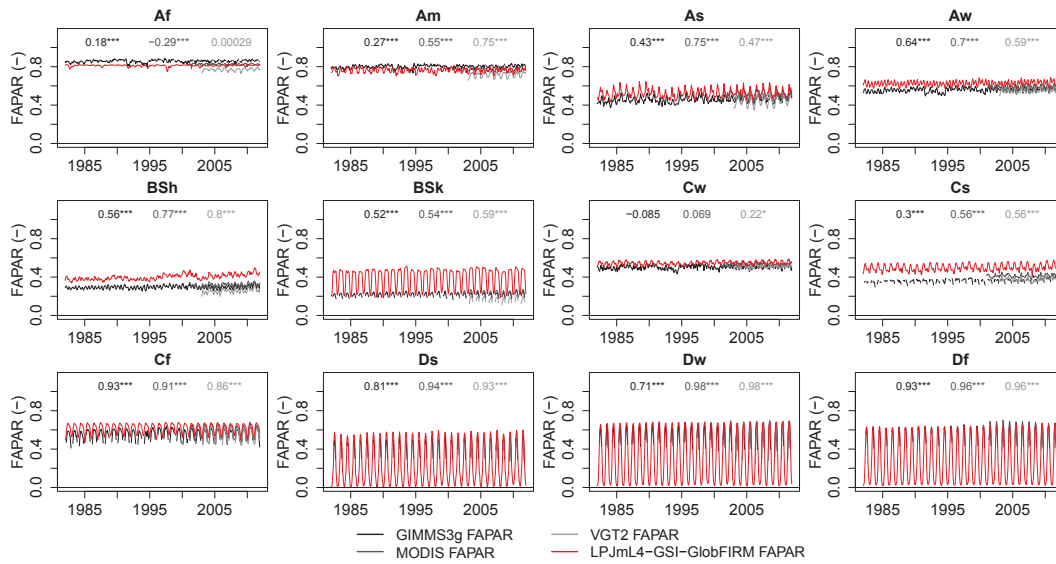


**Figure 70.** FAPAR comparison of seasonal dynamic for Köppen-Geiger classification against 3 different remote sensing products: MODIS FAPAR, GIMMS3g FAPAR, and VGT2 FAPAR.

A map of the Köppen classification can be found [here](http://koeppen-geiger.vu-wien.ac.at) [http://koeppen-geiger.vu-wien.ac.at].

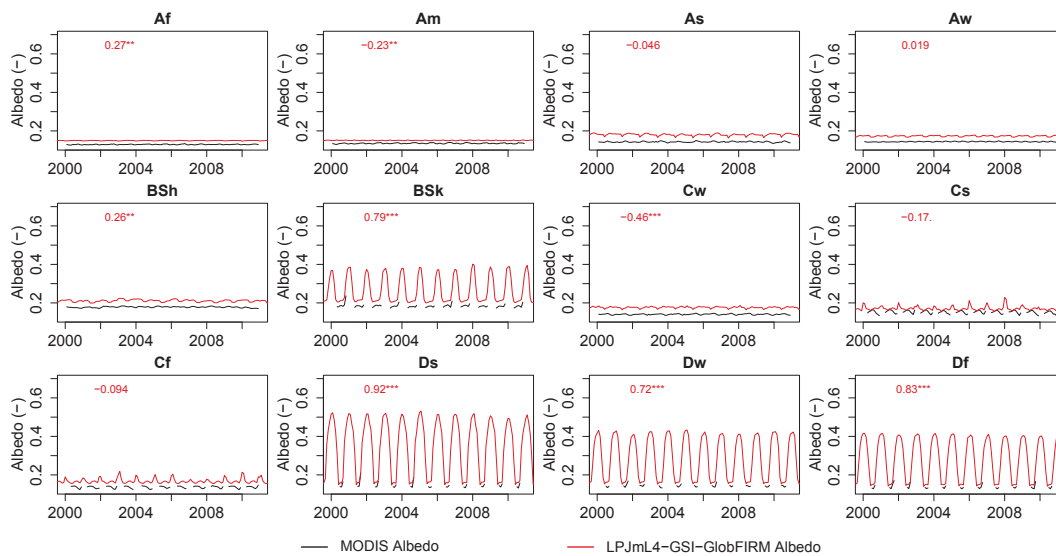


**Figure 71.** Albedo comparison for Köppen-Geiger classification with MODIS remote sensing data.

A map of the Köppen classification can be found [here](http://koeppen-geiger.vu-wien.ac.at) [http://koeppen-geiger.vu-wien.ac.at].

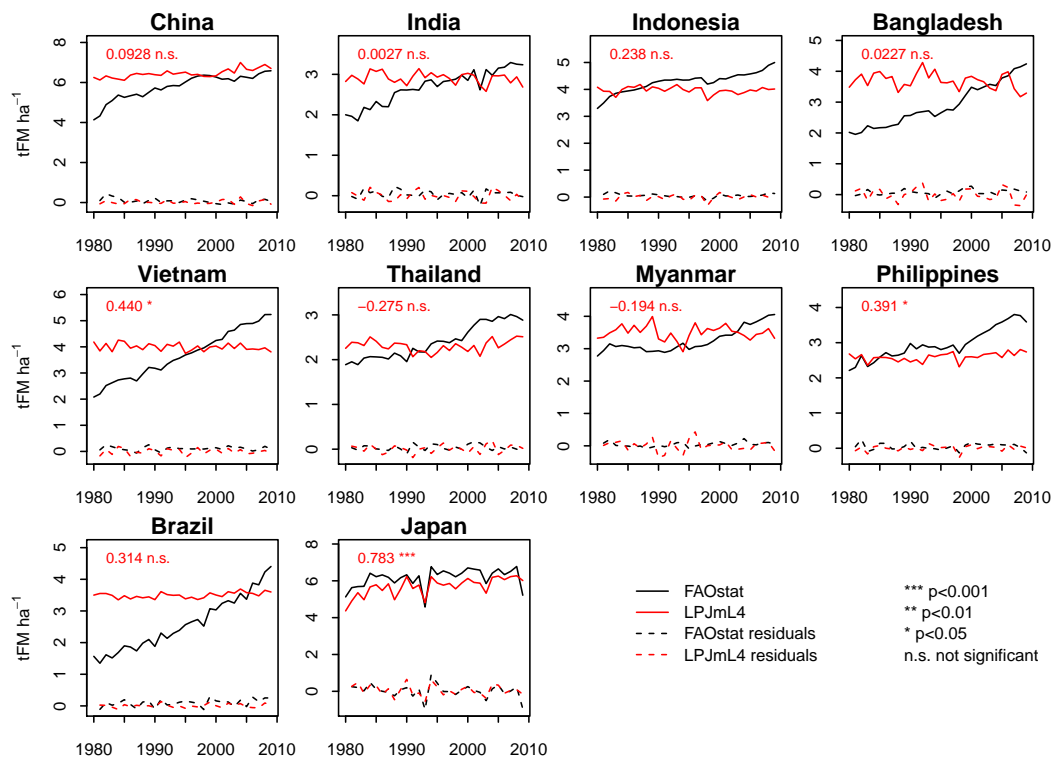


Figure 72. Evaluation of crop variability comparing rice yields computed by LPJmL4 with FAO yield data.

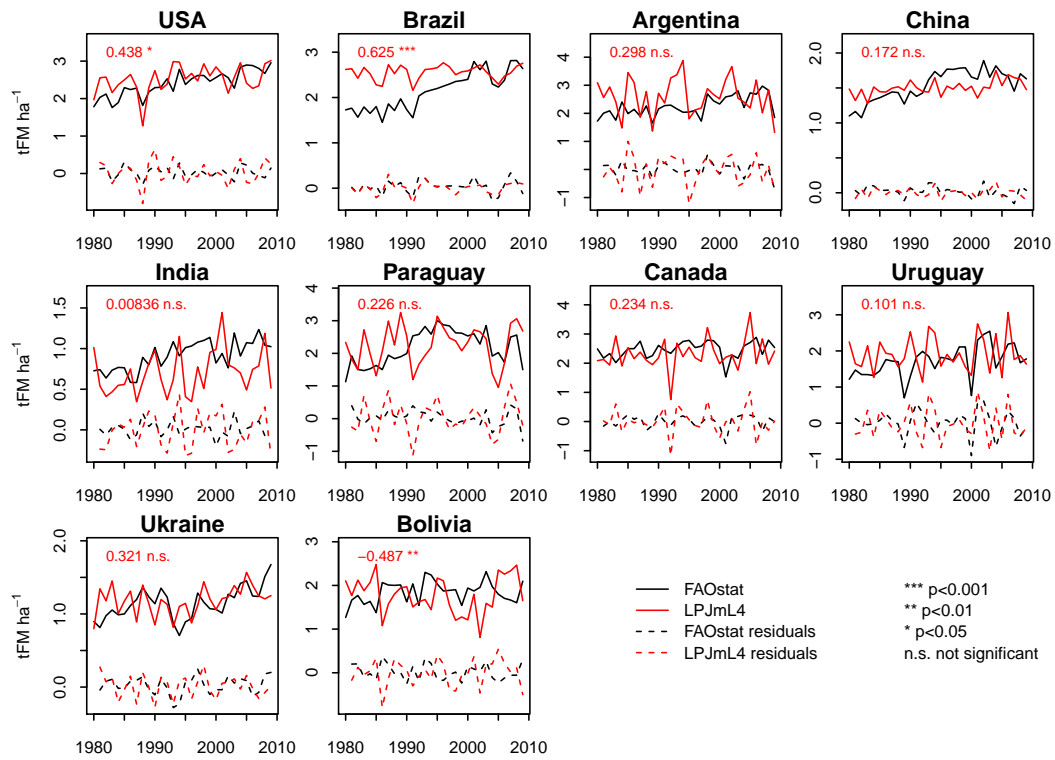


Figure 73. As Fig. 72 for soy.



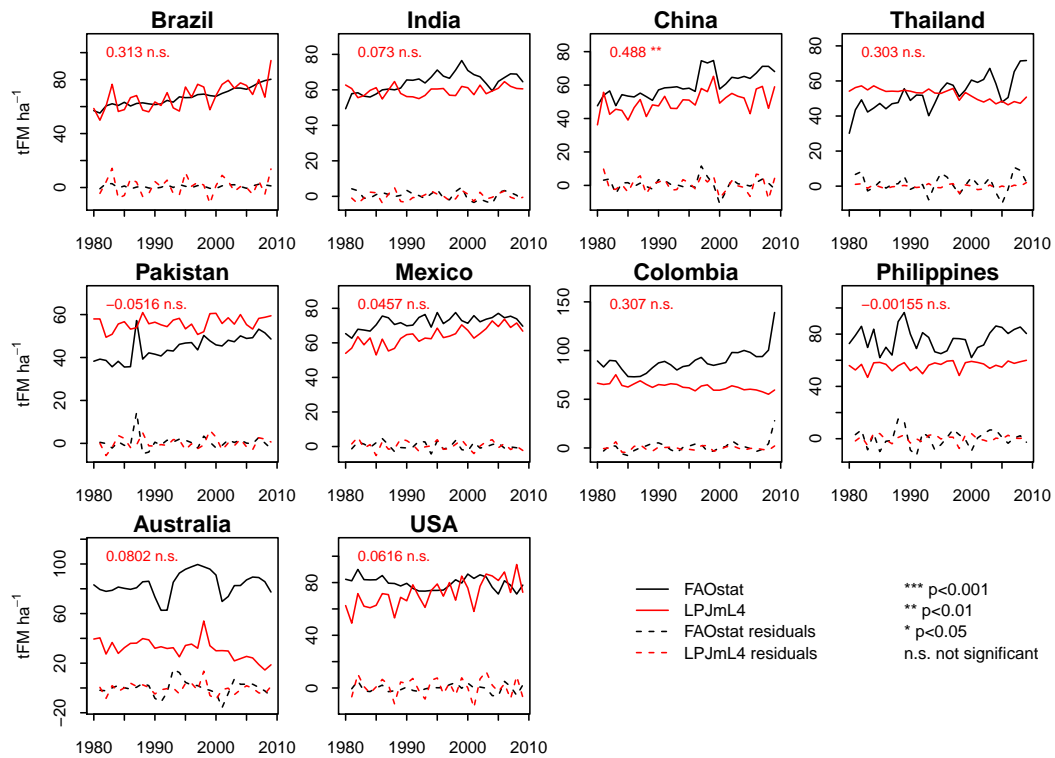


Figure 74. As Fig. 72 for sugarcane.

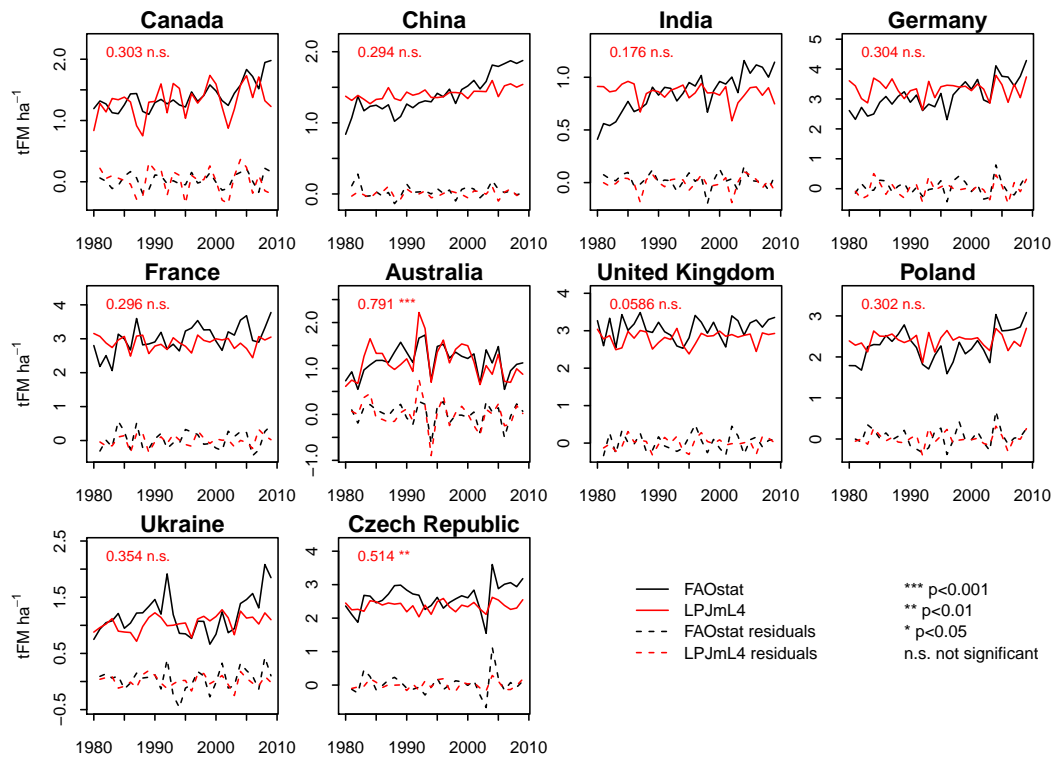


Figure 75. As Fig. 72 for rapeseed.

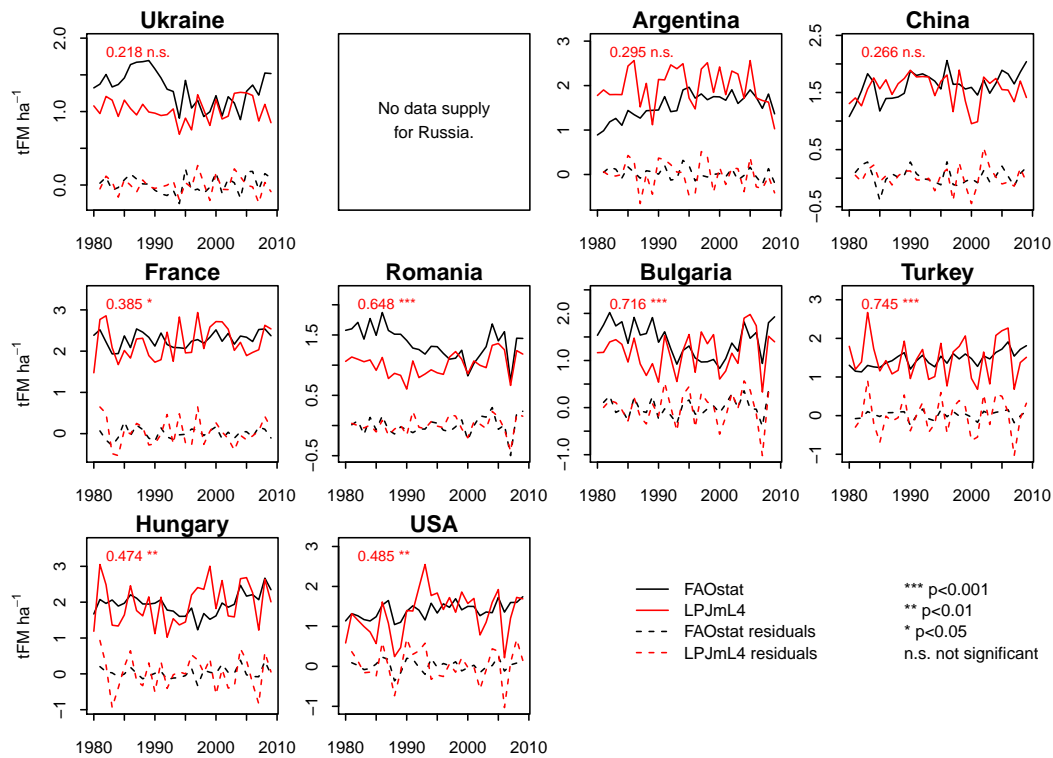


Figure 76. As Fig. 72 for sunflower.

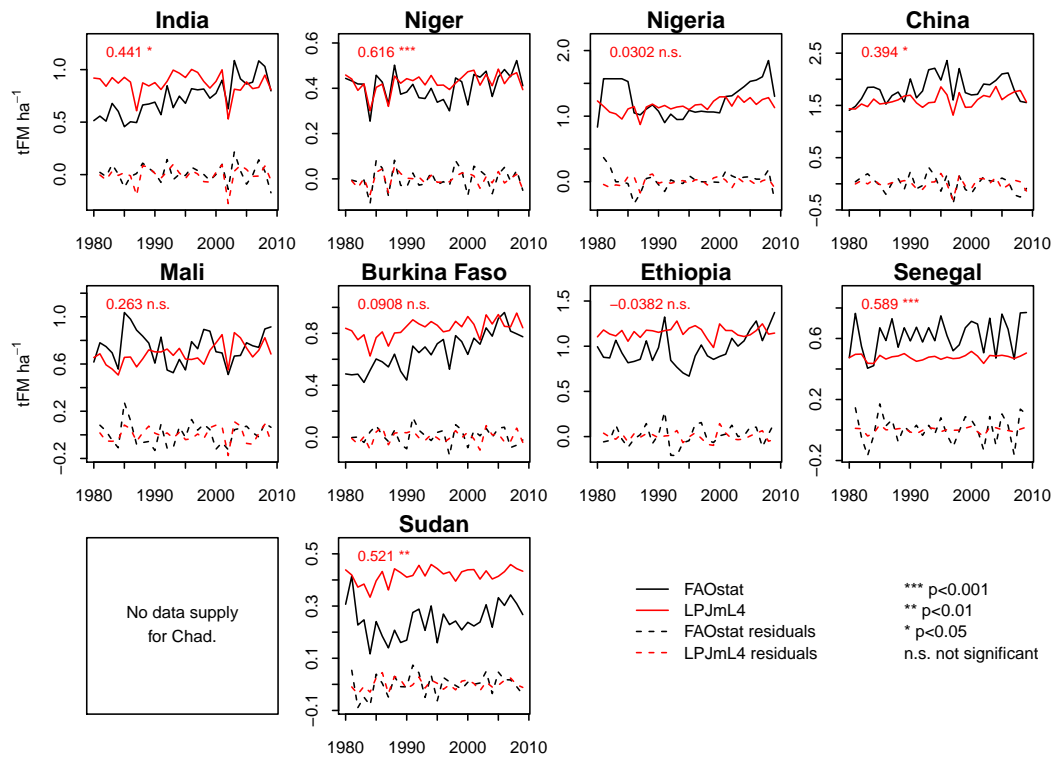


Figure 77. As Fig. 72 for millet.

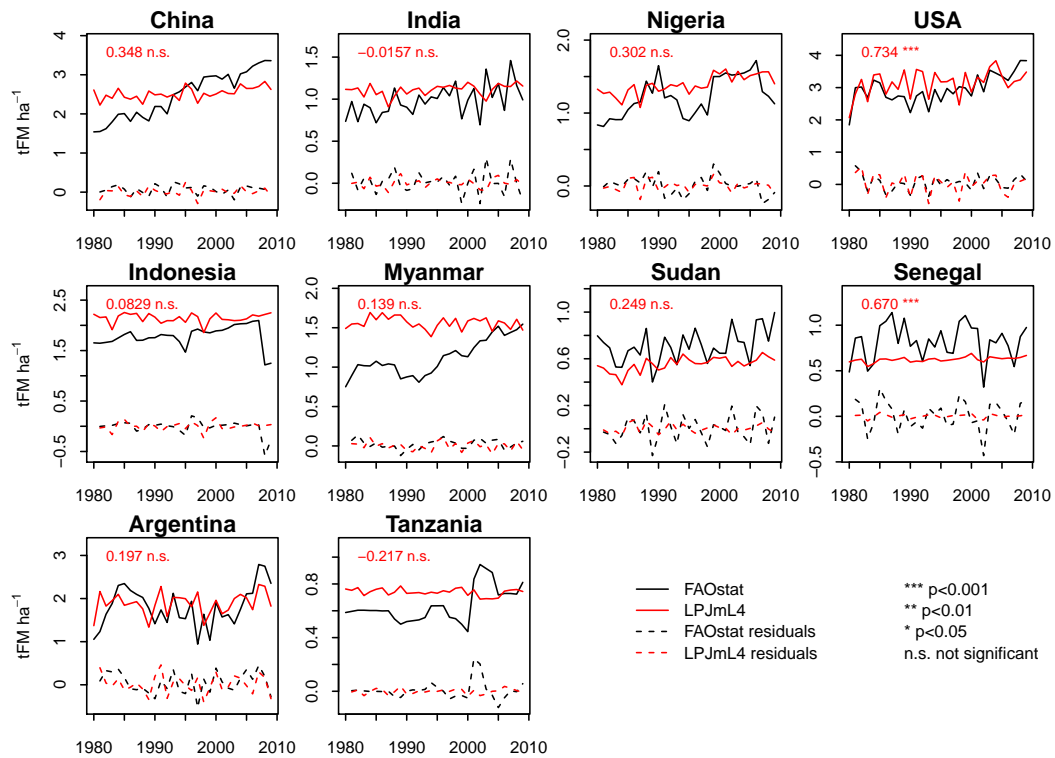


Figure 78. As Fig. 72 for peanut.

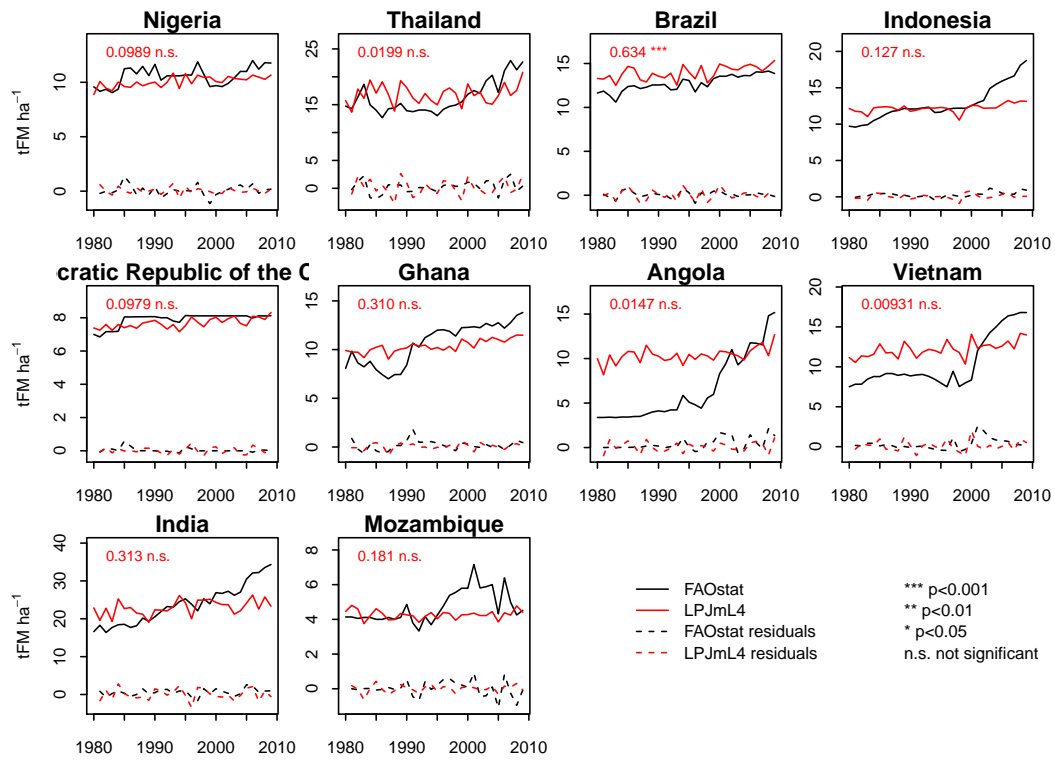


Figure 79. As Fig. 72 for cassava.

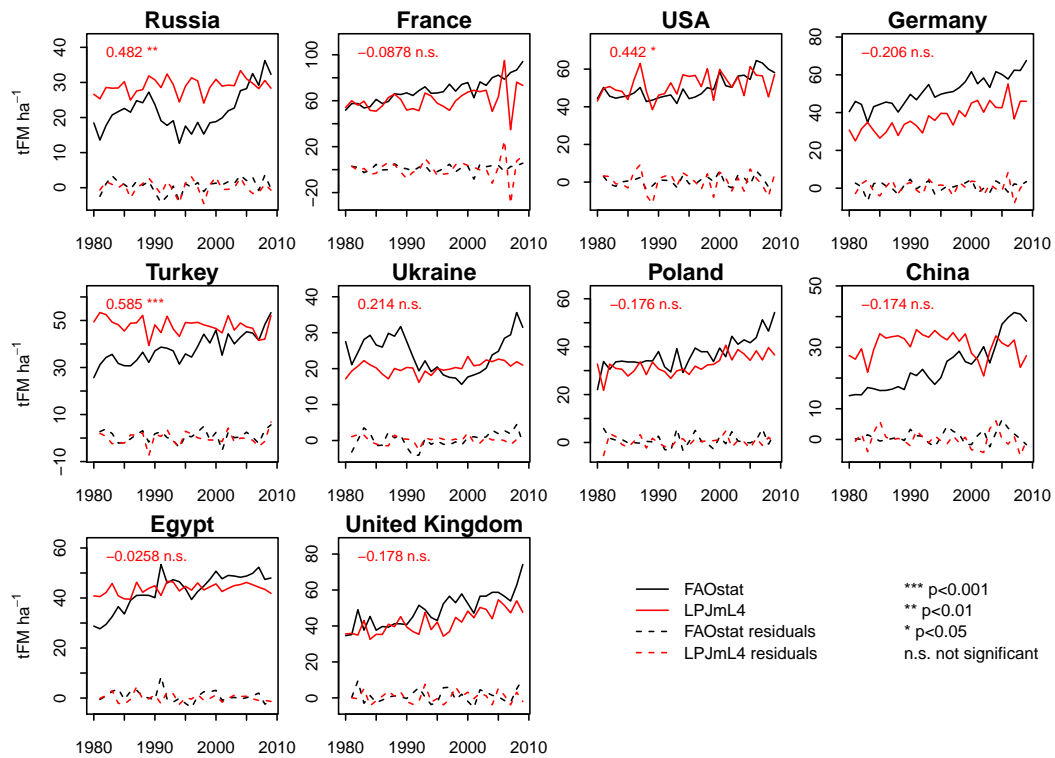
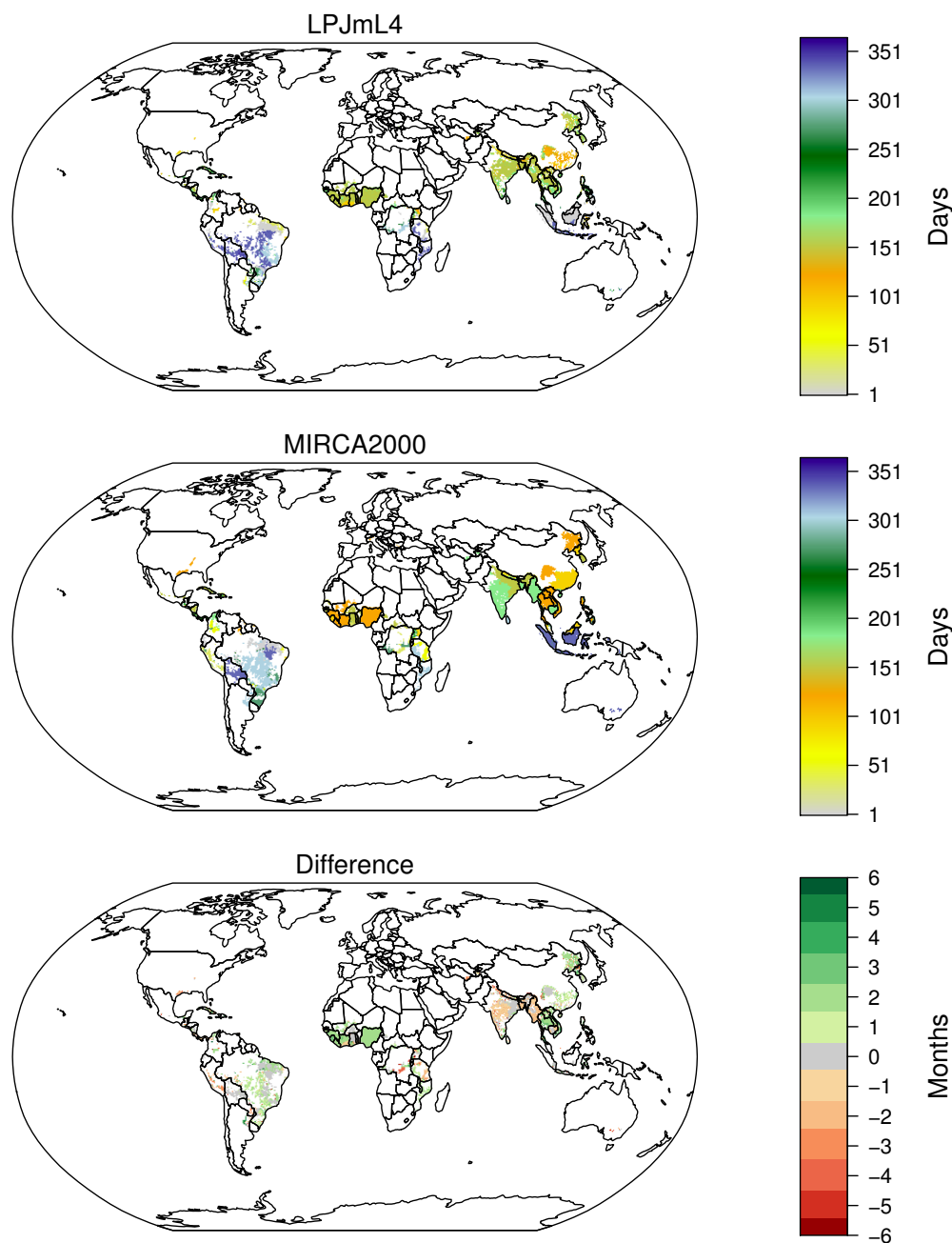
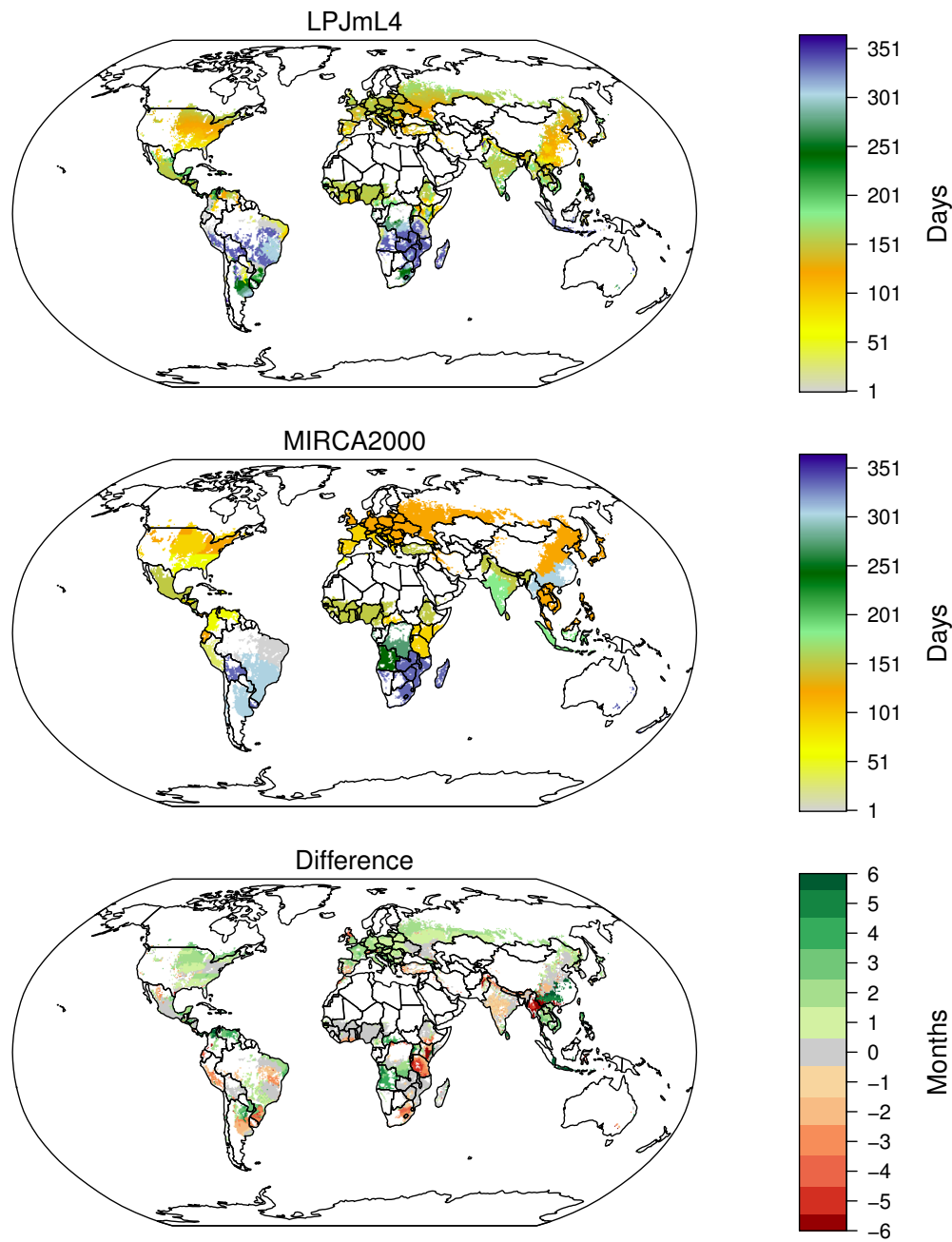


Figure 80. As Fig. 72 for sugar beet.



**Figure 81.** Evaluation of sowing dates of rice: (from top to bottom panel) simulated (LPJmL4) sowing date, observed (MIRCA2000) sowing date and difference between simulated and observed sowing date. Green colours (red colours) in the difference map indicate that simulated sowing dates are too late (too early) compared to observations. White colours indicate crop area smaller than 0.001% of grid cell area. Sowing dates in regions without seasonality are not shown.





**Figure 82.** Evaluation of sowing dates of maize: Caption as for Fig.81.

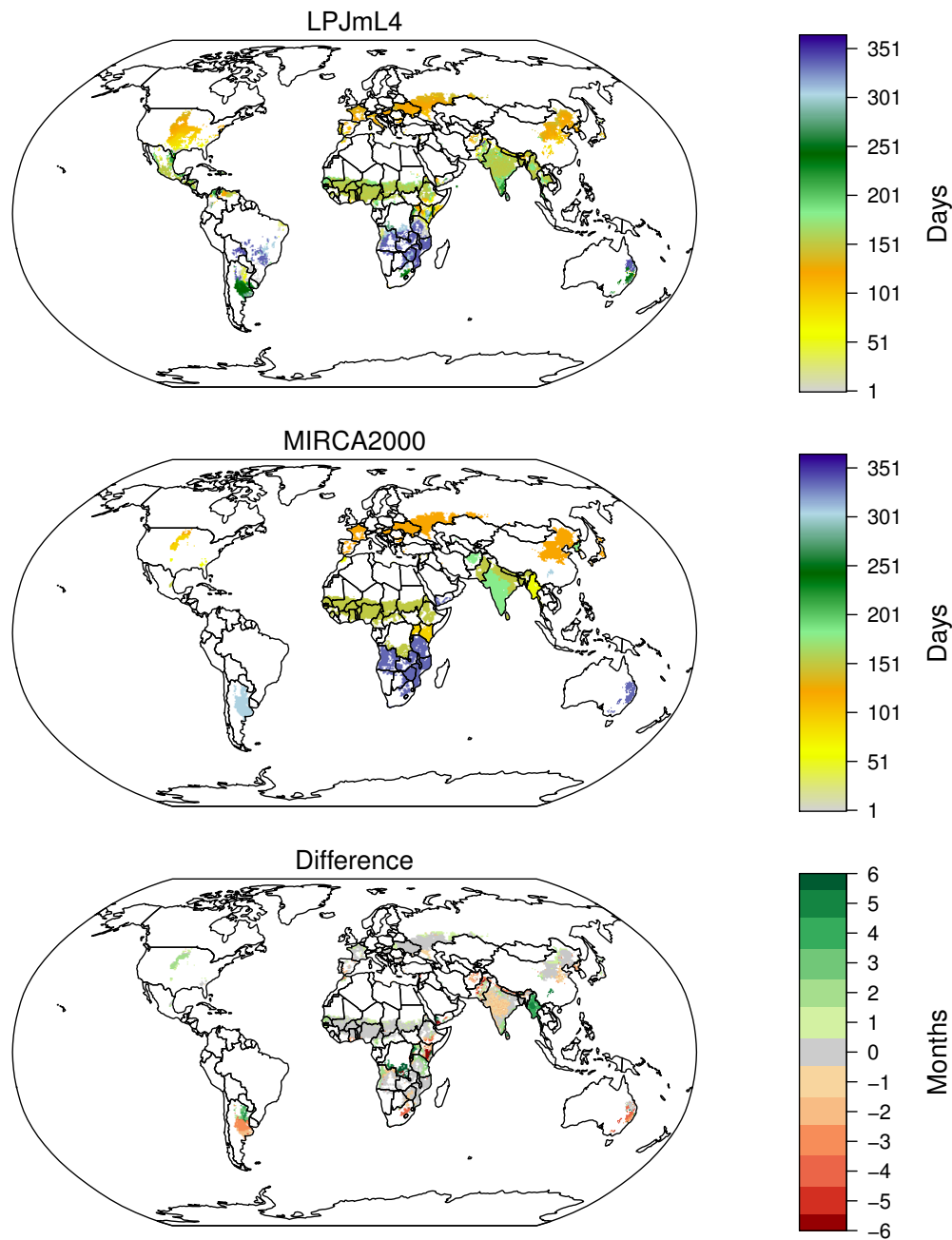


**Figure 83.** Evaluation of sowing dates of millet: Caption as for Fig.81.

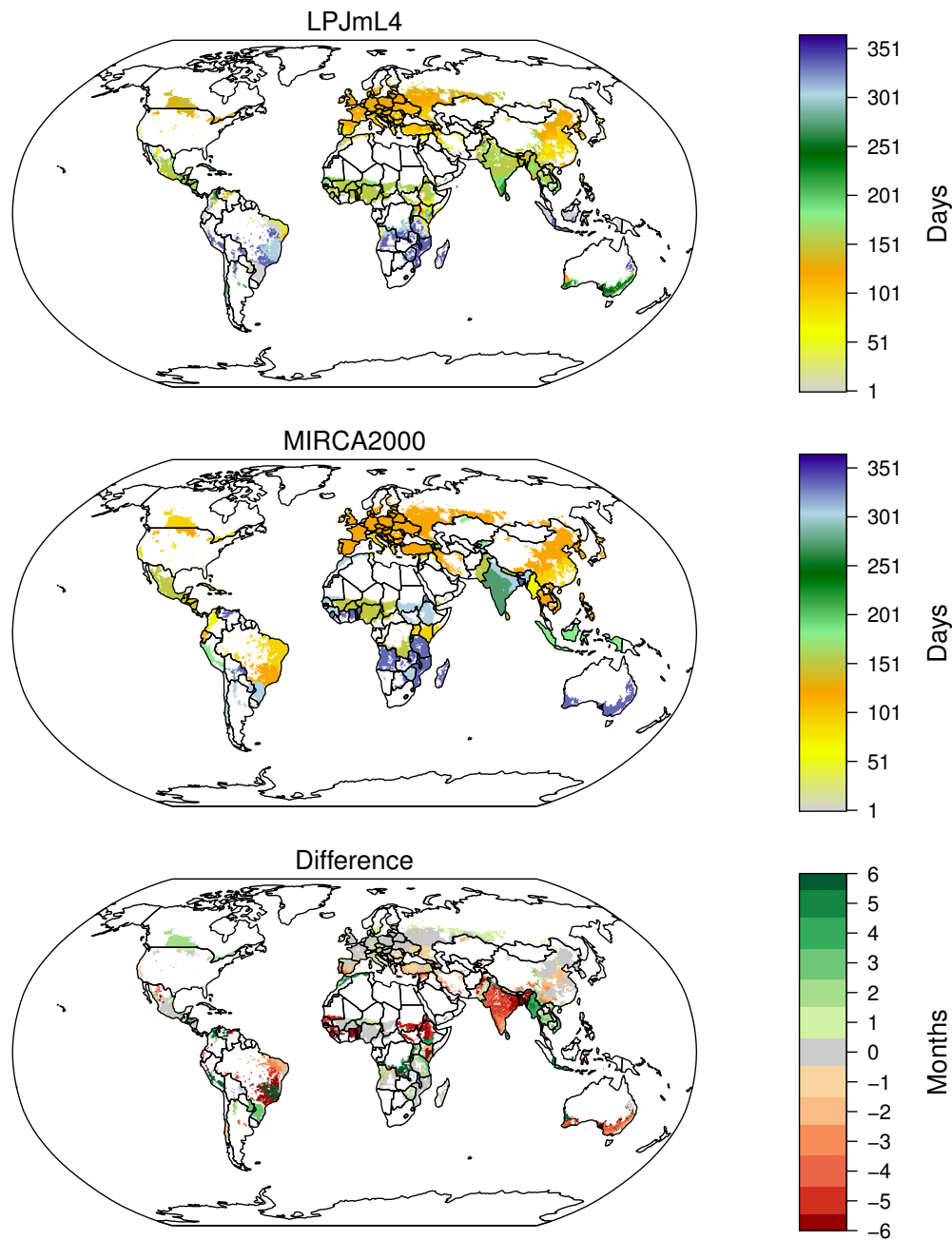


**Figure 84.** Evaluation of sowing dates of pulses: Caption as for Fig.81.

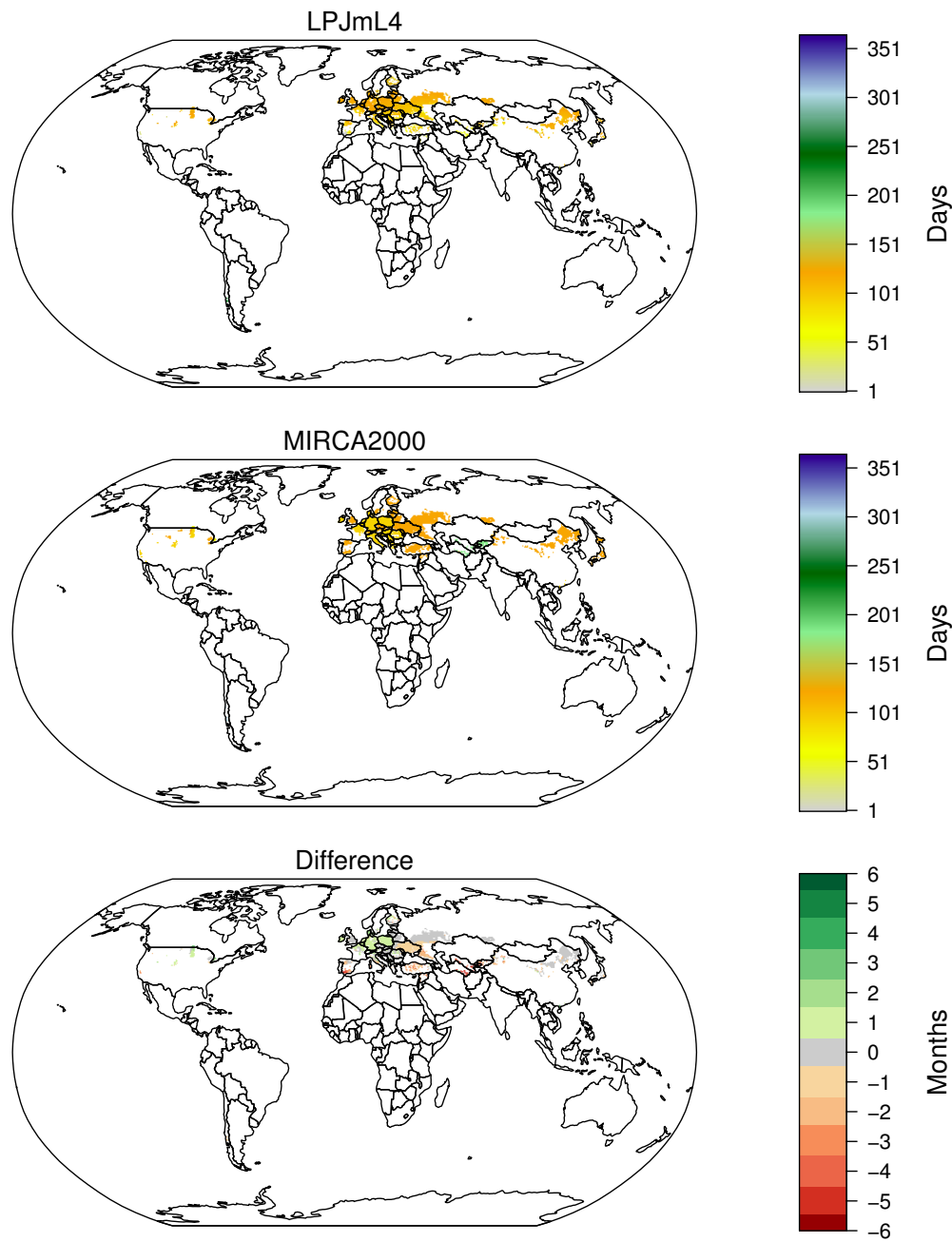
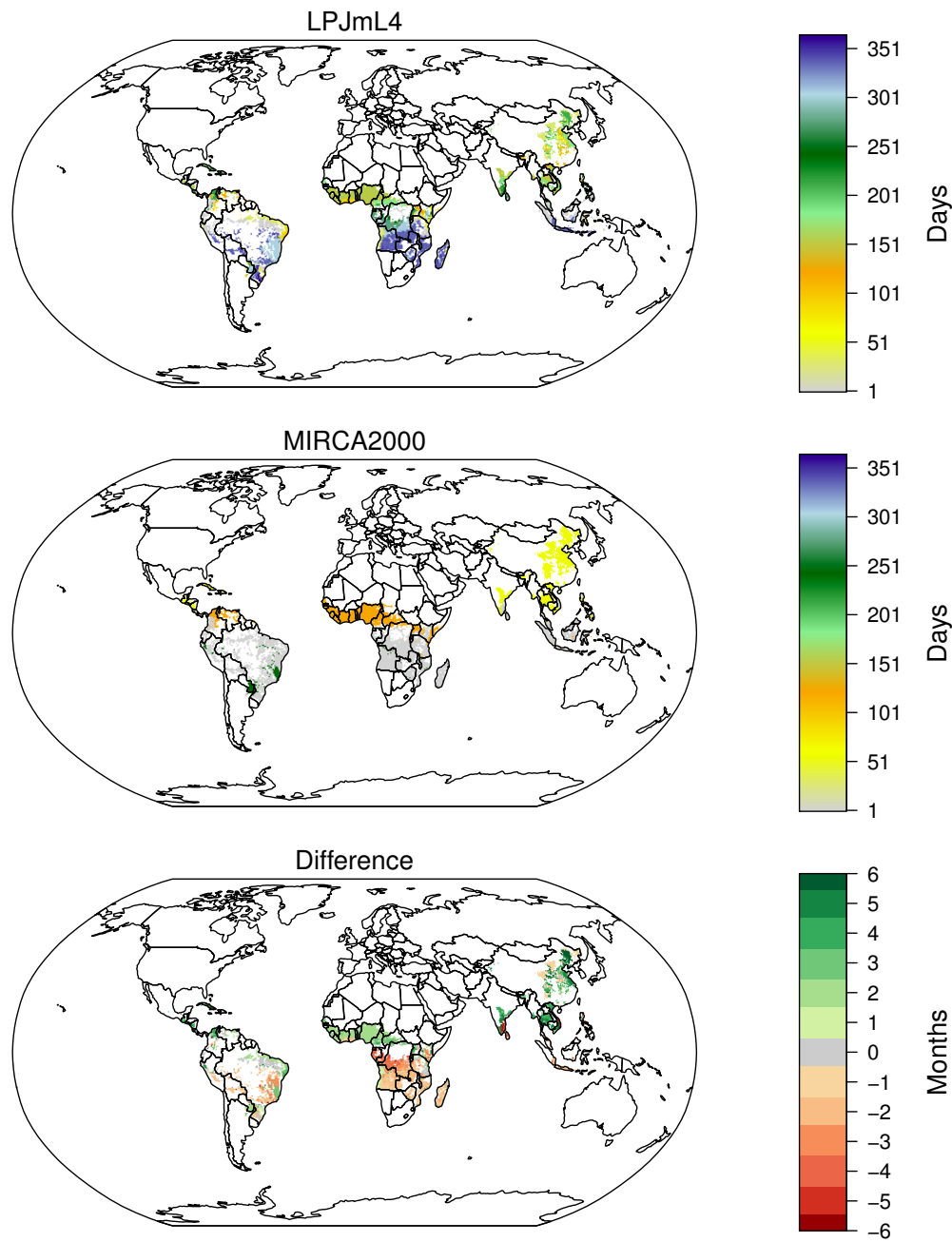
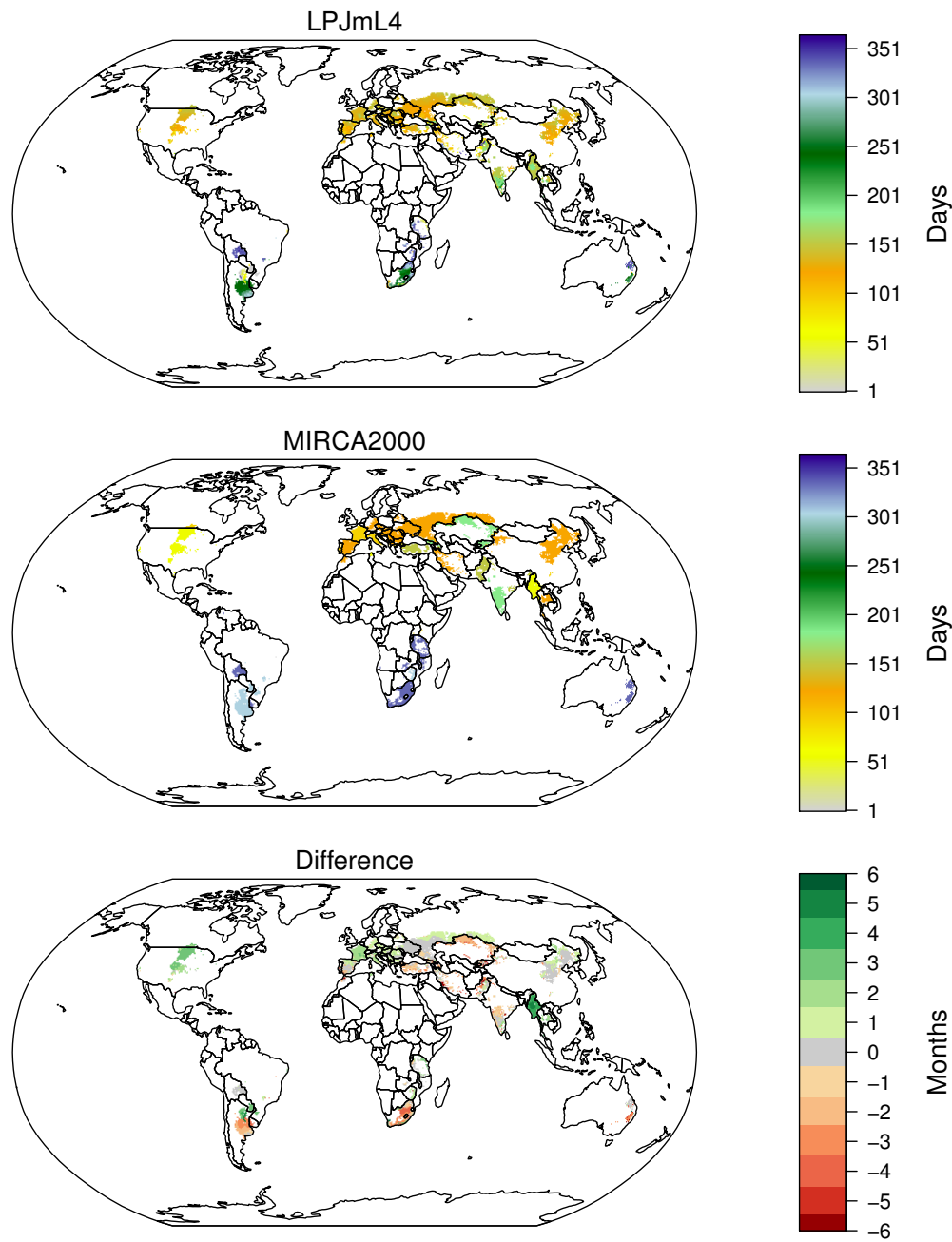


Figure 85. Evaluation of sowing dates of sugarbeet: Caption as for Fig.81.



**Figure 86.** Evaluation of sowing dates of cassava: Caption as for Fig.81.



**Figure 87.** Evaluation of sowing dates of sunflower: Caption as for Fig.81.

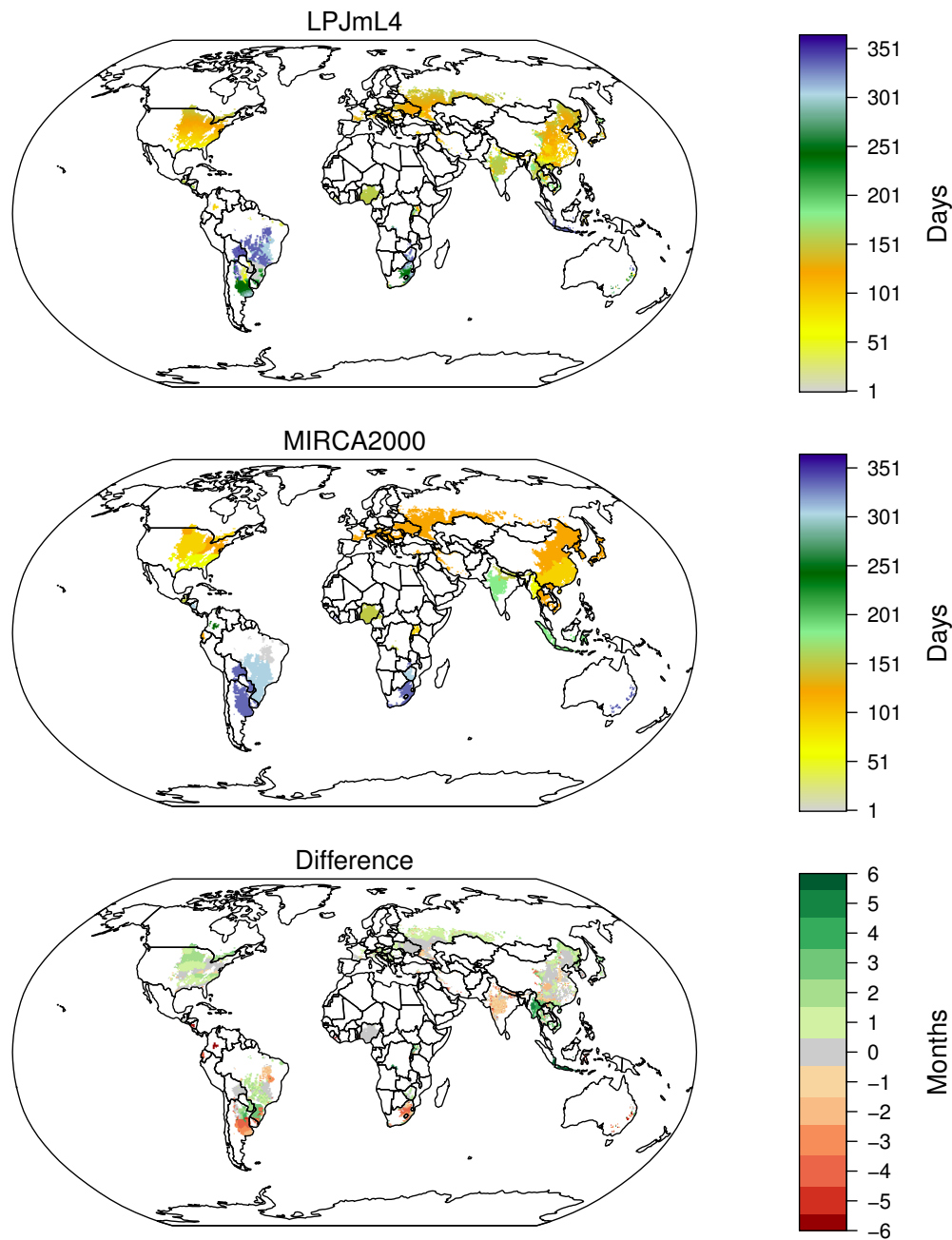


**Figure 88.** Evaluation of sowing dates of soybean: Caption as for Fig.81.

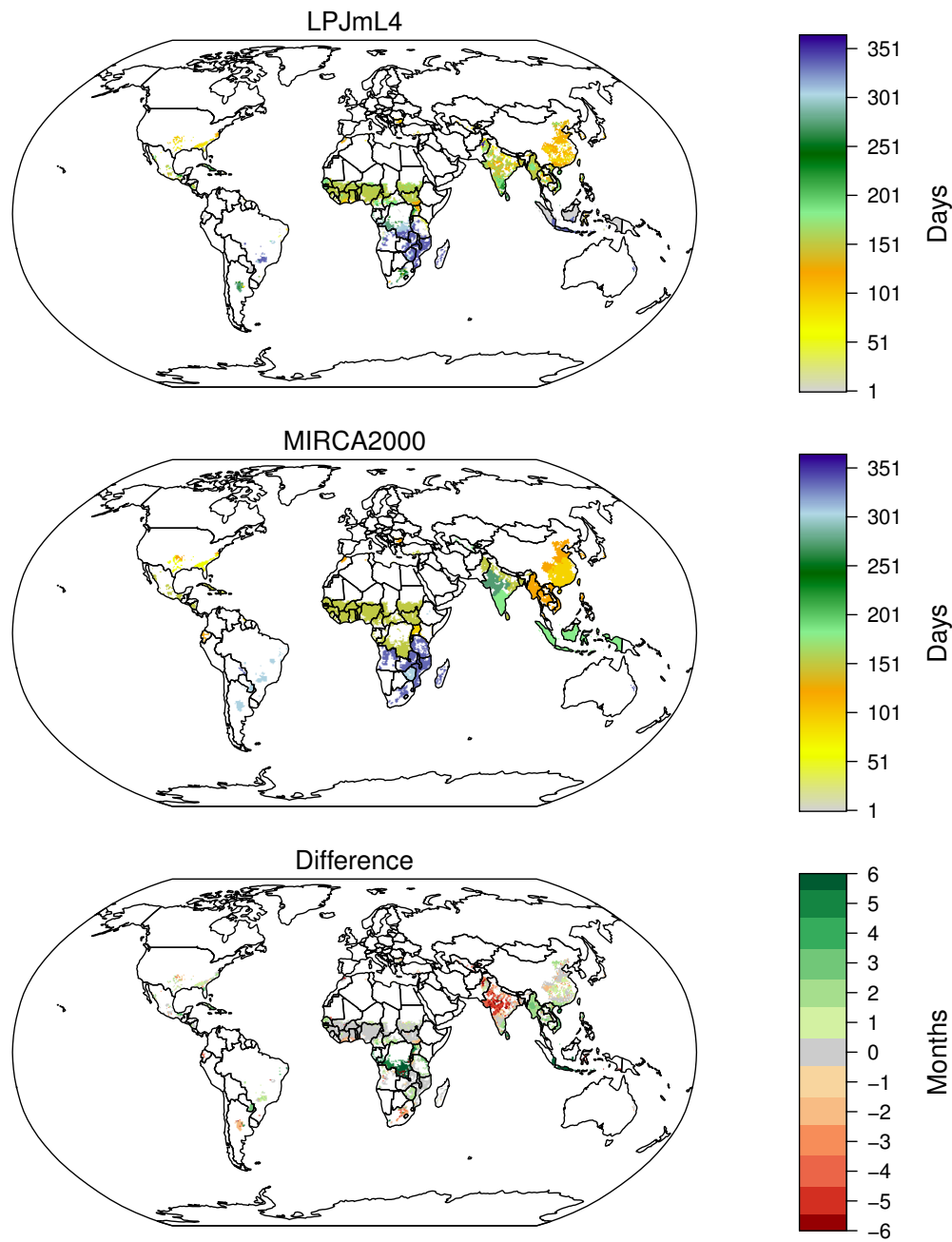


**Figure 89.** Evaluation of sowing dates of groundnut: Caption as for Fig.81.



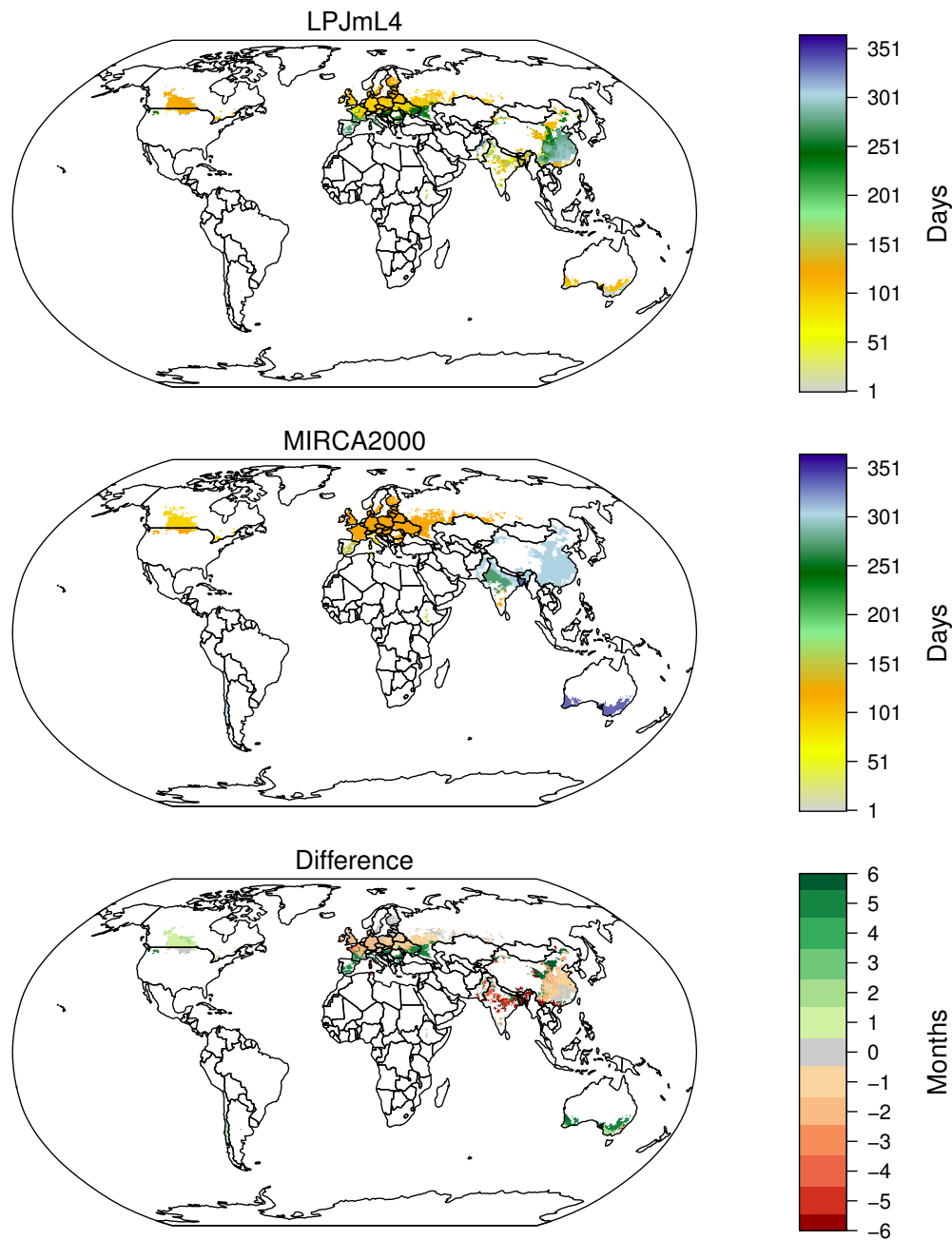


**Figure 90.** Evaluation of sowing dates of rapeseed: Caption as for Fig.81.

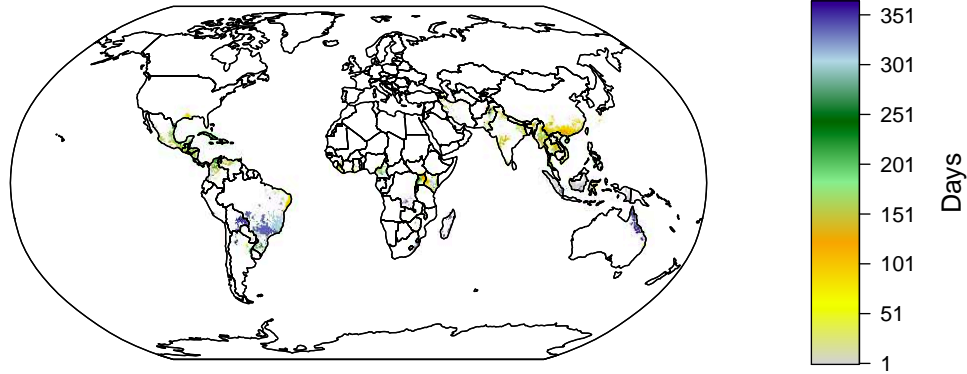


**Figure 91.** Simulated sowing dates of rainfed sugar cane.

**Table 1.** Comparison of field application efficiencies

World region	Surface	Sprinkler	Drip	Surface	Sprinkler	Drip	Surface	Sprinkler	Drip
	(this study)			(Rohwer et al., 2007)			(Sauer et al., 2010)		
North America	52	78	88	48	68	90	50	85	93
South America	50	77	87	51	68	90	38	75	88
Europe and Russia	52	80	90	53	73	90	52	86	93
Mena	62	89	95	49	69	90	22	60	80
SSA	51	70	90	54	75	90	28	64	82
Central and East Asia	50	79	82	48	68	90	42	79	89
South Asia	47	85	92	48	68	90	32	68	84
SE Asia and Oceania	48	67	85	48	71	90	38	75	88
World	50	79	89	49	70	90	42	78	89

For reasons of comparison, we employ here the traditional definition: consumed per applied irrigation water for major world regions compared with literature values in %. This study's results are area-weighted averages, based on current distribution of irrigation systems (source: Jägermeyr et al. (2015)). MENA – Middle East and North Africa; SSA – sub-Saharan Africa.

## References

- 15 Carvalhais, N., Forkel, M., Khomik, M., Bellarby, J., Jung, M., Migliavacca, M., Mu, M., Saatchi, S., Santoro, M., Thurner, M., Weber, U., Ahrens, B., Beer, C., Cescatti, A., Randerson, J. T., and Reichstein, M.: Global covariation of carbon turnover times with climate in terrestrial ecosystems, *Nature*, 514, 213–217, [10.1038/nature13731](https://doi.org/10.1038/nature13731), 2014.
- Jägermeyr, J., Gerten, D., Lucht, W., Hostert, P., Migliavacca, M., and Nemani, R.: A high-resolution approach to estimating ecosystem respiration at continental scales using operational satellite data, *Global change biology*, 20, 1191–1210, doi:[10.1111/gcb.12443](https://doi.org/10.1111/gcb.12443), 2014.
- 20 Jägermeyr, J., Gerten, D., Heinke, J., Schaphoff, S., Kummu, M., and Lucht, W.: Water savings potentials of irrigation systems: global simulation of processes and linkages, *Hydrology and Earth System Sciences*, 19, 3073–3091, doi:[10.5194/hess-19-3073-2015](https://doi.org/10.5194/hess-19-3073-2015), 2015.
- Jung, M., Reichstein, M., Margolis, H. A., Cescatti, A., Richardson, A. D., Arain, M. A., Arneeth, A., Bernhofer, C., Bonal, D., Chen, J., Gianelle, D., Gobron, N., Kiely, G., Kutsch, W., Lasslop, G., Law, B. E., Lindroth, A., Merbold, L., Montagnani, L., Moors, E. J., Papale, D., Sottocornola, M., Vaccari, F., and Williams, C.: Global patterns of land-atmosphere fluxes of carbon dioxide, latent heat, and sensible heat derived from eddy covariance, satellite, and meteorological observations, *Journal of Geophysical Research: Biogeosciences*, 116, doi:[10.1029/2010JG001566](https://doi.org/10.1029/2010JG001566), 2011.
- 25 Liu, Y. Y., van Dijk, A. I. J. M., de Jeu, R. A. M., Canadell, J. G., McCabe, M. F., Evans, J. P., and Wang, G.: Recent reversal in loss of global terrestrial biomass, *Nature Clim. Change*, 5, 470–474, doi:[10.1038/nclimate2581](https://doi.org/10.1038/nclimate2581), 2015.
- Rohwer, J., Gerten, D., and Lucht, W.: Development of functional irrigation types for improved global crop modelling - PIK report No. 104, Tech. Rep. 104, Potsdam Institute for Climate Impact Research, Potsdam, Germany, <https://www.pik-potsdam.de/research/publications/pikreports>, 2007.
- 30 Sauer, T., Havlík, P., Schneider, U. a., Schmid, E., Kindermann, G., and Obersteiner, M.: Agriculture and resource availability in a changing world: The role of irrigation, *Water Resources Research*, 46, doi:[10.1029/2009WR007729](https://doi.org/10.1029/2009WR007729), 2010.
- Schaphoff, S., Forkel, M., Müller, C., Knauer, J., von Bloh, W., Biemans, H., Gerten, D., Heinke, J., Jägermyer, J., Lucht, W., Rammig, A., Thonicke, K., and Waha, K.: The LPJmL4 Dynamic Global Vegetation Model with managed Land: PART II - Evaluation of a global consistent vegetation, hydrology and agricultural model, *Geoscientific Model Development*, submitted.
- 40